Title
Methanosarcina mazei G&#65533;1 Proteomic Response to Methylotrophic Substrates

Author
Jarrett, Deborah

Publication Date
2019

Peer reviewed|Thesis/dissertation

UNIVERSITY OF CALIFORNIA

Los Angeles

Methanosarcina mazei Gö1 Proteomic Response to Methylotrophic Substrates

A Dissertation submitted in partial satisfaction of the

requirements for the Degree of Philosophy

in Biochemistry and Molecular Biology

by

Deborah Jarrett

2019

ABSTRACT OF THE DISSERTATION

Methanosarcina mazei Gö1 Proteomic Response to Methylotrophic Substrates

by

Deborah Jarrett

Doctor of Philosophy in Biochemistry and Molecular Biology

University of California, Los Angeles, 2019

Professor Joseph Ambrose Loo, Chair

Transcriptomics is often touted to be the silver bullet to determining the protein levels within a microorganism when comparing such proteins under two or more different biological conditions. However, designating the transcriptome as a surrogate for protein abundance can be misleading and impractical when determining the effect of environmental stresses on the phenotype of an organism. While the transcriptome is significant for identifying genes that are linked to, or act as co-regulators in the response to stressors, it is best to consider proteomic analyses, in addition to transcriptional profiling, as a complementary tool in order to determine the effect of different environmental factors on the fitness and phenotype of the microorganism in question. *Methanosarcina mazei* are mesophilic archaea microorganisms that grow under anaerobic conditions and produce methane via an energy-conservation process, known as methanogenesis, which is the terminal step in the degradation of organic matter during the

carbon cycle. While the *Methanosarcina* are versatile in their ability to grow on numerous substrates, such as methanol and other compounds such as monomethylamine (MMA), dimethylamine (DMA), and trimethylamine (TMA), it is more thermodynamically favorable for the cells to grow on methanol ($\Delta G'^{o}$ = -106 kJ/ mol methane) than the methylamines ($\Delta G'^{o}$ = -77 kJ/ mol methane). Therefore, the lower free energy change in using the methylamines necessitates *M. mazei* cells to have an efficient energy-conserving system to deal with the thermodynamic limitations. Consequently absolute quantitation using a label-free proteomics strategy was applied to determine the intercelluar protein abundances of the *Methanosarcina mazei* proteome with different methylotrophic substrates (i.e., methanol, MMA, DMA, and TMA). Specifically, the aims of this project are to use quantitative proteomics to: (1) establish how *M. mazei* uses enzymes involved in methanogenesis to convert chemical energy into biomass; (2) determine how methanogenic process depends upon substrate type during the mid-log and stationary phases of growth; (3) determine whether different salt concentrations affect the glycosylation pattern of surface of the protein, and in turn methanogenesis; (4) understand the effect of methylotrophic substrate availability on a different methanogen, *M. barkeri*. At least 40% of all of the proteins were found to be methyltransferases and methylcoenzyme-M reductases in *M. mazei* cells grown under mid-log and stationary phase conditions. Furthermore, the protein abundances varied in a substrate-specific manner, indicating that the *M. mazei* cells may have evolved to be prepared for a potential carbon source switch.

The Dissertation for Deborah Jarrett is approved.

James W. Gober

Robert P. Gunsalus

Joseph A. Loo, Committee Chair

University of California, Los Angeles

2019

Table of Contents

List of Figures

List of Tables

EDUCATION

California State University, Los Angeles, CA **6/06-6/08**
Master of Science, Biochemistry, GPA 3.74
Graduate Thesis Project: Investigate the peroxiredoxin/ sulfiredoxin pathway to remove reactive oxygen species (ROS) in cardiac porcine cells using High Performance Liquid Chromatography (HPLC).

University of Southern California, Los Angeles, CA **8/01-5/05**
Bachelor of Science, Biochemistry, GPA 3.14
Undergraduate Research Project: Investigate the relationship between tea catechins and genotypes (COMT, SULT1A1, and UGT1A1) on Breast Cancer Risk.

INDUSTRY EXPERIENCE

Bachem, Inc., Torrance, CA **4/12-6/13**
Research Scientist
Peptide synthesis, cleavage, and purification, utilizing Fmoc-Solid phase peptide synthesis strategy. Increased production of peptide pharmaceutical products within R&D team by developing products within a 6-week turn-around. Composed written analytical reports after project completion.

Phenomenex, Inc., Torrance, CA **2/10-4/12**
Research Associate
Develop 2 key HPLC products: Aeris Widepore/Peptide and Kinetex XB-C18 columns, used to characterize biomolecules for protein chemistry and small molecules. HPLC method development and optimization. United States Pharmacopeia testing. **Publication: *LCGC* on "Optimized Sunscreen Method Used for Impending 2012 Enforcement of FDA Regulation in Characterizing Their Active Ingredients"**

Peptisyntha, Inc., Torrance, CA **1/08-2/10**
Production Chemist
Peptide synthesis, cleavage, and purification utilizing Fmoc- and Boc-Solid phase peptide synthesis strategies. Preparative purification of peptides in R&D and GMP laboratories, while maintaining a GLP notebook. **Award: 2008 Employee of the Year Award for dedicated performance within the company**

TEACHING/ TUTORING/ ADMINISTRATIVE

UCLA, Los Angeles, CA **1/19-3/19**
Graduate Teacher's Associate Chemistry 184/ Chemical Instrumentation
Instructed 2 laboratory sections per week for advanced undergraduate UCLA students. Implemented laboratory curriculum for the use of analytical instruments, such as LC/MS-ESI, MALDI-TOF, and HPLC in the quantitative and qualitative analysis of small molecules, protein digests, and polymers, while also using bio-informtic databases.

Loyola Marymount University **8/18 – 12/18**
Instructor of Biochemistry and General Chemistry I Lab Lecture
Instruct courses in Introductory Biochemistry and General Chemistry I Lab Lecture. Designed Exams and lecture presentations using PowerPoint. Provided homework, Exam-like questions, Exam review sessions, and weekly office hours to upper-division undergraduates to facilitate student-centered learning.

UCLA, Los Angeles, CA **6/18-8/18 & 6/17-8/17**
Graduate Teacher's Assistant Chemistry 153A/ Biochemistry: Introduction to Structure, Enzymes and Metabolism
Instruct 2 discussion sections per week for the 1st Summer 2018 session of Chemistry 153A to UCLA upper division students. Provided homework, exam and biochemistry assistance to UCLA students during weekly office hours, in addition to instructing exam preparation sessions

UCLA, Los Angeles, CA **8/16-9/16**
Graduate Teacher's Assistant Chemistry 14B/ Thermodynamics, Electrochemistry, Kinetics, and O. Chemistry
Instructed 2 discussion sections per week for the 2nd Summer 2016 session of Chemistry 14B to UCLA students. Provided homework, exam, and general chemistry assistance to UCLA students during weekly office hours, in addition to instructing exam preparation sessions

UCLA Career Center, Los Angeles, CA **9/14-2/15**
Graduate Student Peer Advisor
Increased graduate student access to and use of professional development resources by: presenting career development opportunities to STEM graduate student associations; advising graduate students in one-on-one environments; and increasing graduate-level engagement in professional activities via designing a bi-weekly newsletter, tabling Fellowship events, and designing/posting career-related activity flyers

AWARDS/ FELLOWSHIPS

UCLA, Los Angeles, CA
Chemistry Biology Interface Program Fellow **9/14-Present**
Eugene Cota-Robles Fellowship **9/13-Present**

California State University, Los Angeles
Graduate Equity Fellowship **1/07-1/08**

University of Southern California, Los Angeles, CA
University Dean's List (GPA 3.55 and 3.66) **12/04 & 5/05**
7th Annual Undergrad. Research Symposium **5/05**
Ronald E. McNair Scholar **5/02-5/05**

CONFERENCES/ SYMPOSIA

66th Annual ASMS, San Diego, CA **6/18**
Poster: Deborah A. Jarrett, Farzaneh Sedighian, Hong Hanh Nguyen, Robert P. Gunsalus, Joseph A. Loo, Rachel O. Loo. *Methanosarcina mazei* proteomic responses to different methylotrophic substrates

CHAPTER 1

Quantitative Proteomic Analysis of *Methanosarcina mazei* Gö1

Introduction

This chapter describes how methanogens, methane-producing archaea, conserve their energy to synthesize ATP by producing methane gas (Buan, 2018). By essentially converting chemical energy from various C1 substrates, such as methanol and methylamines, into biomass, *Methanosarcina mazei* Gö1, which is the methanogen studied in this thesis, are "special" microorganisms that are said to be living life close to the 'thermodynamic edge', meaning that they can grow autotrophically on inorganic substrates in the absence of light (Buan, 2018). The scope of this project is to use quantitative proteomics to establish how these "special" microorganisms are able to use crucial enzymes that are involved in the methanogenic process in order to convert chemical energy into biomass, and determine how such a process depends upon substrate availability during different stages of growth: mid-log **(Chapter 2)** versus stationary **(Chapter 3)**; and under two different salt concentrations **(Chapter 4)**. The thesis culminates with an **Appendix** that focuses on a different methanogen, *Methanosarcina barkeri* Fusaro, which exhibits similar proteomic characteristics as *Methanosarcina mazei*; however, it also utilizes up to two different surface-layer proteins depending upon its substrate availability. By determining the enzymes involved in the energy conservation process of methanogens, such as *M. mazei* and *M. barkeri,* via quantitative proteomics, researchers can target such enzymes with the aim to mitigate the levels of methylamine substrates produced through agricultural processes, which account for one-tenth of the greenhouse gases generated, and eventually harness the methane produced as a "clean" fuel.

Methanogens / *Methanosarcina*

Methanogenic Pathways

Methanogens belong to the domain Archaea, kingdom Monera, and phylum *Euryarcheota*, of which there exist 5 orders: *Methanococcales, Methanobacteriales, Methanosarcinales, Methanomicrobiales, and Methanopyrales. Methanosarcina mazei* Gö1 belongs to the *Methanosarcinales* order. *Methanosarcina* species are methanogens, which belong to the domain *Archaea*, and they exist in anoxic environments from freshwater sediments to rice paddies. The methane that is produced by methanogens plays two significant yet different roles in the global ecology of the earth. On the one hand, methane acts as a greenhouse gas that contributes to global warming; however, on the other hand, methane serves as a combustible gas that can be used as an energy source for industrial applications. Three major pathways for methane-production exist for methanogens and they include the 1) hydrogenotrophic, 2) aceticlastic, and 3) methylotrophic pathways. The hydrogenotrophic pathway is believed to be the ancestral pathway for methanogens, and uses hydrogen and carbon dioxide as substrates that are metabolized to methane. The aceticlastic pathway, which only exists in the order *Methanosarcinales*, uses acetate as a substrate. Furthermore, the methylotrophic pathway is found in *Methanomassiliicoccales* (a new order belonging to *Euryarchaeota)*, *Methanobacteriales*, and *Methanosarcinales*; all of which use various methylated compounds, such as methanol, methylamines, and methylsulfides.

In the first step of the hydrogenotrophic pathway **(Figure 1.1)**, carbon dioxide is reduced and activated to form **formylmethanofuran** using reduced ferredoxin (Fd_{red}) as the electron donor. In the second step, **formylmethanofuran** is reduced to form **formyl-tetrahydromethanopterin**, which is then dehydrated to form **methylene- H_4MTP**, and then reduced to form **methyl-H_4MTP**. The electron donor in the second step is $F_{420}H_2$. The

methylene-H_4MTP reduction uses electrons from reduced F_{420} ($F_{420}H_2$). The methyl group of methyl- H_4MTP is then transferred to coenzyme-M, thus forming **methyl-coenzyme M**, which is then reduced to **methane** by using coenzyme-B as the electron donor. These reactions occur in the cytoplasm of the *Methanosarcina* cells where the F_{420} cofactor resides, serving as the central electron carrier in methanogens (Sorgenfrei et al, 1997). The hydrogenase system is responsible for donating electrons to the heterodisulfide reductase enzyme, which then reduces the subsequently formed coenzyme-M-S-S-coenzymeB heterodisulfide, once methane is formed. *Methanosarcina acetivorans* cannot grow on hydrogen and carbon dioxide because it is not equipped with a functioning hydrogenase system.

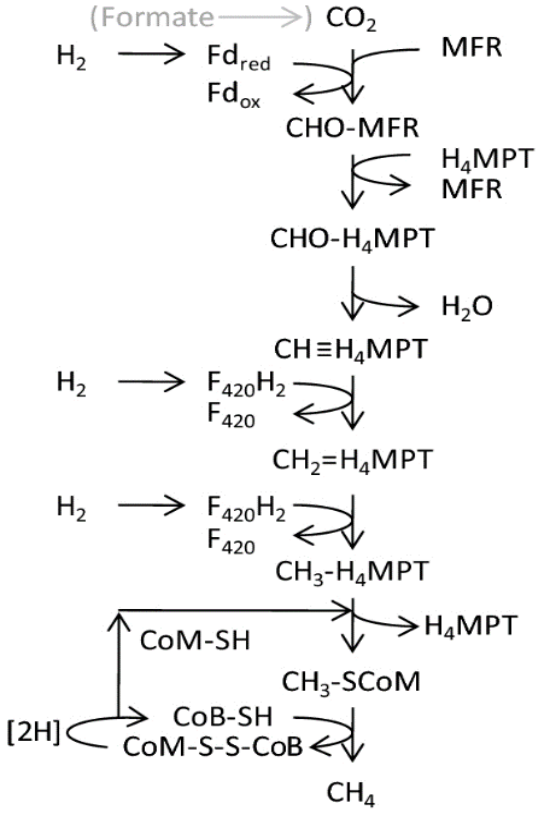

Figure 1.1 Diagram of Hydrogenotrophic Pathway of Methanogenesis (Enzmann, 2018). (Figure reprinted with permission.)

Along the *M. acetivorans* aceticlastic pathway **(Figure 1.2)**, acetate is activated by reacting with coenzyme A and ATP to form acetyl CoA. Afterwards, the carbon monoxide dehydrogenase (CODH)/acetylCoA synthase complex splits acetyl CoA into 2 groups: 1) the carbonyl group, which is oxidized to carbon dioxide and 2) the methyl group that is transferred to tetrahydrosarcinopterin (tetrahydromethanopterin in methanogenic archaea outside of the genus *Methanosarcina*). The methyl group is then transferred to coenzyme M where it is reduced to methane with electrons from oxidizing the carbonyl to CO_2. More specifically, the first step of the aceticlastic pathway of methanogenesis is the phosphorylation of the carboxyl group of acetate, and the transfer of the acetyl group to coenzyme A. The acetyl CoA synthase/carbon monoxide dehydrogenase enzyme then cleaves the C-C- and C-S- bonds in acetyl CoA and oxidizes CO to CO_2. The methyl group in acetyl CoA is then transferred to tetrahydro methanopterin and the electrons derived from the oxidation of CO are then used to reduce ferredoxin, which is an electron carrier. Afterwards the methyl group is transferred from methyltetrahydromethanopterin to coenzyme M. The methyl coenzyme M is reductively cleaved as it was in the hydrogenotrophic pathway, producing methane as a by-product and the CoM-S-S-CoB heterodisulfide, which is cleaved by the reduced ferredoxin (Fdred): heterodisulfide oxidoreductase system.

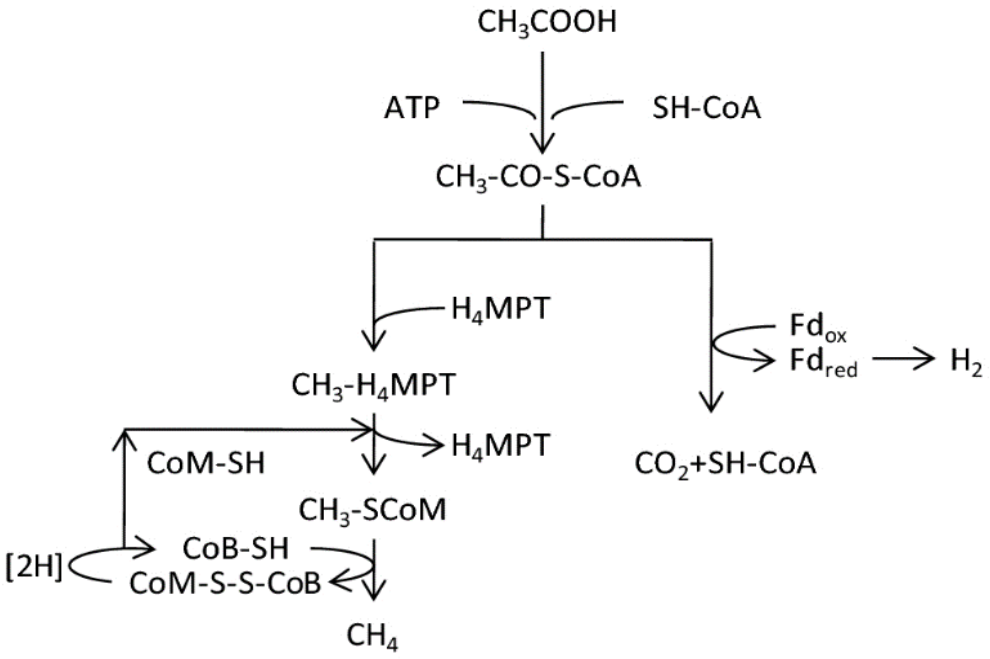

Figure 1.2 Diagram of Aceticlastic Pathway of Methanogenesis (Enzmann, 2018). (Figure reprinted with permission.)

In the methylotrophic pathway **(Figure 1.3)**, the methylated substrate is transferred to a corrinoid protein by a substrate-specific methyltransferase, known as methyltransferase 1 (MT1). Another substrate-specific methyltransferase (MT2) then transfers the methyl group to coenzyme M, thereby forming methyl coenzyme M. Out of every four methyl-coenzyme-M molecules, one is oxidized to carbon dioxide via the oxidative branch of the methylotrophic pathway (the reverse of the hydrogenotrophic pathway), while the remaining three methyl-coenzyme-M molecules are reduced to form methane via the reductive branch of the pathway, a process that uses the electrons derived from oxidizing methyl-coenzyme-M (Welte and Deppenmeier 2014). During the oxidative branch of methanogenegsis, the methyl group is transferred from methanol to coenzyme M, and then transferred to tetrahydromethanopterin in an endergonic process that is driven by an electrochemical sodium ion gradient. As the oxidation of the methyl group from methanol to form CO_2 occurs, the electrons that are lost are used to reduce F_{420}. On the other hand, during the reductive branch of the methylotrophic

pathway, CoB provides the electrons necessary for the reductive cleavage of methyl CoM, thereby producing methane and CoM-S-S-CoB. Furthermore, the $F_{420}H_2$:heterodisulfide oxidoreductase system is responsible for the reduction for the heterodisulfide.

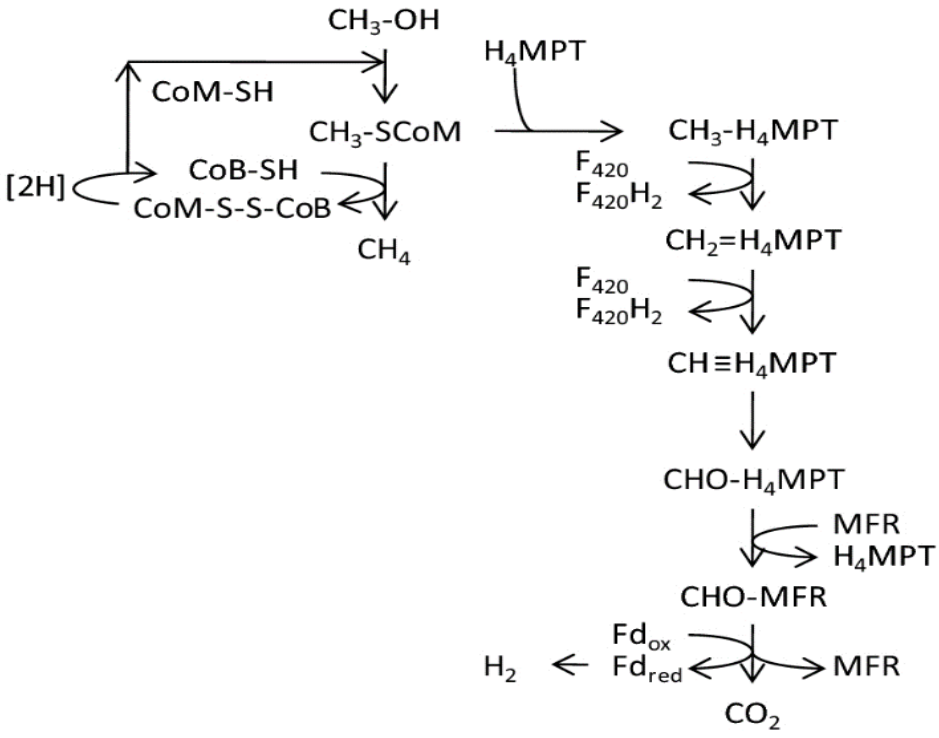

Figure 1.3 Diagram of Methylotrophic Pathway of Methanogenesis (Enzmann, 2018). (Figure reprinted with permission.)

Nonetheless, all of the heterodisulfide oxidoreductase systems from each of the three different methanogenic pathways (hydrogenotrophic, aceticlastic, and methylotrophic) are membrane-bound electron transport systems. Also, the electron transport systems are accompanied by proton translocation across the cytoplasmic membrane. The movement of the protons across the membrane generates an electrochemical proton gradient that is used to drive ATP synthesis from ADP and inorganic phosphate with the A_1A_0 type ATP synthase enzyme. Both *M. mazei* and *M. barkeri* use their anaerobic respiratory chain, which includes the heterodisulfide oxidoreductase systems, to translocate 4 moles of protons for every 1 mole of reduced CoM-S-

S-CoB heterodisulfide. Both of the aforementioned methanogens also contain the H_2:heterodisulfide and $F_{420}H_2$:heterodisulfide oxidoreductase systems. The $F_{420}H_2$ dehydrogenase from the $F_{420}H_2$:heterodisulfide oxidoreductase system is comparable to the NADH dehydrogenase from complex I of the electron transport chain in prokaryotes. The $F_{420}H_2$ dehydrogenase transfers electrons from $F_{420}H_2$ to a hydrophobic cofactor that exists in the cytoplasmic membrane, known as methanophenazine, which is a 2-hydroxy phenazine derivative connected to a pentaprenyl side chain via an ether linkage **(Figure 1.4)**.

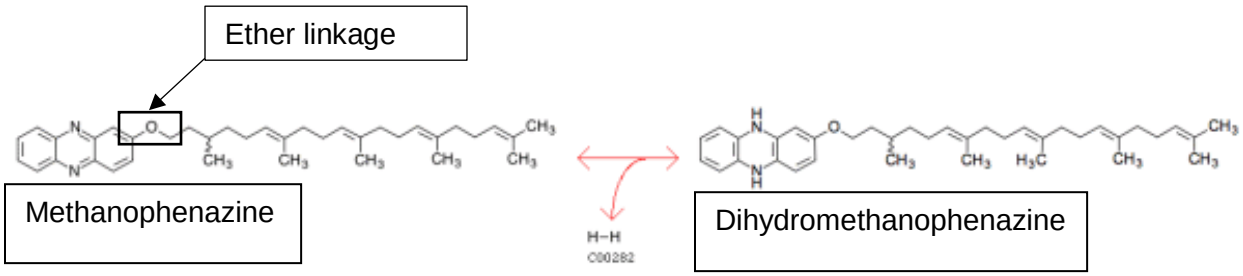

Figure 1.4 Ether linkage of methanophenazine.

The transfer of electrons from $F_{420}H_2$ to methanophenazine is coupled to a proton transfer across the cytoplasmic membrane, and 2 protons are transferred per electron. Then the heterodisulfide from the oxidoreductase system transfers electrons from dihydro-2-hydroxy phenazine to CoM-S-S-CoB, a reaction that is also coupled to proton translocation, for a total of 4 protons transferred per 2 electrons for the $F_{420}H_2$:heterodisulfide oxidoreductase system. At this time, it is important to highlight the fact that the $F_{420}H_2$-dependent hydrogenase is responsible for reducing coenzyme F_{420} to form $F_{420}H_2$, and the $F_{420}H_2$ dehydrogenase is responsible for oxidizing $F_{420}H_2$ to form F_{420}, and the resulting electrons are transferred to methanophenazine, at which time 2 protons are translocated across the cytoplasmic membrane.

The $F_{420}H_2$ dehydrogenase has 5 different subunits, contains non-heme iron, has an acid-labile sulfur atom, and has an FAD that serves as the electron carrier within the enzyme. As

mentioned earlier, the $F_{420}H_2$ dehydrogenase (except for its FpoF and FpoO subunits) have DNA sequence similarity to the NADH:quinone oxidoreductase system found in prokaryotes and eukaryotes. FpoF serves as the input site for the entrance of $F_{420}H_2$, which is subsequently oxidized to form F_{420}; and FpoO participates in the reduction of methanophenazine. Nonetheless, while the differences between the $F_{420}H_2$ dehydrogenase and the NADH:quinone oxidoreductase system exists with the presence of FpoF and FpoF, their similarities abound. For instance, 1) they both have flavin and iron-sulfur containing proteins, 2) significant homology exists between their hydrogenase and proton transporting modules, 3) both utilize the small non-proteinaceous hydrophobic electron carriers of methanophenazine and quinones, respectively, and 4) their electron donors $F_{420}H_2$ and NADH, respectively, are reversible hydride donors.

Methanosarcina species have 3 types of [NiFe] hydrogenases, the F_{420}-reducing hydrogenase, the F_{420}-nonreducing hydrogenase, and the Ech hydrogenase, each of which have a small and large subunit, whereby the large subunit serves as the catalytic site with the NiFe bimetallic center, and the small subunit contains 2-4 FeS clusters and is responsible for electron transport from the catalytic site. The heterodisulfide reductase in methylotrophic methanogens consist of HdrD and HdrE; with HdrD containing the active site for the reduction of the heterodisulfide and comprises of two [4Fe-4S] clusters and HdrE containing a b-type cytochrome and two heme molecules (Deppenmeier, U. 2004).

Methylotrophic Substrates

Methylotrophic substrates, such as methanol and the methylamines, monomethylamine (MMA), dimethylamine (DMA), and trimethylamine (TMA) can serve as carbon sources and energy sources for the growth of *Methanosarcina mazei* cells. Their nitrogen source can be either molecular nitrogen (N_2), under nitrogen-limiting conditions, or ammonium (NH_4^+) under nitrogen-

sufficient conditions. When the *M. mazei* cells are grown using molecular nitrogen as its nitrogen source, the *nif* genes, which encode a molybdenum-containing nitrogenase allowing nitrogen fixation, are induced. Veit and colleagues investigated the regulation of soluble methyltransferases in *Methanosarcina mazei* cells grown under different carbon and nitrogen sources (Veit et al. 2005). Seven different operons code for the methylamine methyltransferases and their respective corrinoid proteins (2 different operons code for TMA methyltransferase and corrinoid protein, 3 different operons code for DMA, and 2 different operons code for MMA). Additionally, 3 different genes code for the methyl cobalamine:CoM methyltransferase (mtbA1-3). All methylamine methyltransferases encode an internal amber codon UAG, which is responsible for encoding the 22nd amino acid, pyrrolysine.

Veit and colleagues performed transcriptional study experiments to determine that the homologous genes for the various methylamine substrates are present in *M. mazei* cells in order to ensure adaptability of the cells to different growth conditions (Veit et al. 2005). Furthermore, due to the observation that the two different MMA methyltransferase/ corrinoid protein operons were differentially regulated, mtmB2C2 being nitrogen-regulated and mtmB1C1 being regulated by a carbon source, it is speculated that they serve different functions within the cell. On the other hand, the methylcobalamine:CoM methyltransferase, which is encoded for by mtbA genes, were significantly, but only slightly differentially regulated under nitrogen-limiting conditions indicating that the basal transcription of mtbA allows the production of enough ammonium for the cells to grow in MMA.

It was also demonstrated that TMA can serve as a carbon and nitrogen source due to the observation that *M. mazei* cells grown in methanol under nitrogen-limiting conditions (+N_2) or nitrogen-depleted conditions, either reduced their yield or did not grow at all when compared to their growth on nitrogen-sufficient conditions (+NH_4), respectively. However when *M. mazei* cells

were grown in TMA under nitrogen-limiting or nitrogen-depleted conditions, the yield of the cells remained relatively the same. Also, when cells were grown in TMA under nitrogen-limiting conditions, it would be expected that the *nif* genes would be induced, because they encode the nitrogenases that are necessary for nitrogen fixation; however, the *nif* genes were instead repressed. This occurred because when the cells are grown in TMA, the degradation of the substrate leads to the formation of ammonium, which can repress the *nif* genes and switch the cells to a nitrogen-sufficient environment (Veit et al, 2005). Similarly, we speculate that the presence of the different methylotrophic substrates can represses the expression of a transcript/ protein or induction of a gene belonging to another methylotrophic substrates' methyltransferase and corrinoid protein. Such results were observed in our proteomic study of *M. mazei* cells grown under different methylotrophic substrate conditions in the mid-log and stationary growth phases. Veit and colleagues also demonstrated that the differential transcription of mtmB1C1 of the mazei cells on TMA versus methanol was not growth-phase dependent. Our proteomic study results are consistent with Veit's results.

Also when different substrate specific methyltransferases are present in different growth conditions, they may be present so that the cells are prepared for a potential carbon source switch (Zinder et al., 1985). A report by Ding *et al.* (Ding, Y.H. et al., 2002) also speculated that multiple homologues of a gene are differentially expressed to expedite a switch between different methylotrophic substrates.

Cytochromes in Methanogens

Methanogens can be divided into 2 groups: 1) methanogens without cytochromes and 2) methanogens with cytochromes. *Methanosarcina* are methanogens that have cytochromes. Methanogens without cytochrome have methyl- H_4MTP:coenzyme M methyltransferase (Mtr), which couples methyl transfer from H_4MTP to coenzyme M with formation of a primary

electrochemical Na^+ gradient over the membrane. Methyl-viologen-hydrogenase-heterodisulfide reductase (Mvh-Hdr) catalyzes the H_2-dependent reduction of CoM-S-S-CoB and couples this exergonic process to the endergonic reduction of oxidized ferredoxin (Fd_{ox}) via flavin-based electron bifurcation (2 distinctly divided reactions whereby the electrons from one reaction power a second reaction). The A_1A_O ATP synthase has a Na^+ ion binding motif in its c subunit, and the Na^+ gradient can facilitate ATP synthesis.

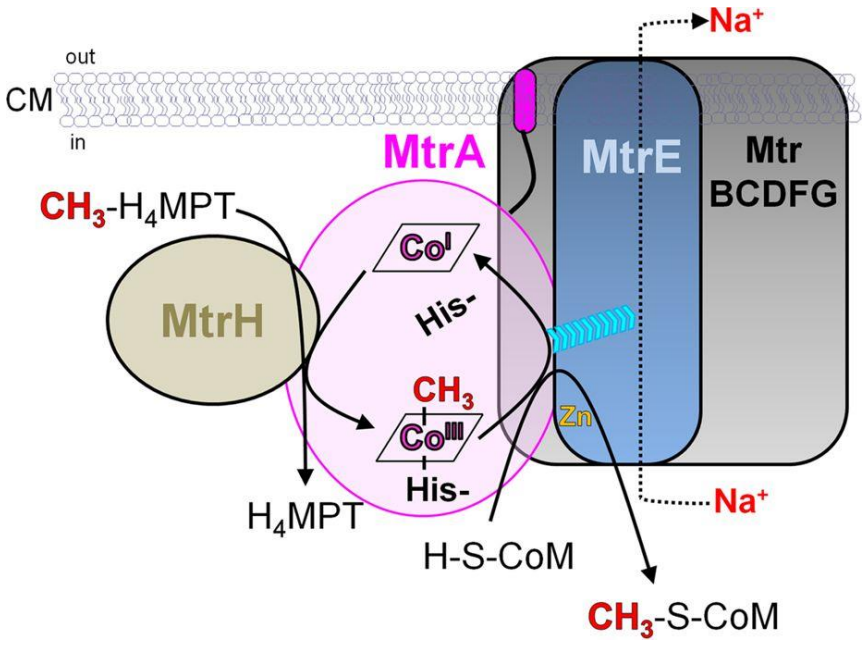

Figure 1.5 Mtr pumps sodium ions out of the cell to facilitate a sodium ion gradient (Wagner et al. 2016). (Figure reprinted with permission.)

Cytochrome-containing methanogens also have Mtr to generate a Na^+ ion gradient **(Figure 1.5)**. However, reduction of the CoM-S-S-CoB is performed by the HdrED complex, which is membrane bound and has a cytochrome b subunit that gets electrons by oxidizing dihydromethanophenazine and couples the reaction to a proton motive force. *Methanosarcina acetivorans* use an Rnf complex to transfer electrons from Fd_{red} to methanophenazine to make a proton gradient. The electrons are then transferred from reduced methanophenazine to HdrED, and generates a proton gradient.

Methylotrophic oxidation requires reduction of the cofactor F_{420} to form $F_{420}H_2$. The reoxidation of $F_{420}H_2$ is catalyzed by the $F_{420}H_2$ dehydrogenase (Fpo), which transfers electrons to methanophenazine to establish a proton gradient over the membrane and Hdr, and a sodium gradient at Mtr (Enzmann et al. 2018).

Methanogens can have biotechnological applications and be used in sewage water treatment, solids treatment and that of micro-biogas systems, which would be useful in developing countries. The primary application of methanogens is their use in the production of biogas via the digestion of organic matter, such as proteins, fats, and sugars. The production of biogas involves a 4 step process: 1) hydrolysis of the complex organic matter into simple monomers (Vavilin et al. 2008); 2) fermentation or acidogenesis of the simple monomers via oxidation into compounds, such as propionate, acetate, hydrogen and carbon dioxide; 3) acetogenesis via oxidation of the fermentation products to form mostly acetate and carbon dioxide (McInerney et al. 2008), and then 4) methanogenesis, whereby the products from acetogenesis, including methylated compounds, carbon dioxide and hydrogen, are converted to methane gas, which can be used as fuel for vehicles, the production of electricity, or the base chemical for various synthetic reactions (Ren et al. 2008). Hence biogas production relies upon a syntrophic (cross-feeding association where species live off of the product of another species) relationship between bacteria and archaea. Methanogens that can metabolize acetate are preferred in the biogas systems, which require the precise control of process parameters such as temperature (Venegas and Bartlett 2013) and ammonia concentration (Karakashev et al. 2005).

Methanogens can also be used to clean sewage water by removing pathogens from the sludge as well as reducing the amount of sludge needed to be disposed via the degradation of the complex organic matter. This process requires less energy than aerobic processes (Martin et al. 2001). Additionally, methanogens can be used to treat animal manure and slurry (liquid form)

(Holm-Nielsen et al. 2009) to reduce pathogens, thereby rendering the manure more nutrient-rich to serve as a better fertilizer (Sahlstrom 2003). When using micro-biogas systems in developing countries the natural gas can be used directly for heating and cooking (Enzmann et al. 2018). While such endeavors in developing countries would necessitate government funding, the process of making micro-biogas units, which are 10 m^3, the deforestation in certain areas would decrease because the wood is no longer needed for heating or cooking (Enzmann et al. 2018).

When complex biopolymers such as proteins, carbohydrates, and lipids are degraded by bacteria they can produce simple molecules such as amino acids, sugars, and fatty acids, respectively, via a hydrolysis reaction. The monomers can then undergo acidogenesis/ fermentation to form acetate, hydrogen and carbon dioxide, all of which can enter methanogenic pathway to produce methane as a byproduct created by methanogens (Purwantini et al. 2014). The natural source of methylamines are betaine and choline, from which betaine, an amino acid (trimethyl glycine), is derived (Purwantini et al. 2014).

S-Layer Protein

The Archaea are similar to both Eukarya and Bacteria (Rodrigues-Oliveira et al., 2017) due to the presence of genes involved in replication, transcription and translation, and genes involved in metabolic pathways, respectively, which represent both domains (Rivera et al, 1998). A characteristic distinguishing archaea from bacteria involves their cell walls, which lack the peptidoglycans that are present in bacteria. However, archaeal cell walls can contain psudomurein or methanochondroitin and, in almost all archaea, a surface layer protein defines the outermost layer of the cell. Surface layer proteins have been elucidated to possess lattice symmetries that are composed of one, two, three, four, or six protein units that form regularly spaced pores (Sletyr et al. 2007). Consequently, the S-layer protein (SLP) can serve many roles

in the archaeal cell. For instance, SLPs can act as protective coats, molecular sieves, molecule and ion traps, and they can even play significant roles in surface recognition and cell shape maintenance (Sletyr et al. 2014). The presence of negatively charged amino acids on S-layer proteins allows them to function as charge and size barriers, thereby restricting access to the periplasmic-like space (Arbing et al., 2012).

The archaeal species studied in our research, *Methanosarcina mazei*, is a methanogen that possess different morphologies based upon the salinity of its environment. In freshwater environments (low salinity), four cell aggregates are formed and each cell is surrounded by an S-layer protein, with the outermost layer being a coat of glycan moieties that form the methanochondroitin. Under marine conditions (high salinity) the *mazei* cells become isolated and surrounded only by the S-layer protein.

S-layer proteins can also be post-translationally modified with sugars, and the glycosylation pattern and density of those modifications may contribute to the proteins' stabilities in harsh environments such as high temperatures (Jarrell et al., 2014 and Wildgruber et al., 1982). Previous research has demonstrated that the S-layer proteins are composed of DUF1608 domains that are N-glycosylated with α-D-linked mannose or α-D-glucose (Francoleon et al., 2009). In other S-layer proteins, salt concentrations have been suggested to change a protein's N-glycosylation pattern, with modifications to both the type of glycan and the site of glycosylation (Abu-Qarn et al., 2007). N-glycosylation of the surface-layer protein appears to be important for maintaining a stable cell envelope and survival in hypersaline environments (Abu-Qarn et al., 2007).

Salt Adaptation

Methanosarcina mazei is a non-halophilic methanogen that is able to adapt to survival in 0.8 – 1 M sodium chloride. However, it is well documented that, for non-halophiles, salinity can induce a stress response that involves water loss, cell shrinkage and eventual cell death, if no proper processes are employed to adequately remove the excess salt from the organism (Galinski et al, 1994). *Methanosarcina mazei* are irregularly shaped cocci, arranged in sarcina (packets of eight or more cocci cells), are mesophilic (meaning that they grow at temperatures between 20 – 45^{o}C), and grow optimally at neutral pH. Microbes increase their cellular solute/ osmolyte concentration when externally exposed to elevated saline concentrations, in order to prevent excessive water efflux. At low salt (NaCl) concentrations, approximately 0.040 M, the *mazei* species exist in the aggregated form with a sugar coating known as methanochondroitin. At higher concentrations, such as 0.4 M NaCl, the cells synthesize glutamate as an osmoprotective solute; however, as the concentration of sodium chloride increases to 0.8 M, the osmoprotective solute Nε-acetyl-b-lysine is also synthesized (Pfluger et al. 2005, 2003). While the osmoprotectants are temporarily present, another means to re-establish a steady-state of ionic strength the cells includes having an influx of potassium and chloride ions into the cells, which then is followed by an influx of water.

Methanosarcina mazei, as demonstrated through various studies, adapts to high salt concentrations by transporting osmoadaptability regulators, such as glycine betaine into the cell, or accumulating glutamate or N$^{\varepsilon}$-acetyl-β-lysine (Roeßler et al., 2002). In a microarray study conducted by Pfluger and colleagues, it was confirmed that *mazei* grown under 0.8 M NaCl with 0.1 M methanol as a carbon and energy source, regulated specific genes to adapt to high salt. In *mazei* cells, MM1409 was the highest upregulated gene, being expressed 300 times stronger when grown in 0.8 M NaCl compared to 0.0385 M NaCl. MM1409 is a hypothetical protein; however, it is shown to have 81% similarity to MA0122 of *Methanosarcina acetivorans* C2A,

which is also a hypothetical protein. High salt concentrations also demonstrate a higher demand for phosphate-binding proteins. Phosphate and poly-phosphate (polyP), which can serve many functions, such as an ATP substitute and energy source, a phosphate reserve or a chelator of electron-deficient metal ions (Kornber, 1995; Kulaev et al., 2000), may be acting as counter-ions for potassium ions thatare accumulated by methanogens (Pfluger et al., 2007). The upregulation of phosphate binding proteins and polyP was indicated by the expression of the *PstC* (phosphate transporter operon), which has a functional connection with polyphosphate kinase (Ppk) (MM1375). The *ablA* and *ablB* genes are responsible for synthesis of the compatible solute N^{ε}-acetyl-β-lysine, under high salt conditions. Pfluger and colleagues used quantitative PCR analysis to show a 2-5-fold increase in expression with respect to otaC, which encodes the substrate-binding protein of a glycine betaine transporter that is relevant for salt adaptation (Roeßler et al., 2002). Interestingly enough, the expression levels of two annotated surface layer proteins, MM1589 and MM2587, was increased 5-fold in the presence of high salt conditions, possibly conferring the cell with higher osmostability (Pfluger et al., 2007). Other genes that were upregulated were the transcriptional regulators, such as MM1605, MM1882, MM0077 and MM1671; general stress response genes such as MM1254 and MM1452; and the putative ATP-driven sodium pump, MM1056 (Pfluger et al., 2007).

The saline environment of archaeal cells can cause shock to the cells; however, they can adapt to the new extracellular saline conditions via osmoadaptation and osmoregulation, which is adapting to external osmotic pressures, and the development of mechanisms to achieve this osmoadaptation (Roberts, 2004). Under hypo-osmotic conditions, in which the external cellular environment has low salt concentration (greater water pressure outside versus inside the cell, causing water to flux into the cell), the cells respond by first sensing the change in water pressure, opening aquaporin water channels as well as ion, such as the potassium (K+) channels, and the synthesis and accumulation of osmolytes that are used to re-establish a

steady-state of the cells (Roberts, 2004). A similar pathway for osmoadaptation and osmoregulation is used, for cells exposed to hyper-osmotic environments, except the extracellular environment has high salt concentration (lower water pressure outside versus inside the cell, causing water to efflux out of the cell).

From sudden changes in osmolarity, such as during hypo- or hyper-osmotic shock, aquaporins can facilitate the large flux of water across the membrane of the archaeal cell. Once water rushes into or out of the cell, respectively and K+ channels open. During hyperosmotic shock, NaCl concentrations are high on the outside of the cell, water rushes out of the cell, and K+ ions then enter the cell via mechanosensitive channels to create a balance of positively charged ions; water follows the K+ ions into the cell being internalized by the aquaporins. The K+ ions then decrease in concentration to a steady state environment. This flux of K+ ions is coupled to osmolytes being increased in concentration within the cell. There are 3 types of organic solutes found commonly in archaeal cells are: 1) zwitterions (e.g., amino acids such as glycine betaine or L-alpha-glutamate); 2) neutral solutes; and 3) anionic solutes. The zwitterion glycine betaine is actively transported into the cell to create a balance in solutes under hyper-osmotic conditions, rather than being synthesized de novo. Under low external salt conditions, alpha-glutamate osmolytes are the dominant solutes; however at extracellular NaCl concentration > 0.5 M, N-epsilon-acetyl-beta-lysine zwiterionic solute dominates.

Nonetheless, the major types of osmolytes in archaea are anionic solutes, which can be represented by the addition of negatively charged groups to carbohydrates and polyols that frequently exist within eukarya and bacteria. Osmolytes offer a protective property towards proteins in the folded state and raises the melting temperature via stabilization of the proteins (Timasheff, 1992). Stabilization of the proteins via osmolytes occurs via two mechanisms: 1) osmolytes have a solvophobic effect on the protein and destabilizes the unfolded protein more

than water does, so proteins prefer to stay in the folded state in the presence of osmolytes, and 2) osmolytes maintain the equilibrium between bulk water and water adjacent to the macromolecule, preferring water in the bulk position, while the osmolytes are at the protein interfaces. Furthermore, osmolytes can reduce pressure denaturing and the rate of proteolysis of enzymes. Even though the exact biosynthetic pathway for osmolytes is not known, osmolyte synthesis occur after the end of the extended lag phase, once the cell has been exposed to hyper-saline environments. After the accumulation of osmolytes, the synthesis of stress proteins subsequently follows. Examples of stress proteins within the cell include heat shock proteins and chaperonins, which increase in concentration during heat and osmotic shock in order to refold misfolded proteins.

Quantitative Proteomics

Quantitative proteomics relies upon principles of relative or absolute quantification. Relative quantification determines the ratio of peak area of a specific peptide under 2 or more different conditions, and hence determines the relative abundance of a protein. Absolute quantitation can be used to determine the exact amount of a protein within a sample through the use of an internal standard, such as a synthetic peptide that is similar to the endogenous proteins within the sample and spiked into the mixture or a radiolabeled amino acid that is used in the growth medium of the cell and incorporated into the proteins (Silva et al. 2006). Consequently absolute quantitation allows for the intracellular and intercellular determination of protein abundance.

Absolute quantitative techniques can involve both a labelled and a label-free approach. The labeled approach is used for absolute quantitation in the application of the isobaric tags for relative and absolute quantitation (iTRAQ), in which the N-terminus and amine side chains are tagged with an iTRAQ reagent. Even though the labelled approach is common in the proteomics field, it can be a time-consuming and cost-intensive process. Therefore, the label-free approach

has been employed for absolute quantitation, whereby the known concentration of a synthetic tryptic digested peptide is spiked into the analyte peptide mixture. Through the use of this internal standard, a universal signal response factor can be determined in units of counts per mole of protein. Silva and colleagues demonstrated a linear relationship between the average mass spectrometry signal of the three most intense peptide ions and the amount of the protein. The amount of protein is calculated by determining the counts (average MS signal of the three most intense peptides) of the unknown protein and dividing this value by the universal signal response factor of the internal standard.

Data-Dependent versus Data-Independent Acquisition

Data-dependent acquisition (DDA) monitors the intensity of peptides then isolates and fragments precursor ions in the order of decreasing intensity, with a dynamic exclusion window preventing a previously MS2 analyzed peptide from being re-fragmented. However, by using the data-independent acquisition (DIA) approach with elevated mass spectrometer (MS^E) technology, all of the peptides within a specific mass range and that are above a specific threshold are exposed to fragmentation at once. LC-MS^E alternates between low-energy collisions in the MS mode and high-energy collision energy in the MS^E mode. The advantage of DIA over DDA is that the former provides a more complete picture of the proteins involved in various biological processes. In our instrument, the Protein Lynx Global Server (PLGS) software is subsequently used to align the precursor and product ions of each peptide according to their retention time. The precursor and product fragment peptide ions must have identical retention times.

Prior to the identification and quantification of proteins using data-independent acquisition, data-dependent acquisition was used most commonly. DDA relied upon the first mass analyzer to select ions for fragmentation to further identify the peptides within a peptide mixture. However, a

major limitation of data-dependent acquisition was that only peptides with the highest intensity were being selected for fragmentation, therefore diminishing the dynamic range of proteins being sampled for identification and quantification as well. Because, low abundant peptide ions were being excluded from analysis, Venable and colleagues (Venable et al., 2004) developed data-independent acquisition, whereby the first mass analyzer serves only to scan the complete spectrum using an isolation window of, for instance, 10 *m/z* for a specified mass range, and fragments all of the peptides within the isolation window for data-independent acquisition. Furthermore, peptides can be more easily detected in MS/MS mode than in MS mode alone, and therefore have a higher signal-to-noise ratio, thereby increasing the dynamic range of the mass spectrometer, and peptide specificity (correctly matching fragment ions to the precursor ions to accurately identify the peptides). By generating a greater amount of fragment ions in DIA, the ion intensities can be averaged to produce more accurate quantitative measurements than DDA.

In 2004, when Venable and colleagues compared the effectiveness of DIA to DDA, they used trypsin-digested proteins from the soluble fraction of yeast lysates to determine the qualitative facets of analysis. Interestingly enough, the number of peptide and protein identifications made by DIA and DDA were comparable in their study, thereby demonstrating that DIA is on par with DDA, and may have even identified more peptides/ proteins if the researchers had the adequate tools to reliably extract information from the multiplexed spectra generated in DIA. In order to validate the quantitative effectiveness of DIA, Venable and colleagues utilized Multi-dimensional Protein Identification Technology (MudPIT) for the analysis of trypsin-digested unlabeled and N15-labeled yeast whole-cell lysates at two different ratios (1:1 and 10:1 unlabeled: labeled ratio). MudPIT eliminates the need for gel fractionation (e.g., 1D and 2D gel electrophoresis), and instead allows for many proteins to be digested and generate an enormous amount of peptides, which are then separated by liquid chromatography before mass spectrometry

analysis. It was discovered that DIA analyzed peptides (i.e., peptides quantified directly from tandem mass spectra rather than being pre-selected in MS1 mode) had an average of 350% increase in signal-to-noise ratio. Furthermore, the dynamic range of the mass spectrometer appeared to be more linearly correlated to the signal-to-noise ratio in DIA than DDA. This data revealed that DDA is more prone to systematic error than DIA.

Benefits of Using Data-Independent Acquisition

After analyzing the proteome of *C. elegans* to determine protein abundances during its two different phases of development (eggs and young adults) by using DIA, Venable and colleagues were able to quantify 333 proteins. Furthermore, they were able to corroborate the tandem mass spectrometry-determined protein abundance levels for 3 proteins by western blot analysis, thereby further validating their DIA approach.

Nonetheless, even though DIA proved itself to be a valid and reliable technique for identification and quantification of peptides and subsequently proteins, it does pose some limitations, which include 1) reduced mass accuracy of the precursor ions, possibly caused by a large isolation window that may contain product ions from non-specific precursor ions (ones that are not of interest), which makes it more challenging to match the correct fragment ion to the precursor ion reliably, and increasing the chances for false positive identifications; and 2) convolution caused by the simultaneous isolation and fragmentation of isobaric peptides (peptides that have identical *m/z* ratio or mass). However, these limitations are not only outweighed by the quantitative power of DIA, they are resolved by implementing strict spectral filtering requirements, that include using 2 or more peptides per locus, and utilizing the inherently larger dynamic range for peptides in a complex mixture, which produces ion series that can accurately be identified and quantified, respectively. Also, if a precursor region is sufficiently sampled, the mass spectrometer will be able to obtain tandem mass spectra of one of the peptides, as long

as the “pseudo-isobaric” peptides do not perfectly co-elute. In summary, DIA proved to be qualitatively on par with DDA and quantitatively superior to DDA, demonstrating higher signal-to-noise ratios, dynamic range, and specificity of peptides analyzed (Venable et al., 2004).

Transition from Stable Isotope Labeling to Label-Free Approach for Quantitation

Quantitative proteomics has relied upon stable-isotope labelling as a popular means to determine the relative abundance of proteins analyzed under two different environmental conditions. The three major means of performing stable-isotope labelling involve chemical, metabolic, and enzymatic modifications. However, such processes can be cumbersome, and therefore, alternative methods have been created to quantitatively assess the global protein profile of an organism. Hence, label-free techniques can be used by spiking a known concentration of any peptide(s) (digested or undigested) into a protein/ peptide mixture, and using chromatographic and mass spectrometer information to quantify the proteins identified relative to the spikes.

Relative Quantitation using Stable-Isotope Labeling

In order to obtain relative quantification of proteins/ peptides via stable isotope labeling, identical peptides from 2 different experimental conditions will be labeled (one being light labeled and the other being heavy labeled). The 2 identical peptides will then be combined into one solution, with their only distinction being the isotope labeling (light vs. heavy). The isotope labeled peptides will have the same retention times in the liquid chromatography system, and different *m/z* ratios in the mass spectrometers. In fact, when analyzed in the MS mode, the 2 identical peptides will have a mass difference (shift in mass) that correlates to the difference in their stable isotope labeling; one will see the *m/z* of the light and that of the heavy in the same spectra. The ratio of the intensity of the 2 identical peptides (one light and the other heavy) will determine the relative abundance of the identical peptides under 2 different experimental

conditions. When using absolute quantification for proteins via stable isotope labeling a standard of known concentration in the form of a synthetic peptide, intact protein, or peptide concatemer is labeled instead of the endogenous protein/peptide, and then spiked into the peptide/ protein mixture. The labeled peptide standard will have a sequence similar to the endogenous peptide/ protein being measured, and the ratio of the endogenous peptide to the labeled standard is being used to determine the absolute quantity of the peptide/ protein.

Relative Quantitation using Label-Free Approach

When using the label-free approach for relative quantification, quantification can be based upon peak intensity. For instance, instead of labeling identical peptides with different stable isotopes, and then combining the samples for simultaneous mass spectral analysis, each sample, which was generated from 2 different experimental conditions, is introduced separately to the mass spectrometer. The peptide peak intensities from the 2 different conditions are then compared to each other to determine their relative abundance. On the other hand, when using the label-free approach for absolute quantification, whereby a peptide standard of known identity and concentration is spiked into the experimental peptide mixture, peak intensities or spectral counts can be used. With peak intensity, the intensity of the 3 most abundant peptides ascribed to the identified protein are averaged and then compared to the average of the 3 most abundant peptides from the protein standard. When comparing 3 means for assessing protein abundance and their correlation to known values: the percentage of the protein's sequence recovered from the peptides analyzed, the number of peptides identified, and spectral counts, spectral count was found to have the highest positive correlation. Spectral count measures the number of MS/MS spectra recorded and matched to a specific protein. Previous research demonstrated that 1) high abundance proteins generate more peptides, and hence there would be more MS/MS spectra, which provides the amino acid sequence of each isolated peptide; and 2) larger proteins (ones with more amino acid residues) have more peptides that are detected in MS

mode, which will eventually generate more MS/MS spectra as well. While such statistics indicate that the label-free approach may be error prone for low-abundant proteins (proteins that may even have fewer than 3 peptides that can identify them), or proteins that may actually be identical in amount however have fewer amino acid residues than a larger protein, and thereby producing fewer peptides, these errors can be corrected via normalization with observable peptides. In the case of normalization with observable protein, a factor known as the protein abundance index (PAI) can be used. PAI is calculated by dividing the number of actual peptide ions for a unique protein generated in the MS mode by the number of theoretical peptides expected for that unique protein. Furthermore, an abundance index can be used for normalization by dividing the MS/MS spectral count by the number of observable peptides. For normalization with protein size, spectral count is divided by protein molecular weight (Kito et al, 2008).

Benefits and Limitations of Stable-Isotope Labeling and Label-free Approach

Relative and absolute quantitative proteomics can be performed using a label, primarily the stable-isotope labeling, or a label-free approach, both of which have their advantages and limitations, depending upon the purpose of the experiment. When using stable-isotope labeling, a critical difference between relative and absolute quantification is that the peptides within the sample mixture are being measured when using relative quantitative techniques, while on the other hand, an external synthetic peptide standard is being labeled when using absolute quantitative techniques. Furthermore, another stark difference between the two quantification techniques is that when using absolute quantification, the concentration of the stable isotope-labeled synthetic peptide that is spiked into the sample peptide or protein mixture (before digestion) is known. When using stable isotopes for labeling, the procedure can be performed chemically, enzymatically, or metabolically. Chemical modification involves using C13 or N15 isotopes; enzymatic modification uses ^{18}O- labeling; and metabolic modification involves

cultivating cells in a medium that possesses stable isotopes of amino acids that are incorporated into the proteins during the growth of the organism.

Absolute Quantification Achieved Through Bio-Informatic Tools

Silva and Geromanos showed that bioinformatics software could reduce the complexity of LC/MS data into a list of simplified components (Silva et al. 2006). The software uses both accurate mass measurements as well as liquid chromatography retention time parameters, in addition to ion intensities of precursor and product peptide ions to determine the quantity and identity of a protein. Specifically, accurate mass, retention time (AMRT) components were used for absolute quantification. While Radulovic and colleagues initially used nominal mass (integer mass of the most abundant naturally occurring isotope) measurements to sort the peptide ions (Radulovic et al., 2004), Silva and colleagues determined that nominal mass sorting would be limiting, because many unique peptides would be inaccurately binned together due to them having the same integer mass. The AMRT components that are used to quantify the proteins identified include 1) weight-averaged monoisotopic mass and charge state, 2) mass deviation, 3) deisotoped and charge-state reduced sum intensity, 4) chromatographic peak area, 5) intensity deviation, 6) retention time of the apex (highest point of intensity) of the peptide peak, and 7) start and stop time of ion detection. These components are determined for both the precursor and product ions, which are then matched to each other by retention-time alignments.

Algorithms for the bioinformatics software were used for 1) ion detection in order to deisotope and charge-state reduce the *m/z* detections to a monoisotopic m/z for each of the LC/MS data, 2) clustering of the peptide components by mass and retention time of chemically identical components in replicate injections from the same sample or multiple samples, and 3) data normalization to a set of AMRT components from standards known to be constant in all of the different samples and statistical analysis using a student's *t-test* for each of the binary

comparisons. The data selection process involved using a set of statistical parameters, such as applying a replication requirement in which AMRTs had to be present in at least 2 out of the 3 injections for each condition; the coefficient of variation of the normalized intensities of an AMRT was less than or equal to 30%; and the mass precision had to be less than 10 ppm (Silva et al. 2004). While Silva and colleagues used the Expression Informatics tool to perform the quantification of the proteins in their study of 6 standards spiked into a serum matrix, we used MassLynx as our ion detection, clustering and statistical analysis tool. MassLynx is equipped with all of the features attributed to the Expression Informatics software, and was used to generate AMRT components for quantification of the identified proteins. Furthermore, in order to ensure the highest quality of data for proteins identified and quantified, we selected proteins that were identified in at least 3 out of 4 technical replicate injections, with amount of protein on column (fmol) having a coefficient of variation of less than or equal to 30%, and a mass accuracy of less than approximately 10 ppm.

Conclusion

Methanosarcina mazei are methane-producing microorganisms that play a pivotal role in the global carbon cycle by facilitating the final conversion of organic waste matter into the natural gas methane. The goal of this research is to further elucidate the process of methane production in *Methanosarcina mazei* by quantitatively analyzing the proteins that play a significant role in *M. mazei*'s ability to adapt to different substrate growth conditions, specifically growth on various methylotrophic substrates, such as methanol, mono-, di-, and tri-methylamine. In the following chapters, I describe how the proteins, both in type and in quantitative levels, change in response to growth on each of the 4 different aforementioned methylotrophic substrates, when *M. mazei* cells are harvested during the mid-log, also known as the exponential, phase of growth. Afterwards protein type and quantitative levels are compared when *M. mazei* cells are harvested during the stationary phase of growth, when it is expected

for the cells to have a constant rate of production and death. Furthermore, due to the outermost structure of the *M. mazei* cells changing under fresh water and saline conditions, we also determined the major proteins of *M. mazei* cells that were grown in methanol under relatively high and low salt concentrations. This research can be used to mitigate methane production in methanogens, such as *M. mazei*, by targeting the proteins identified as having high levels within the cells under different phases of growth (i.e., mid-log and stationary).

References

1. Abu-Qarn, M.; Yurist-Doutsch, S.; Giordano, A.;Trauner, A.; Morris, H.R.; Hitchen, P.; *Haloferax volcanii* AglB and AglD are involved in N-glycosylation of the S-layer glycoprotein and proper assembly of the surface laer. *J. Mol. Biol.* **2007,** *14,* 1224-1236.
2. Arbing, M.A.; Chan, S. ; Shin, A.; Phan, T.; Ahn, C.J.; Rohlin, L.; Gunsalus, R.P. Structure of the surface layer of the methanogenic archaean *Methanosarcina acetivorans*. *Proc. Natl. Acad. Sci. U.S.A.* **2012,** *109,* 11812-11817.
3. Buan, N.R. Methanogens: pushing the boundaries of biology. *Emerging Topics in Life Sciences*, **2018**. *2,* 629-646.
4. Chen, S.; Xing, D.; Call, D.F.; Logan, B.E. Direct biological conversion of electrical current into methane by electromegthanogenesis. *Environ Sci Technol.* **2009,** *43,* 3953-3958.
5. Choi, O.; Sang, B-I. Extracellular electron transfer from cathode to microbes: application for biofuel production. *Biotechnol Biofuels.* **2016,** *9,* 11.
6. Deppenmeier, U. The membrane-bound electron transport system of Methanosarcina species. *J Bioenerg Biomembr.* **2004,** *36(1),* 55-64.
7. Ding, Y. H. R.; Zhang, S. P.; Tomb, J. F.; Ferry, J. G. Genomic and proteomic analyses reveal multiple homologs of genes encoding enzymes of the methanol: coenzyme M methyltransferase system that are differentially expressed in methanol and acetate-grown *Methanosarcina thermophile. FEMS Microbiol. Lett.* **2002,** *215,* 127-132.
8. Enzmann, F.; Mayer, F.; Rother, M.; Holtmann, D. Methanogens: biochemical background and biotechnological applications. *AMB Express.* **2018,** *8:1,* 1-22; doi:10.1186/s13568-017-0531-x.
9. Francoleon, D.R.; Boontheung, P.; Yang, Y.; Kin, U.; Ytterber, A.J.; Denny, P.A. Loo, J.A.; Gunsalus, R.P.; Loo, R.R. S-layer, surface-accessible, and concanavalin A binding proteins of *Methanosarcina Acetivorans* and *Methanbosarcina mazei. J. Proteome Res.* **2009,** *8,* 1972-1982.

10. Galinski, E.A.; Truper, H.G. Microbial behaviour is salt-stressed ecosystems. *FEMS Microbiology Review.* **1994,** *15(2-3),* 95-108.
11. Holm-Nielsen, J.B.; Al Seadi, T.; Oleskowics-Popeil, P. The future of anaerobic digestion and biogas utilization. *Bioresour Technol.* **2009,** *100,* 5478-5484.
12. Jarrell, K.F.; Ding, Y.; Meyer, B.H.; Albers, S.-V.; Kaminski, L.; Eichler, J. N-linked glycosylation in *Archaea:* a structural, functional, and genetic analysis. *Microbiol. Mol. Biol. Rev.* **2014,** *78,* 304-341.
13. Karakashev, C.; Batstone, D.J. Angelidaki, I. Influence of environmental conditions on methanogenic compositions in anaerobic biogas reactors. *Appl Environ Microbiol.* **2005,** *71,* 331-338.
14. Kito, K.; Ito, T. Mass spectrometry-Based Approaches Toward Absolute Quantitative Proteomics. *Current Genomics.* **2008,** *9,* 263-274.
15. Kornber, A. Inorganic polyphosphate: toward making a forgotten polymer unforgettable. *J Bacteriol.* **1995,** *177(3),* 491-496.
16. Kulaev, I.; Kulakovskaya, T. Polyphosphate and Phosphate Pump. *Annual Review of Microbiology.* **2000,** *54,* 709-734.
17. Martin, I.; Pidou, M.; Soares, A.; Judd, S.; Jefferson, B. Modelling the energy demands of aerobic and anaerobic membrane bioreactors for waste-water treatment. *Environ Technol.* **2011,** *32,* 921-932.
18. McInerney, M.J.; Struchtemeyer, C.G.; Sieber, J.; Mouttaki, H.; Stams, A.J.; Schink, B.; Rohlin, L.; Gunsalus, R.P. Physiology, ecology, phylogeny, and genomics of microorganisms capable of syntrophic metabolism. *Ann NY Acad Sci.* **2008,** *1125,* 58-72.
19. Patil, S.A.; Hagerhall, C.; Gorton, L. Electron transfer mechanisms between microorganisms and electrodes in bioelectrochemical systems. *Bioanal Rev.* **2012,** *4*, 159-192.
20. Pfluger, K.; Ehrenreich, A.; Salmon, K.; Gunsalus, R. P.; Deppenmeier, U.; Gottschalk, G.; Muller, V. Identification of genes involved in salt adaptation in the archaeon *Methanosarcina*

mazei Go1 using genome-wide gene expression profiling. *FEMS Microbiology Letter.* **2007,** *277(1),* 79-89.

21. Pfluger,K.; Baumann,S.; Gottschalk, G.; Lin, W.; Santos, H.; Muller, V. Lysine 2,3-aminomutase and beta-lysine acetyltransferase genes of methanogenic archaea are salt induced and are essential for the biosynthesis of N(epsilon)-acetyl-beta-lysine and growth at high salinity. *Appl. Environ. Microbiol.* **2003,** *69,* 6047-6055.
22. Pluger K.; Wieland, H.; Muller, V. Osmoadaptation in methanogenic archaea: recent insights from a genomic perspective. In: Gunde-Cimeerman N, Oren A, Plemenitas A (eds) Adaptation of life in high salt concentrations in *Archaea, Bacteria, and Eukarya. Springer, Dordrecht*. **2005,** 241-251.
23. Purwantini, E.; Torto-Atalibo, T.; Lomax, J.; Setubal, J.C.; Tyler, BM.; Mukhopadhyay, B. Genetic resources for methane production from biomass described with the Gene Ontology. *Frontiers in Microbiology.* **2014,** *5:634,* 1-18.
24. Radulovic, D.; Jelveh, S.; Ryu, S.; Hamilton, T.G., Foss, E.; Mao, Y.; Emil, A. Informatics platform for global proteomic profiling and biomarker discovery using liquid-chromatography mass spectrometry. *Mol. Cell. Proteomics.* **2004,** *3*, 984-997.
25. Ren, T.; Patel, M.; lok, K. Steam cracking and methane to olefins: energy use, CO2, emissions and production costs. *Energy.* **2008,** *33,* 817-833.
26. Rivera, M.C.; Jain, R.; Moore, J.E.; Lake, J.A. Genomic evidence for two functionally distinct gene classes. *Proc Natl Acad Sci U.S.A.* **1998,** *95,* 6239-6244.
27. Roberts, M. F. Osmoadaptation and osmoregulation in archaea: update 2004. *Front Biosci.* **2004,** *9,* 1999-2019.
28. Rodrigues-Oliveira, T.; Belmok, A.; Vasconcello, D.; Schuster, B.; Kyaw, C.M. Archaeal S-Layers: Overview and Current State of the Art. *Front Microbiol.* **2017,** *8,* 2597.

29. Roeßler, M.; Pfluger, K.; Flach, H.; Lienard, T.; Gottschalk, G.; Muller, V. Identification of a Salt-Induced Primary Transporter for Glycing Betaine in the Methanogen *Methanosarcina maxei* Go1. *Appl. Environ. Microbiol.* **2002,** *65(5),* 2133-2139.

30. Sahlstrom, L. A review of survival of pathogenic bacteria in organic waste used in biogas plants. *Bioresour Technol.* **2003,** *87,* 161-166.

31. Silva, J.C.; Denny, R.; Dorschel, C.A.; Gorenstein, M.V.; Kass, I.J.; Li. G-Z.; McKenna, T.; Nold, M.J.; Richardson, K.; Young, P.; Geromanos, S.J. Quantitative proteomic analysis by accurate mass retention time pairs. *Anal. Chem.* **2004,** *77*, 2187-2200.

32. Silva, J.C.; Gorenstein, M.V.; Li, G-Z.; Vissers, J.P.C.; Geromanos, S.J. Absolute Quantification of Proteins by LCMSE. *Molecular and Cellular Proteomics.* **2006,** *122*, 144-156.

33. Sleytr, U.B.; Huber, C.; Ilk, N.; Pum, D.; Schuster, B.; Egelseer, E.M. S-layers as a tool kit for nanobiotechnological applications. *FEMS Microbiol Lett.* **2007.** *267,* 131-144.

34. Sleytr, U.B.; Schuster, B.; Egelseer, E.-M.; Pum, D. S-layers: principles and application. *FEMS Microbiol Rev.* **2014,** *38,* 823-864.

35. Sorgenfrei, O.; Muller, S.; Pfeiffer, M.; Sniezko, I.; Klein, A. The [NiFe] hydrogenases of Methanococcus voltae: genes, enzymes and regulation. *Archives of Microbiology.* **1997,** *167(4),* 189-195.

36. Sydow, A.; Krieg, T.; Mayer, F.; Schrader, J.; Holtmann, D. Electroactive bacteria – molecular mechanisms and genetic tool. *Appl Microbiol Biotechnol.* **2014,** *98,* 8481-8495.

37. Timasheff, S. N. A Physiochemical Basis for the Selection of Osmolytes by Nature. *Water and Life.* 70-84.

38. Vavilin, V.A. Fernandez, B.; Palatsi, J.; Flotats, X. Hydrolysis kinetics in anaerobic degradation of particulate organic material: an overview. *Waste Manag.* **2008,** *28,* 939-951.

39. Veit, K.; Ehler, C.; Schmitz, R. A. Effects of Nitrogen and Carbon Sources on Transcription of Soluble Methyltransferases in *Mehtanosarcina mazei* Strain Go1. *Journal of Bacteriology.* **2005,** *187(17),* 6147-6154.

40. Venable, J.D.; Dong, M.-Q., Wohlschlegel, J.; Dillin, A.; Yates, J.R. Automated approach for quantitative analysis of complex peptide mixtures from tandem mass spectra. *Nat. Methods.* **2004,** *1,* 39-45.

41. Venegas, C.; Bartlett, J. Anaerobic digestion of luminaria digitate: the effect of temperature on biogas production and composition. *Waste Biomass Valorization.* **2013,** *4,* 509-515.

42. Villano, M; Aulenta, F.; Ciucci, C.; Ferri, T.; Giuliano, A.; Majone, M. Bioelectrochemical reduction of CO2 to CH4 via direct and indirect extracellular electron transfer by hydrogenophilic methanogenic culture. *Bioresour Technol.* **2010,** *101,* 3085-3090.

43. Wagner,T; Ermler, U.; Shima, S. MtrA of the Sodium ion pumping methyltransferase binds cobalamin in a unique mode. *Nature Scientific Reports*. **2016**, 1-10; doi: 10.1038/srep28226

44. Welte, C.; Deppenmeier, U. Bioenergetics and anaerobic respiratory chains of aceticlastic methanogens. *Biochimica et Biophysica Acta.* **2014,** *1837*, 1130-1147.

45. Wildgruber, G.; Tomm, M.; Konig, H.; Ober, K.; Richiuto, T.; Stetter, K.O. *Methanoplanus limicola,* a plate-shaped methanogen representing a novel family, the methanoplanaceae. *Arch. Microbiol.* **1982,** *132,* 31-36.

46. Zhen, G.; Lu, X.; Kobayashi, T.; Kumar, G.; Xu, K. Promoted electromethano-synthesis in a two-chamber microbial electrolysis cells (MECs) containing a hybrid biocathode covered with graphite felt (GF). *Chem Eng J.* **2016,** *284,* 1146-1155.

47. Zinder, S. H.; Sowers, K. R.; Ferry, J. G. *Methanosarcina thermophila* sp. nov., a Thermophilic, Acetotrophic, Methane-Producing Bacterius. *International Journal of Systematic Bacteriology.* **1985,** *35(4),* 522-523.

CHAPTER 2

Methanosarcina mazei Gö1 Proteomic Regulation During the Mid-log Stage of Growth

Introduction

Methanosarcina mazei are mesophilic archaea that grow under anaerobic conditions and produce methane via an energy-conservation process, known as methanogenesis, which is the terminal step in the degradation of organic matter during the carbon cycle (Deppenmeier et al. 2007). While *Methanosarcina* are versatile in their ability to grow on numerous substrates, such as methanol and other compounds, such as monomethylamine (MMA), dimethylamine (DMA), and trimethylamine (TMA), it is more thermodynamically favorable for the cells to grow on methanol ($\Delta G'^{o}$ = -106 kJ/ mol methane) than the methylamines ($\Delta G'^{o}$ = -77 kJ/ mol methane). Therefore, the lower free energy change in the methylamines necessitates *M. mazei* cells to have an efficient energy-conserving system to deal with the thermodynamic limitations (Deppenmeir et al. 2004). Consequently, such a system is speculated to be created via an electrochemical ion (proton and sodium) gradient. Thus, the proton gradient is generated when the $F_{420}H_2$ dehydrogenase oxidizes $F_{420}H_2$ to F_{420} and reduces the electron carrier methanophenazine, while translocating 2 protons out of the cytoplasm into the periplasmic-like space of the cell (Baumer et al. 2000). A sodium gradient is created when the methyltetrahydromethanopterin:coenzyme M methyltransferase transfers a methyl group from methyltetrahydromethanopterin to coenzyme M, thereby facilitating the transport of sodium ions across the cytoplasmic membrane (Deppenmeier et al. 2007). Both the proton and sodium gradients that drive the synthesis of ATP via the A_1A_0 ATP synthase ATP synthesis in methanogens are driven by ion-gradient phosphorylation, not substrate-level phosphorylation, and only 2 reaction pathways are exergonic enough to establish the electrochemical gradient (Schlegel and Muller, 2013). One is via the Mtr enzyme, which facilitates the translocation of sodium ions out of the cell of all methanogens, while transferring a methyl group from tetrahydromethanopterin to the thiol form of coenzyme M (Schlegel and Muller, 2013). The second reaction pathway is a bit more sophisticated in methanogens such as *Methanosarcina mazei* that contain cytochromes, which are membrane bound ion carriers that function in an

archaeal electron transport chain (Schlegel and Muller, 2013). If hydrogen is the electron donor, a membrane bound hydrogenase, known as Vho (F_{420} non-reducing hydrogenase), takes the electrons and transfers them to the coenzyme M- coenzyme B heterodisulfide, which is reduced by the heterodisulfide reductase (Hdr) (Schlegel and Muller, 2013). The Hdr also pumps protons out of the cell, thereby creating an electrochemical gradient that then allows another membrane bound energy converting hydrogenase, Ech, to reduce ferredoxin, which is responsible for converting carbon dioxide to formylmethanofuran in the hydrogenotrophic pathway (Schlegel and Muller, 2013). While most ATP synthases / ATPases use protons as coupling ions, some are able to also use sodium ions (Schlegel and Muller, 2013). Furthermore the binding of the sodium ion requires five amino acids, 2 of which, glutamic acid and serine, are well conserved (Schlegel and Muller, 2013).

The goal of this stage of the research project is to examine how protein levels in *mazei* are affected by the medium within which they are grown during the mid-log phase of the cell cycle. The mid-log phase is specifically chosen because it is the phase when the cells are actively growing and demonstrate an exponential rate of growth, after the lag phase, when the cells are becoming acclimated to their respective growth conditions.

Transcriptomic Studies on *M. mazei*

Transcriptomics and DNA microarray analysis are the most frequently used tools to attain a better understanding of methanogenic archaea, such as *Methanosarcina mazei.* The significance of transcriptomic studies has been to identify mRNAs that are in high abundance in methanogenic cells under various environmental conditions (Browne et al. 2013). For instance, in *Methanosarcina barkeri*, one-third of the most abundant mRNAs grown on methanol substrate were methanogenesis-related (Culley et al. 2006). Furthermore transcriptomics was used to elucidate the differential optimization of methanogenesis in a substrate-dependent

manner in *Methanosarcina mazei* Gö1 (Hovey et al. 2005) and *Methanosarcina acetivorans* (Li et al. 2007). However, it has been appropriately noted that minimal correlation exists between absolute levels of mRNA abundance and protein levels (Lange et al. 2007 and Xia et al. 2006). Instead, the global response of the organism with respect to two different environmental conditions, as indicated by transcript levels, is a more improved predictor of protein level. Nonetheless, mRNA abundance studies should not be used in isolation to study the ecological and phenotypic effect of environmental variation on the methanogens. For example, post-transcriptional modifications can alter protein levels and even protein activity, and therefore diminish any correlation between mRNA and protein abundance. The most common post transcriptional modifiers are small RNAs (sRNAs), which may interact with mRNAs at the 5' untranslated region (5'UTR), thereby causing up- or down-regulation of mRNA and impact mRNA turnover, or they may even bind to proteins and influence their activities (Sonnleitner et al. 2009). In *Methanosarcina mazei* it was demonstrated that $sRNA_{162}$ binds the 5'UTR of the MM_2241 transcript, thereby inhibiting the binding of ribosomes necessary for the translating MM_2241 (Jager et al. 2012). The 3'UTR site is also important because polyadenylation of the 3' end of the mRNA controls mRNA degradation in some methanogens (Portnoy et al. 2006). Hence, there is great significance for proteomic studies to elucidate the mechanism of how methanogens regulate and optimize their metabolism in different growth environments.

Transcriptomics is often touted as a silver bullet for determining the protein levels within an organism and for comparing protein levels under two or more different biological conditions. However, designating the transcriptome as a surrogate proteome can be misleading and impractical when determining how environmental stress affects the phenotype of an organism. While useful for identifying genes that are linked to, or that act as co-regulators in the response to stressors, transcriptional profiling is best considered to complement proteomic analyses for

determining how different environmental factors affect the fitness and phenotype of the organism in question (Feder et al, 2005).

Li and colleagues (Li et al, 2007) used a complimentary approach to determine the effect of growing *Methanosarcina acetivorans* under methanol versus acetate conditions. By utilizing the ^{14}N and ^{15}N metabolic labelling of cells, protein abundance ratios were quantitatively measured, while gene expression ratios were determined by DNA microarray analyses. Of the 1081 proteins quantified (with their identity determined by two or more peptide pairs), 255 of those proteins were differentially abundant proteins, 184 proteins were upregulated in methanol grown cells, versus the 71 proteins that were upregulated in acetate grown cells. The microarray genetic analysis of the *M. acetivorans* cells identified 410 differentially expressed genes, with 210 genes being expressed higher in cells grown in methanol, versus the 200 genes that were expressed higher in acetate-grown cells. Out of the 255 differentially abundant proteins identified by proteomics, 88 of their encoding genes indicated a differential expression of 2.5-fold or greater. This data translated to 63 genes being consistently identified as overexpressed by both protein and microarray analyses when cells were grown in methanol, and 17 genes being identified as overexpressed by both analyses when cells were grown in acetate (Li, L. et al, 2007).

Due to the greater abundance and upregulation of proteins and genes, respectively, for *M. acetivorans* grown in methanol, Li and colleagues speculate that both DNA and proteins serve regulator functions that are specific for growth on varying substrates. For example, formyl-methanofuran dehydrogenase (encoded as MA0304-0309) functions in the conversion of methanol to methane, and is found in greater abundance in methanol-grown cells. Furthermore, while approximately 3 times more energy is present for *Methanosarcina* cells grown on methanol ($\Delta G^{o'}$ = -106.5 kJ) versus cells grown on acetate ($\Delta G^{o'}$ = -36 kJ), not much information

is available about the mechanism of gene regulation in a substrate-dependent manner, hence the significance of this study in combining the proteomic and DNA microarray analyses to determine abundance and upregulation of proteins and genes, respectively in methanol versus acetate grown cells. Li's study suggests the significance of genetic and proteomic regulatory systems that are specific for each substrate in *Methanosarcina* cells (Li, L. et al, 2007). Therefore, the purpose of this present research is to highlight the advancement of proteomic analyses in the protein quantification of *Methanosarcina mazei* cells grown in 4 different methylotrophic substrates during the mid-logarithmic growth phase, which to date is limited in the scientific literature.

To date, the literature that examines *Methanosarcina mazei* does so from a transcriptional profiling perspective and negates the regulatory and enzymatic roles that proteins play in the transformation of methylotrophic substrates to methane. For instance, while Kratzer and colleagues (Kratzer et al. 2009) compare the growth of *Methanosarcina mazei* on methanol versus trimethylamine substrates, and suggest the use of an elaborate regulatory network for the optimization of differential substrate usage, the monitoring of transcript levels in the absence of proteomic analyses negates any post-transcriptional regulation that may have resulted and the significant role that the ultimate effector, the protein (prior to being post-translationally modified), plays in the methanogenic process. Nonetheless, the significance of Kratzer's work lies in the results about the genes involved in the transportation of and demethylation of trimethylamine (TMA) into the *mazei* cells. Interestingly enough, it was determined, via assays that specifically measure for monomethylamine (MMA), dimethylamine (DMA), and TMA, that TMA is not immediately converted to methane; however, it is converted in stepwise fashion, first forming DMA, then MMA, then methane (Kratzer, 2009). Because the *mttP1* gene (MM1691 protein) showed higher transcript levels in cells grown in TMA when compared to those grown in methanol, it was suggested that the TMA permease first functions to transport TMA into the

cells, and then MttBC1 demethylates TMA to form DMA, which is then converted to MMA by MtbBC1 (Kratzer, 2009). *Methanosarcina mazei* performs sequential transformation of TMA, rather than an immediate degradation, in order to prevent the exorbitant release of ammonia into the cell, thereby resulting in cell toxicity (Kratzer, 2009). Instead, MMA levels are gradually increased and metabolized (Kratzer, 2009). The schematic for TMA metabolism is also growth-phase sensitive, meaning that as TMA levels gradually decrease until the late-exponential phase, the DNA permease gene, *mtbP*, which is included in the *mtb3* operon (MM2961-MM2964) is upregulated, resulting in the transport of DMA into the cell, and *mtmP* (MM1436-MM1438) levels also increase to transport MMA into the cells, where it is slowly metabolized to form methane, carbon dioxide, and ammonia (Kratzer, 2009). At the point of the late-exponential phase of growth, the *mtb1-mtt1* operon for TMA transport and demethylation is downregulated because TMA is no longer inside of the cell, and MMA is being slowly metabolized (Kratzer, 2009).

Our research will further advance the study of methylotrophic substrates in *mazei* cells by examining the proteins in *M. mazei* that have not only been grown in methanol and TMA, but MMA, and DMA as well; allowing us to compare MMA-, DMA-, TMA- utilizing proteins to methanol proteins. Kratzer and colleagues also noticed that under the TMA-growth conditions, the genes encoding MM0869 – MM0872 proteins, which are involved in the first steps of mevalonate synthesis for the production of ether lipids, are upregulated (Kratzer, C., 2009). It is suggested that the increased production of the ether lipids, which make up the cytoplasmic membrane of the *Methanosarcina* genus, occur because the deprotonated (neutral) TMA is membrane-permeable. Once it enters the cytoplasm it can be reprotonated. Protons then enter the cell to maintain pH. (Kratzer, C., 2009). This process may disrupt the membrane potential, as was demonstrated in *Xenopus laevis* oocytes (Burckhardt, B.C., 1995), and therefore requires the increased production of ether lipids (Kratzer, C., 2009).

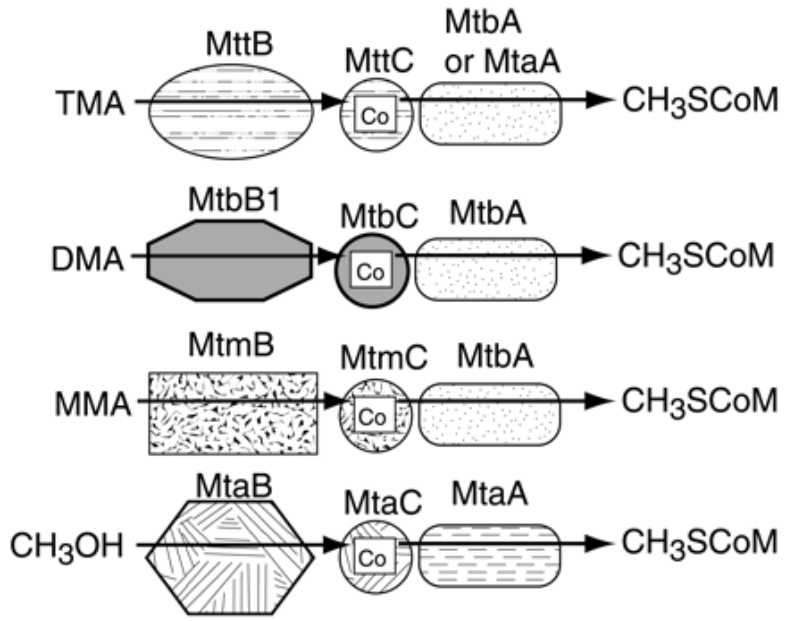

Figure 2.1 General scheme of CH_3-Coenzyme-M formation from MeOH/MMA/DMA/TMA: 1) Methanol (MMA/ DMA/ TMA) → corrinoid protein (enzyme: MT1), 2) Corrinoid protein → HS-CoM (enzyme: MT2), 3) HS-CoM + HS-CoB → heterodisulfide (enzyme: methyl-CoM reductase, reduces CH3 group to CH4). (Ferguson et al, 2000) (Figure reprinted with permission.)

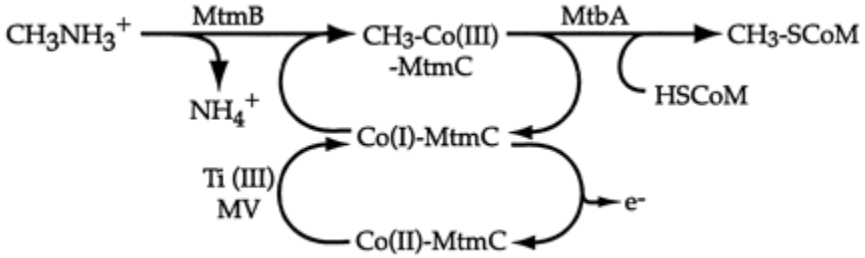

Figure 2.2 Scheme of CH_3-Coenzyme-M formation from MMA: 1) MtmC uses cobalt as a cofactor. Cobalt is active in the Co(I) oxidation state and inactive in the Co(II) oxidation state. *In vitro* assays have shown that Ti(III) and methyl viologen (MV) are responsible to sustaining the activity of MtmC. (Ferguson et al, 2000) (Figure reprinted with permission.)

Role of $F_{420}H_2$ Dehydrogenase in Methanogenesis

The $F_{420}H_2$ dehydrogenase in *M. mazei* Gö1 has been compared to the NADH dehydrogenase that is found in the respiratory chain of bacteria and eukarya alike, NDH-1 and complex I, respectively (Baumer, S., 2000). After inverted vesicles, which contained $F_{420}H_2$ and its dehydrogenase, were pulsed with 2-OH-phenazine, a water-soluble homologue of methanophenazine, the membrane-bound electron carrier found in *M. mazei*, the amount of $F_{420}H_2$ diminished, due to the transfer of electrons from $F_{420}H_2$ to 2-OH-phenazine via the $F_{420}H_2$ dehydrogenase, which also leads to the formation of transfer of electrons from F_{420}; and the external solution became more alkaline (Baumer, S., 2000). The movement of electrons from $F_{420}H_2$ to 2-OH-phenazine also corresponded to the translocation of protons into the lumen of the inverted vesicle, thereby resulting in an alkaline external medium, for which thiocyanate was used as a charge compensating cation in the inverted vesicle solution (Baumer, S., 2000). Based upon the lower amount of $F_{420}H_2$, the electron transport ceased and the proton gradient also diminished, because the protons that once translocated to the lumen of the inverted vesicles passively diffused into the external solution, resulting into a re-acidification process (Baumer, S., 2000). The amount of sodium hydroxide required to re-alkalinize the external solution was used to measure the H+/2e- ratio, and it was determined that 0.9 ± 0.2 protons are translocated per every 2 electrons transported (~2 protons/ 2 electrons, due to 50% of the inverted vesicle being uncoupled), versus 4 protons/ 2e- for the NADH dehydrogenase (Baumer et al. 2000 and Dutton et al 1999).

Consequently, the proton translocation in *M. mazei* cells generated an electrochemical gradient that stimulated the synthesis of ATP, as was measured by the luciferin/ luciferase enzyme (Baumer, S., 2000) via oxidative phosphorylation. The presence of a protonophore degraded the proton gradient and resulted in a decrease in the concentration of ATP (Baumer, S., 2000).

(Inverted vesicles were used to prevent hydrophobic aggregates from forming, with the membrane exposed to the hydrophilic external solution.)

Furthermore, both $F_{420}H_2$ dehydrogenase and NADH dehydrogenase use reversible hydrides as electron donors ($F_{420}H_2$ and NADH, respectively) and shuttle electrons to small hydrophobic nonproteinaceous molecules, namely methanophenazines and quionones, respectively (Baumer, S., 2000). Also, both dehydrogenases contain [Fe4-S4] clusters and the membranous part of their proteins are identical in bacteria; however, the native structure of $F_{420}H_2$ dehydrogenase is still unknown and its proton translocating machinery is slightly modified (Baumer, S., 2000). Therefore, determining the amount of $F_{420}H_2$ dehydrogenase found in the *M. mazei* cells, when they are grown under different methylotrophic pathway substrate conditions, can further elucidate the significance of $F_{420}H_2$ dehydrogenase as well as the hydrogenase during the mid-log and stationary phase of the methanogenic process.

The $F_{420}H_2$ dehydrogenases were characterized by Abken and colleagues via solubilization with the CHAPS detergent, native polyacrylamide gradient electrophoresis, denaturing SDS/PAGE, extensive purification with strategies including anion and affinity based chromatography, and UV/Vis spectroscopy (Abken, H-J. et al., 1997). Native PAGE demonstrated that the molecular weight of the $F_{420}H_2$ dehydrogenase, which was dislodged from the cytoplasmic membrane effectively with CHAPS from *M. mazei*, is 115 kDa (Abken, H-J. et al., 1997). After purification with DEAE, hydroxyapatite, anion exchange (QAE), and affinity (Reactive green) chromatography, the final specific activity of $F_{420}H_2$ dehydrogenase enzyme resulted to be 15 U mg/ protein with a 2.7% yield (Abken, H-J., et al., 1997). SDS/PAGE revealed that the $F_{420}H_2$ dehydrogenase is a multi-subunit system, which has a different subunit profile than the F_{420}–dependent hydrogenase. Also, $F_{420}H_2$ dehydrogenase cannot function as a hydrogenase (Abken, H-J., et al., 1997).

The occurrence of a yellowish color in the concentrated $F_{420}H_2$ dehydrogenase indicated the existence of flavins and/ or iron-sulfur clusters that were verified with UV/Vis spectroscopy (Abken, H-J. et al., 1997). The results indicated the presence of 7 moles of non-heme iron and 7 moles of acid-labile sulfur per mole of enzyme (Abken, H-J. et al., 1997). Moreover, the presence of flavins was confirmed with the disappearance of a 430nm peak after the reduction with Na-dithionite (Abken, H-J. et al., 1997). The flavin was revealed to be 0.2 mol FAD per mole of $F_{420}H_2$ dehydrogenase protein by HPLC (Abken, H-J. et al., 1997).

Our study will quantify and compare the amount of $F_{420}H_2$ dehydrogenase protein found in methanogenic cells, such as *Methanosarcina mazei,* grown under different methylotrophic conditions and will further elucidate the significance of $F_{420}H_2$ dehydrogenase coupling to proton transfer across the cytoplasmic membrane (Abken, H-J. et al., 1997).

Role of ATP Synthase in Methanogenesis

Energy production, in the form of ATP synthesis, within the *M. mazei* cell is crucial for its growth and proliferation. The ATP synthase found in archaea is the A_1A_O ATP synthase, which is a multisubunit, membrane-bound structure that is related to the F_1F_O and V_1V_O ATP synthase found in bacteria and eukaryotic organelles, respectively, has 4 major components: the 1) A_O motor, 2) peripheral stalks, 3) the A_1 motor and 4) the central stalk. The A_O motor is membrane bound and is composed of subunits *a* and *c*; the peripheral stalk is composed of subunits E and H; and the A_1 motor and central stalk is composed of subunits A, B, C, D, and F (Vonck, J., et al, 2009; Esteban, O., et al, 2008; Lau, W.C. et al, 2012; Coskun, M., et al., 2004; and Gruber, G. et al., 2001). It is important to note that subunits *a* and *c* are distinct from subunits A and C. For instance, while subunits *a* and *c* are solely membrane bound, subunits A and C are integral proteins and compose the central stalk. The rotation of the central stalk leads to structural

changes in the A_1 motor, thereby allowing ATP synthesis to ensue (Muller, V. et al., 2003 and Stock, D., et al 1999). Gloger and colleagues' ability to produce ATP synthase from *M. mazei*, a mesophilic archaeaon, inside of *E. coli*, allowed for the study of *M. mazei*'s A_1A_O ATP synthase on a molecular level (Gloger, C., et al., 2015). Even though the enzyme from *M. mazei* did not facilitate the growth of *E. coli* on succinate as the carbon source due to orders of magnitude lower ATP synthase activity being produced than required for *E. coli* growth, the use of inverted membrane vesicles allowed for the analysis of the A_1A_O ATP synthase, its ATP synthesis driving forces, and mutagenesis (Gloger, C., et al., 2015).

Firstly, subunit *a*, from the A_O motor of the A_1A_O ATP synthase, was detected in the cytoplasmic fraction and, more notably in the membrane fraction of the *E. coli* pA40 and *E. coli* pRIL pA40 plasmids (with the pRIL pA40 plasmid possessing 1.5 times more ATP synthase subunit A vesicles than the pA40 plasmid) (Gloger, C., et al., 2015). When NADH was added to the inverted membrane vesicles, NADH was oxidized (ATP concentration was measured by the luciferin/ luciferase assay) (Gloger, C., et al., 2015). The results indicated that pRIL pA40 plasmid showed the highest concentration of ATP; and after the addition of Dicyclohexylcarbodiimide (DCCD) or Diethylstilbesterol (DES), both of which are inhibitors of ATP synthesis, the concentration of ATP decreased, thereby indicating that ATP synthesis is coupled with and driven by NADH oxidation (Gloger, C., et al., 2015). Furthermore, ATP synthesis was also driven by a potassium-diffusion potential and a pH gradient, whereby a ΔpH of 3 elicited the greatest production of ATP, and corresponded to a membrane potential of -180 mV (Gloger, C., et al., 2015). However, an electric potential alone was not sufficient enough to drive ATP synthesis in the inverted membrane vesicles of the pRIL pA40 plasmid (Gloger, C., et al., 2015). Based upon the mutagenesis experiments, it was discovered that the glutamic acid residue at position 65 of subunit *c* is crucial for ATP synthesis as well as the 2 conserved arginine residues at positions 625 and 563 of subunit *a* (Gloger, C., et al., 2015), with *a*R563

assuming the role of the stator charge that is responsible for the proton translocation (Deckers-Hebestreit, G., et al., 1996; and Fillingame, R.H., 1992).

Our research plans to examine the protein abundance of the A_1A_O ATP synthase, along with other substrates that play a pivotal role in methanogenesis in *M. mazei* cells when grown in different methylotrophic substrates (methanol, MMA, DMA, and TMA). Our data may also elucidate the presence of subunits *a* and *c* of the A_O motor, as well as any $F_{420}H_2$ dehydrogenases that would oxidize $F_{420}H_2$ to F_{420}; whereby it would be expected for the $F_{420}H_2$ oxidation to be coupled with ATP synthesis by the A_1A_O ATP synthase in *M. mazei*.

Singh and colleagues demonstrated that the F subunit of the A_1A_O ATP synthase is crucial for ATP hydrolysis in the A_3B_3-headpiece, which is located in the cytoplasm of *Methanosarcina mazei* Gö1, and contains domains for ATP binding, phosphoryl transfer and catalytic activation (Singh et al., 2016). In solution, the F subunit has an N terminal globular region and a flexible and positively charged C terminal region, which can also enable cross-linkage to the B subunits (Schafer et al., 2006; Gayen et al., 2007; and Coskun et al., 2004). In the A_1A_O ATP synthase, the A_1 domain is water soluble and contains the catalytic site, while the A_O motor is involved in the translocation of the proton; hence, archaeal ATP synthases are able to synthesize ATP and utilize ATP as a driving force to create a proton gradient when fermentation ensues (Deppenmeier et al., 2008; Gruber et al., 2014; Boekema, E.J., et al., 1999; Cross, R.L., et al., 2004; and Marshansky, V., et al., 2014). In the absence of the F subunit in the A_3B_3D-headpiece, the headpiece shows 4 times less ATP hydrolytic activity, when compared to the presence of the F subunit (Singh, D., et al., 2016). Nonetheless, even though the Michaelis-Menten V_{max} was greater for A_3B_3DF, the K_m was the same, which indicated that the F-subunit may not be involved in the binding of ATP to the catalytic binding site of subunit A; however, it may impact and stabilize the transition state of the B subunits, and hence the cleavage of ATP

to ADP and P_i (Singh, D., et al., 2016). The C-terminus of the F subunit was found to be of great significance in the enhancement of ATP hydrolysis activity (Singh, D., et al., 2016). For instance, when the F subunit was in the truncated form that lacks the C-terminus, ATP hydrolysis activity was diminished by approximately 4-fold (4.6 µmol/min/ mg protein for wild type A_3B_3DF versus 1.0 µmol/min/ mg protein for $A_3B_3D + F_{1\text{-}91}$) (Singh, D., et al., 2016). When different residues within the F subunit were mutated, ATP hydrolysis activity was not significantly different than the $A_3B_3D+F(_{WT})$, except in the case where arginine 88 was mutated to leucine, which resulted in a 20% decrease in hydrolytic activity (Singh, D., et al., 2016).

Furthermore, when the A_3B_3D headpiece was combined with the F subunit from *Saccaromyces cerevisiave* V-ATPase, in order to create a hybrid complex, it was demonstrate to still function as an ATPase, but however not at the full potential of the $A_3B_3D+F(_{WT})$ complex (Singh, D., et al., 2016). These results are consistent with data that shows the F subunit of eukaryotic V- and archaeal A-ATPase to share sequence (<23%) and structural similarity (Basak, S., et al., 2013), which is more so than for the bacterial F-ATPase. Therefore, when the F subunit of $A_3B_3D+F(_{WT})$ was replaced with *Mtε*, a subunit involved in the coupling of ATP hydrolysis to proton translocation, and rotation of the bacterial F-ATP synthase (Aggeler, R., et al., 1996 and Noji, H., et al., 1997), ATP hydrolysis activity was reduced by 1.5-fold (Singh, D., et al., 2016).

Our proteomic results were sensitive enough to detect the F subunit of the archaeal-ATPase, and we aim to also analyze the significance of its abundance in a methylotrophic substrate-dependent manner. Therefore, given all of the genetic information and partial protein analysis, we hypothesize that *Methanosarcina mazei* cells have an expansive regulatory system of proteins that augments substrate usage differently in the methylotrophic pathway of methanogenesis during the mid-log and stationary growth phase, via the use of whole-cell proteomic analysis. Furthermore, the proteins that are optimized are the methyltransferases.

Methods

Cells were grown in 0.4 M sodium chloride at 37ºC, then lysed in a solution of ammonium lauryl sulfate, deoxycholic acid, and the reducing agent, tris(2-carboxyethyl)phosphine (TCEP), in 100 mM ammonium bicarbonate. An exchange buffer composed of urea was used to remove ammonium lauryl sulfate from the solution. Then the reduced proteins were alkylated with iodoacetamide then digested overnight with the trypsin protease. Urea was exchanged with a solution of ammonium bicarbonate by ultrafiltration. Once digested, the deoxycholic acid in the peptide solution was acidified and then treated with water-saturated ethyl acetate to separate the peptides from the ethyl acetate-soluble deoxycholic acid (Erde et al. 2014).

Once dried in a speedvac and resuspended in mass spectrometry-amenable solvents, four technical replicates of two biological replicate samples were injected on a Waters Acquity M-class liquid chromatography system to then be introduced onto the Waters Xevo QTof G2XS mass spectrometer via an electrospray ionization inlet. Data independent acquisition in the form of MS^E allowed for the fragmentation of precursor ions using alternating low-energy and high-energy collision induced dissociation. PLGS is the software used to further identify and quantify the proteins within the *M. mazei* cells. Approximately 0.9 µg of protein was loaded onto a reversed-phase C18 nanoLC column, which accommodated a flow rate of 300 nL/ min. Prior to analysis by LC/MS, protein amounts were quantified via the micro-bicinchoninic acid assay (Thermo Scientific), whereby proteins within the cells were measured using a spectrophotometer at 562 nm and compared to several diluted standards of bovine serum albumin (BSA).

Error limits for loading amounts of protein (in fmols) on column were determined by using coefficient of variation values of <30%. Two biological replicates and 4 technical replicates were

analyzed for each of the substrates (MeOH, MMA, DMA and TMA). Only proteins that were identified 3 or more times were included in Tables 2.1-2.3.

Results

Relative abundance of proteins in methanol and C1-methylotrophic substrates

At least 40% of all of the protein found in the *M. mazei* cells comprised methyltransferases and methylcoenzyme-M reductases. This phenomenon was demonstrated in all of the methylotrophic-grown cells, for MeOH **(Figure 2.3)**, MMA **(Figure 2.4)**, DMA **(Figure 2.5)** and TMA **(Figure 2.6)**. Most notably the type of methyltransferase (including the corrinoid protein) interchanged in a substrate-specific manner. For instance, when growth medium changed, the methyltransferases that were specific to methanol grown cells were replaced with, or found in lower abundance when compared to, methyltransferases specific to dimethylamine grown cells. Furthermore, MM_1976, the S-layer protein specific to *Methanosarcina mazei* cells was also found to be among the most abundant proteins within the cell. The hypothetical protein, MM_1357 is shown to be highly abundant in methanol- and monomethylamine-grown cells. Proteins similar to MM_1357 include translation initiation factor proteins (IF subunit 2) in different strains of *M. mazei* (C16 and LYC). Strain C16 was isolated from marine sediments (Maestrojuan et al. 1992) and LYC was isolated from an alkaline sediment from an oil exploration drilling site (Liu et al. 1985).

Not only were different methyltransferases employed according to substrate **(Figures 2.7 and 2.8)**, the corrinoid proteins were also regulated with significant specificity **(Figure 2.9)**.

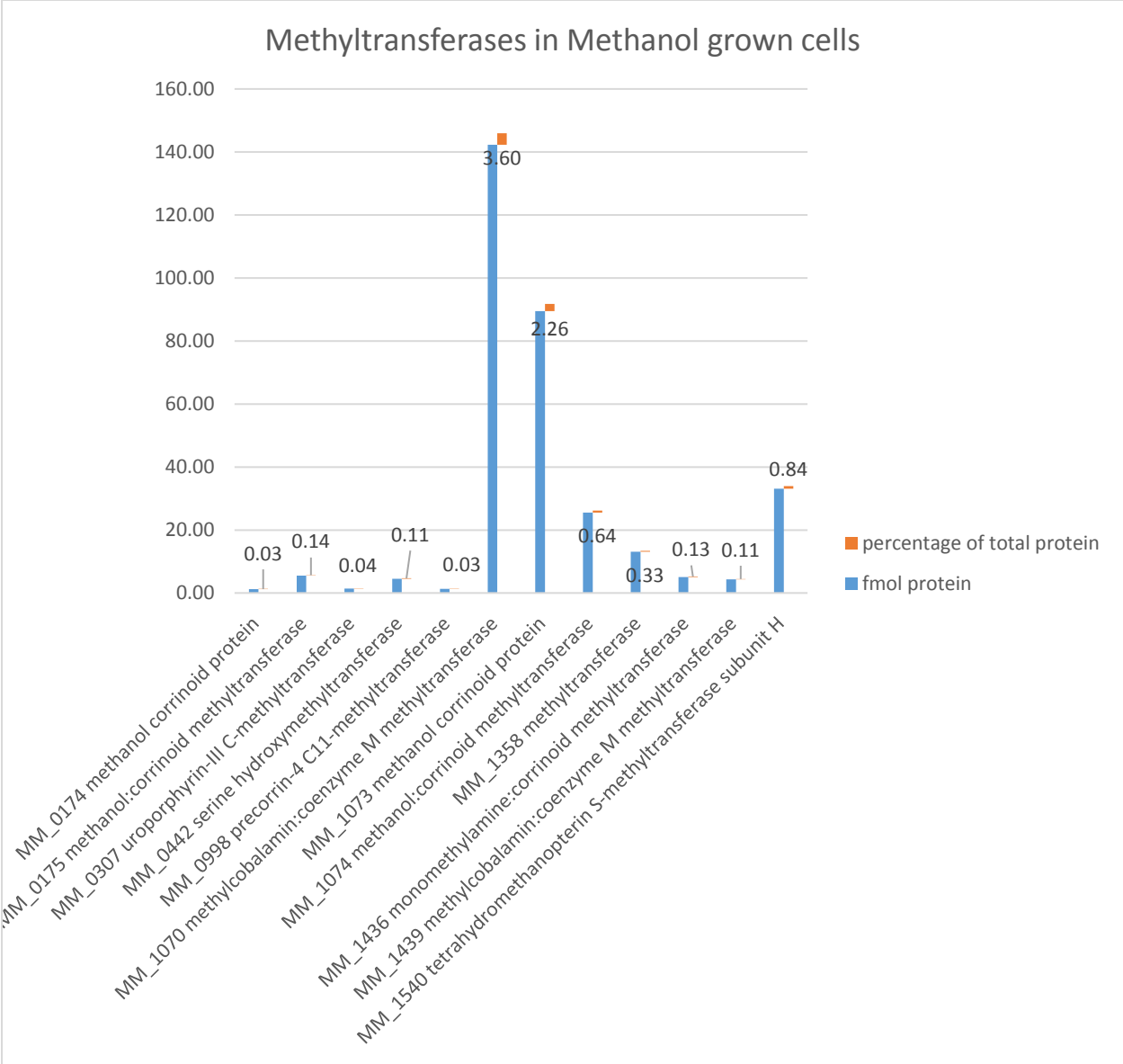

Figure 2.3a Methanol-grown *Methanosarcina mazei* cells. Methyltransferases (e.g., *mtaB, mtaC, mtaA*) account for ~30% of total amount of proteins identified (See Figure 2.3b)

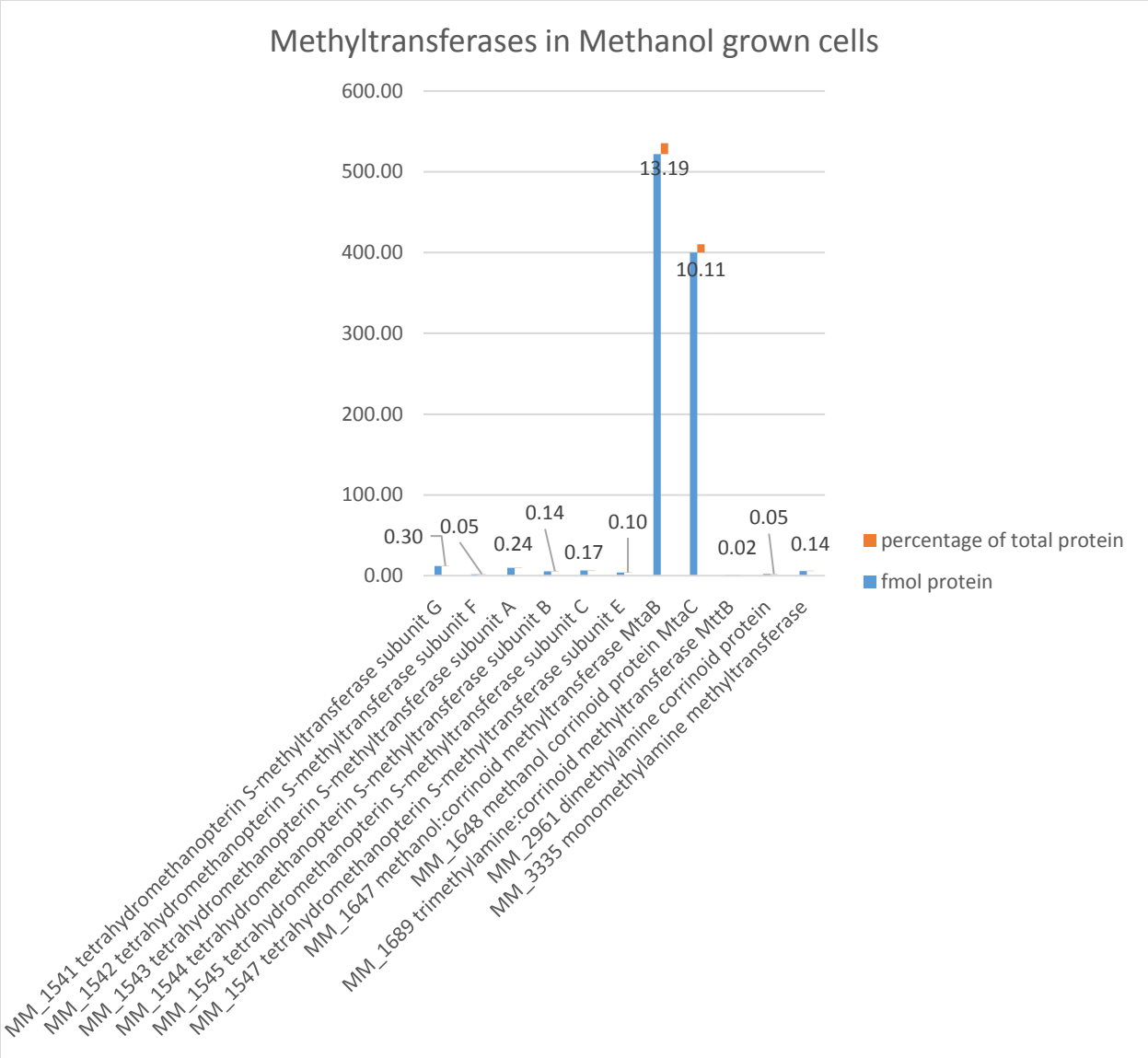

Figure 2.3b Methanol-grown *Methanosarcina mazei* cells. Methyltransferases (e.g., *mtaB, mtaC, mtaA*) account for ~30% of total amount of proteins identified (See Figure 2.3a)

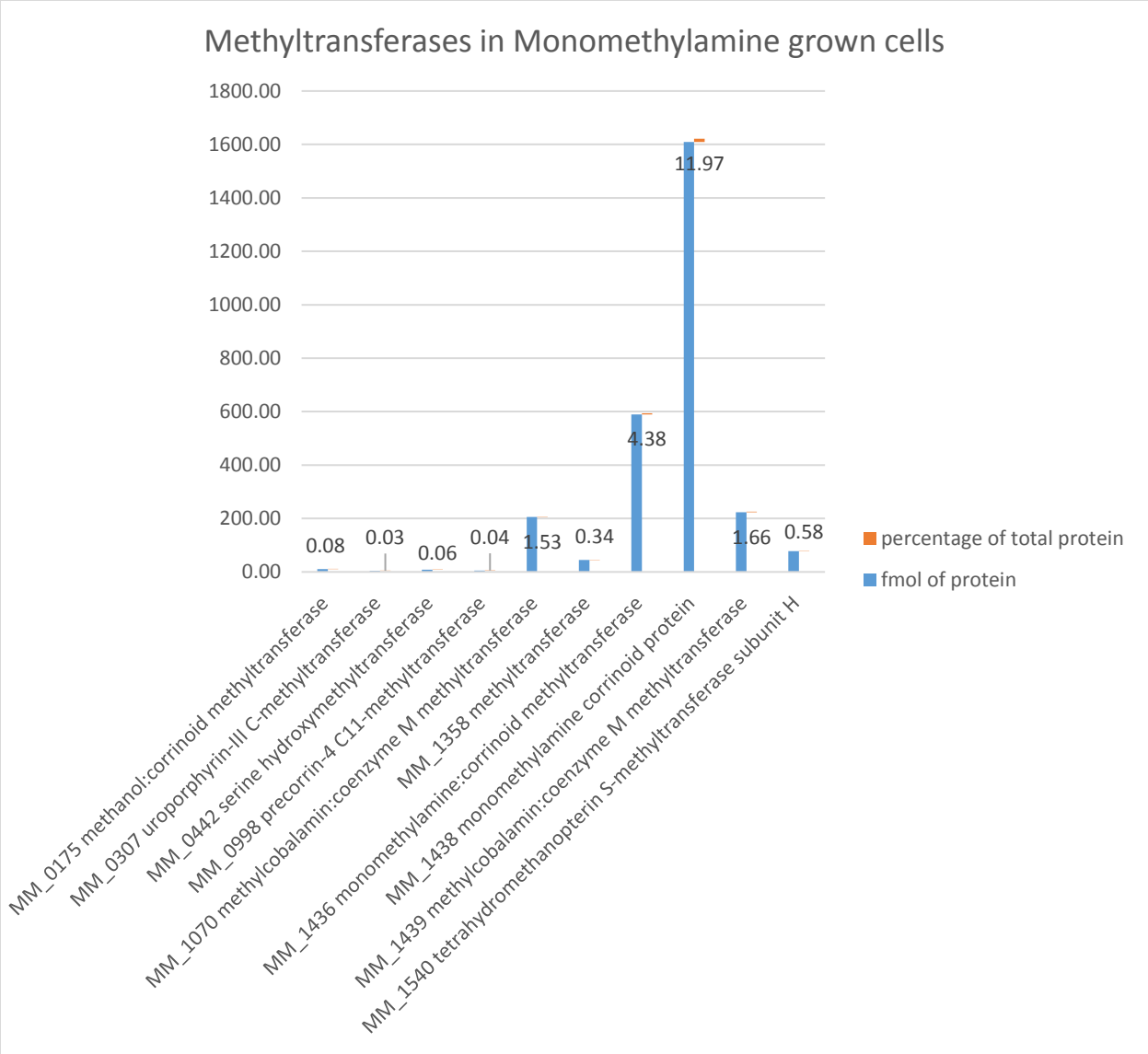

Figure 2.4a MMA grown *Methanosarcina mazei* cells. Methyltransferases (e.g., *mtmB, mtmC, mtmA*) account for ~23% of total amount of proteins identified (See Figure 2.4b)

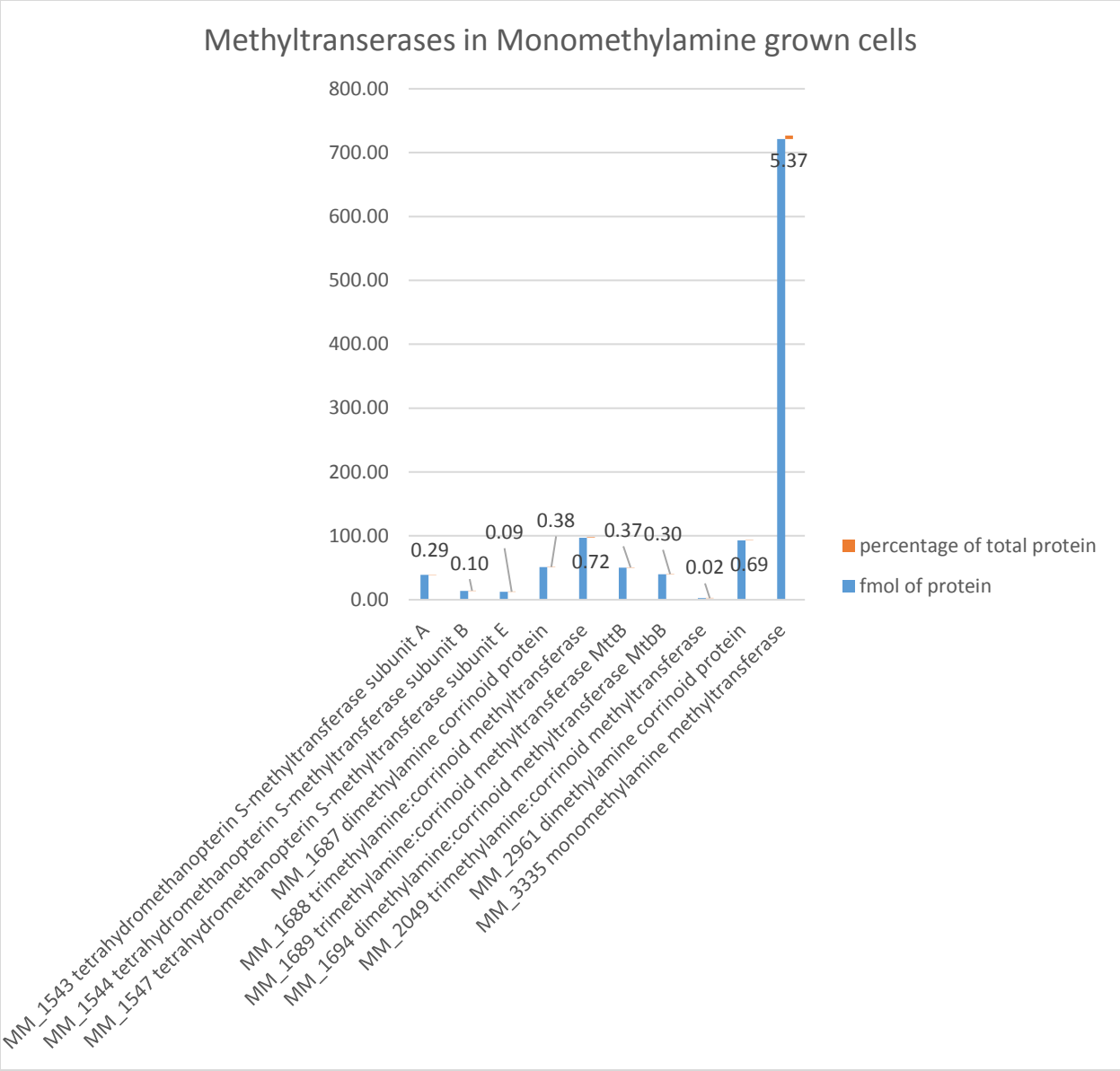

Figure 2.4b MMA grown *Methanosarcina mazei* cells. Methyltransferases (e.g., *mtmB, mtmC, mtmA*) account for ~23% of total amount of proteins identified (See Figure 2.4a)

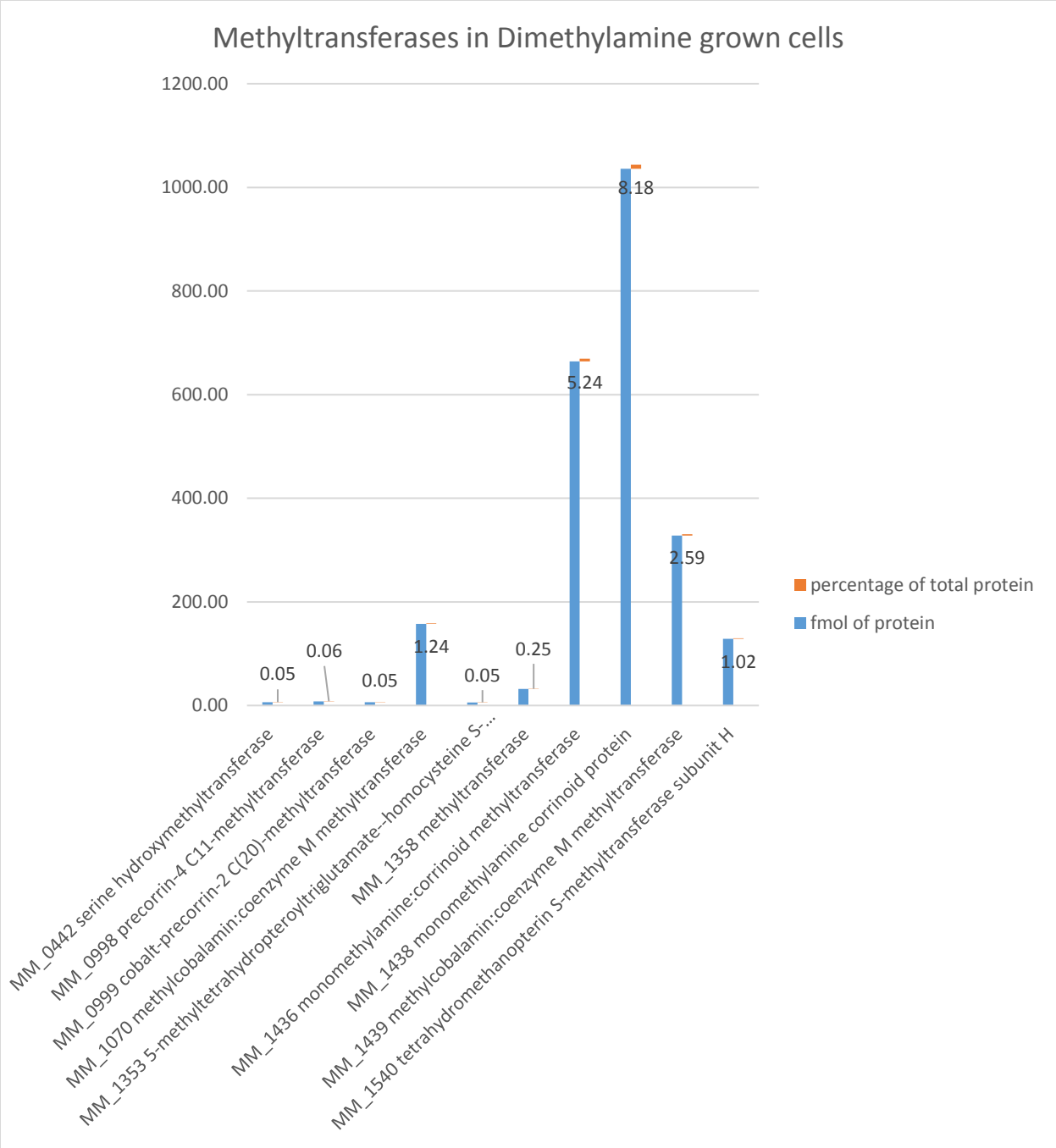

Figure 2.5a DMA grown *Methanosarcina mazei* cells. Methyltransferases (e.g., *mtbB, mtbC, mtbA*) account for ~26% of total amount of proteins identified (See Figure 2.5b)

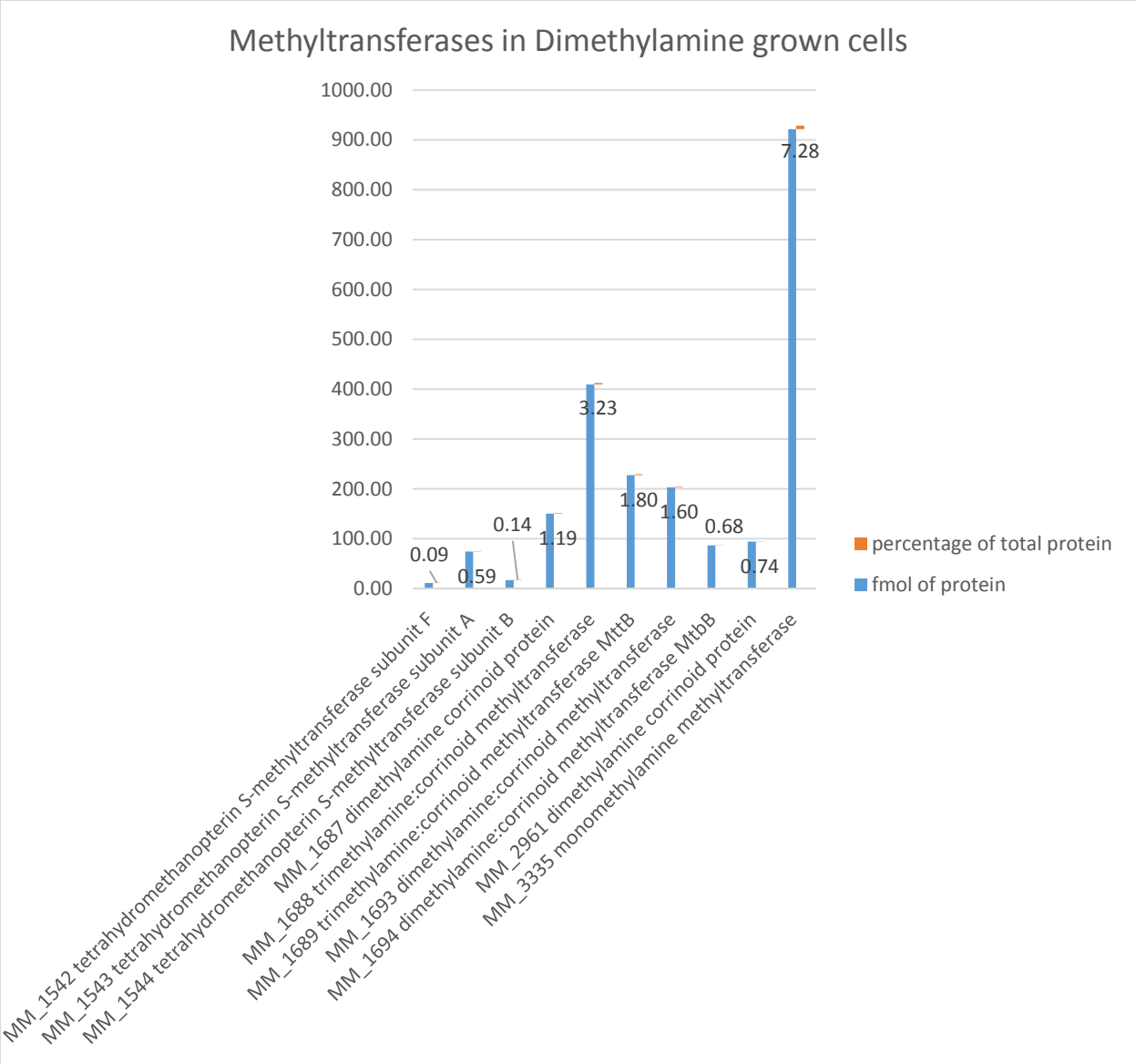

Figure 2.5b DMA grown *Methanosarcina mazei* cells. Methyltransferases (e.g., *mtbB, mtbC, mtbA*) account for ~26% of total amount of proteins identified (See Figure 2.5a)

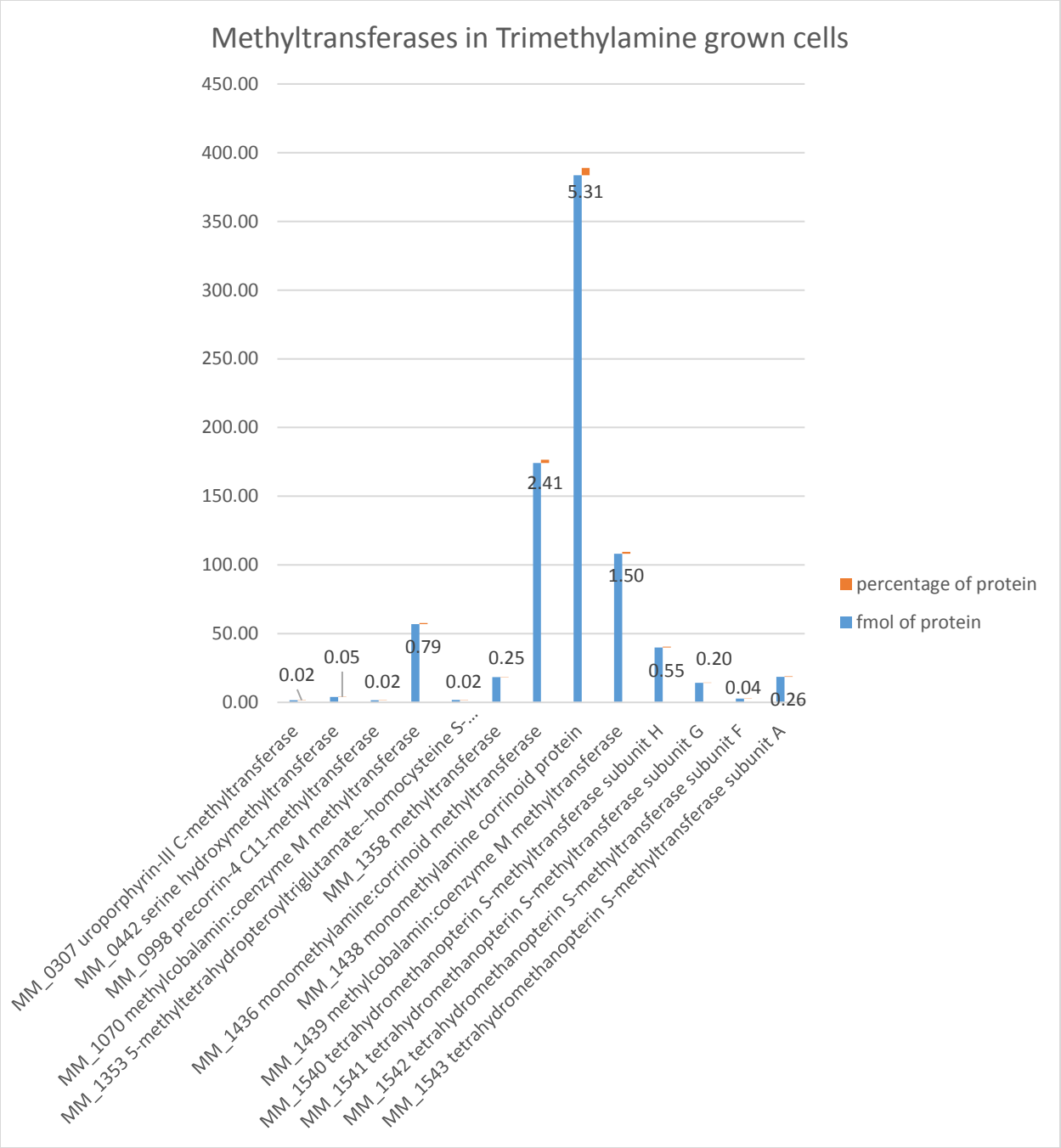

Figure 2.6a TMA grown *Methanosarcina mazei* cells. Methyltransferases (e.g., *mttB, mttC, mttA*) account for ~34% of total amount of proteins identified (See Figure 2.6b)

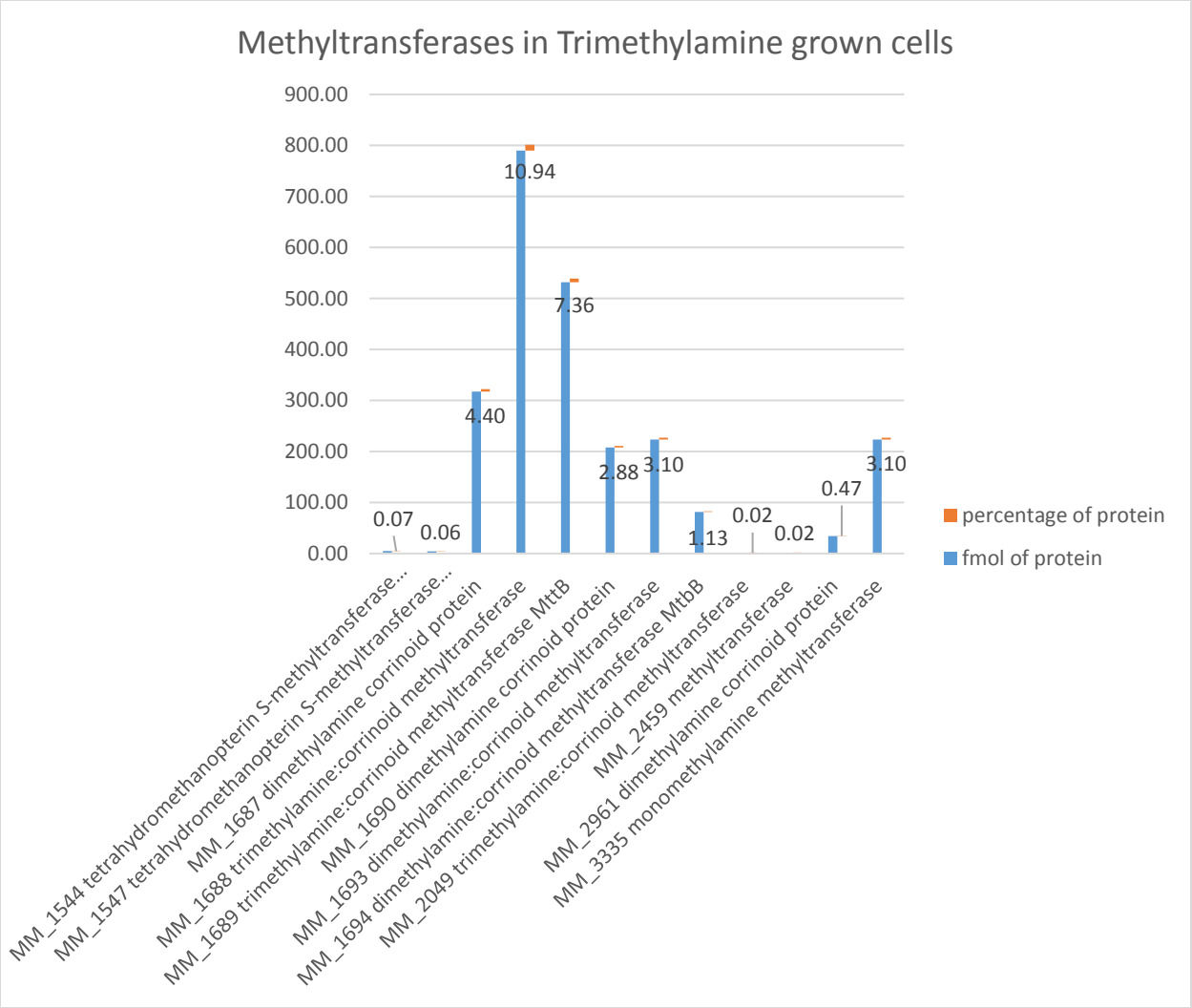

Figure 2.6b TMA grown *Methanosarcina mazei* cells. Methyltransferases (e.g., *mttB, mttC, mttA*) account for ~34% of total amount of proteins identified (See Figure 2.6a)

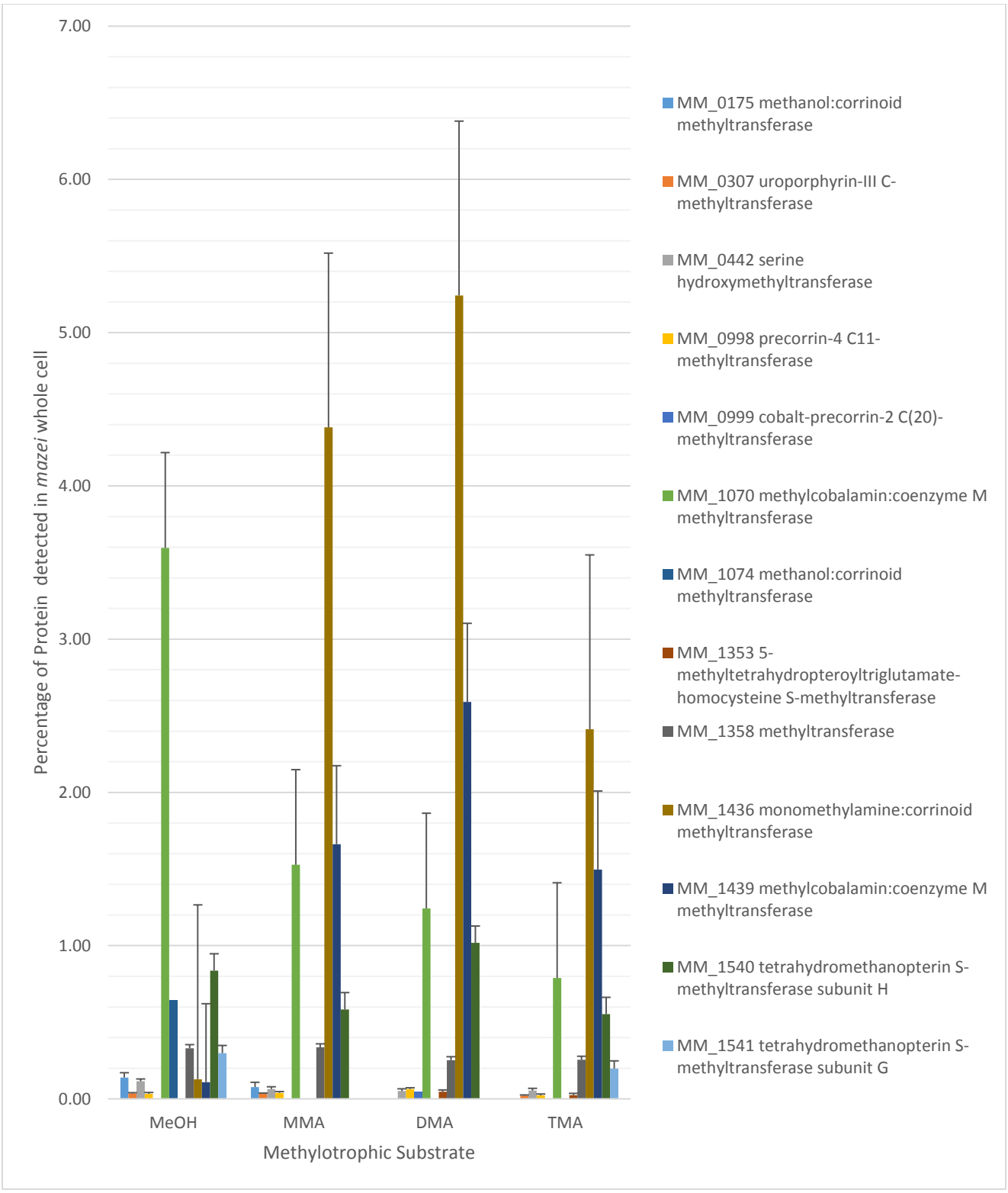

Figure 2.7 Methanol corrinoid methyltransferase and MMA corrinoid methyltransferase were in highest abundance in MeOH and MMA-grown cells, respectively

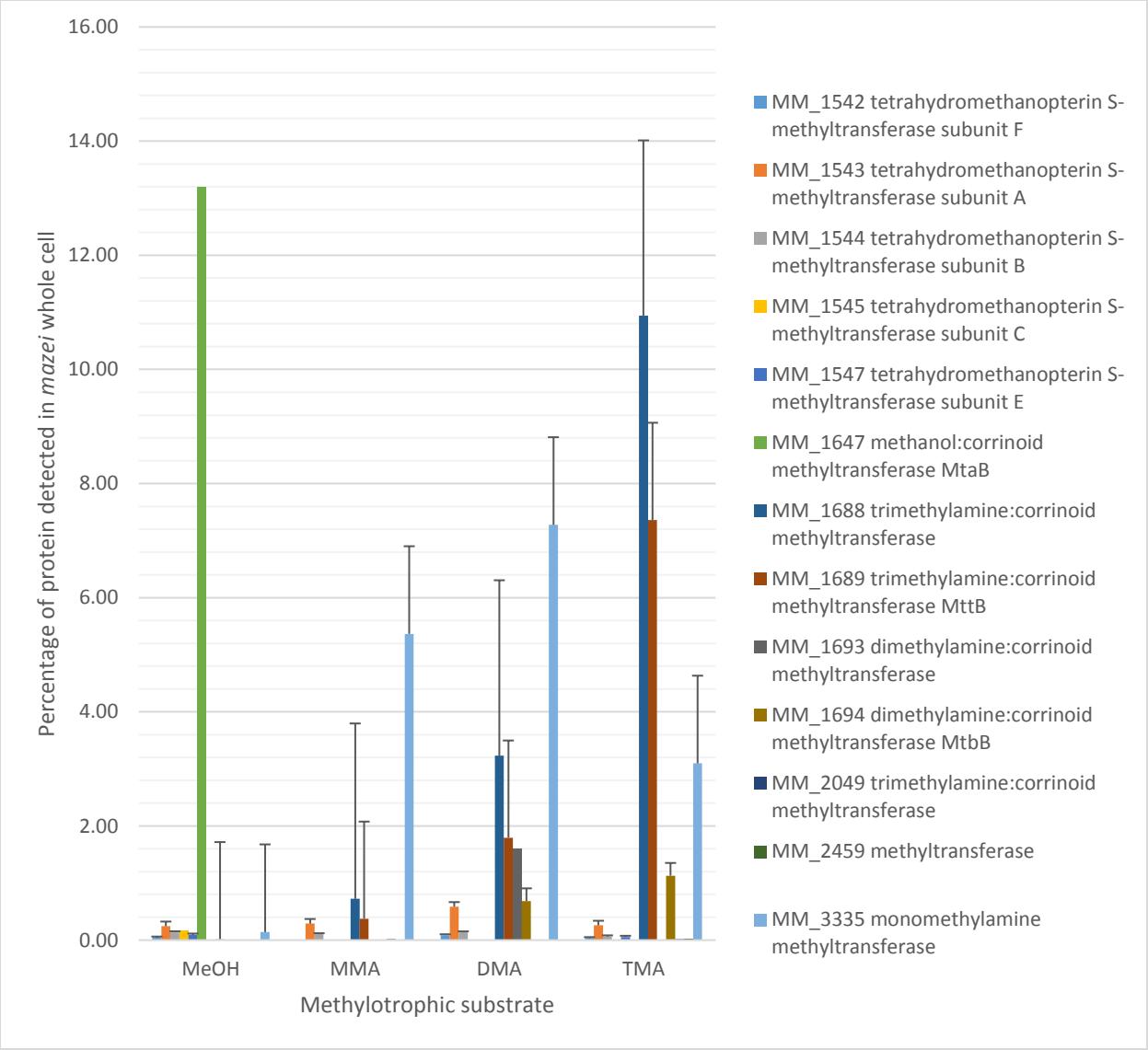

Figure 2.8. Methanol corrinoid methyltransferase and TMA corrinoid methyltransferase were in highest abundance in MeOH and TMA-grown cells, respectively

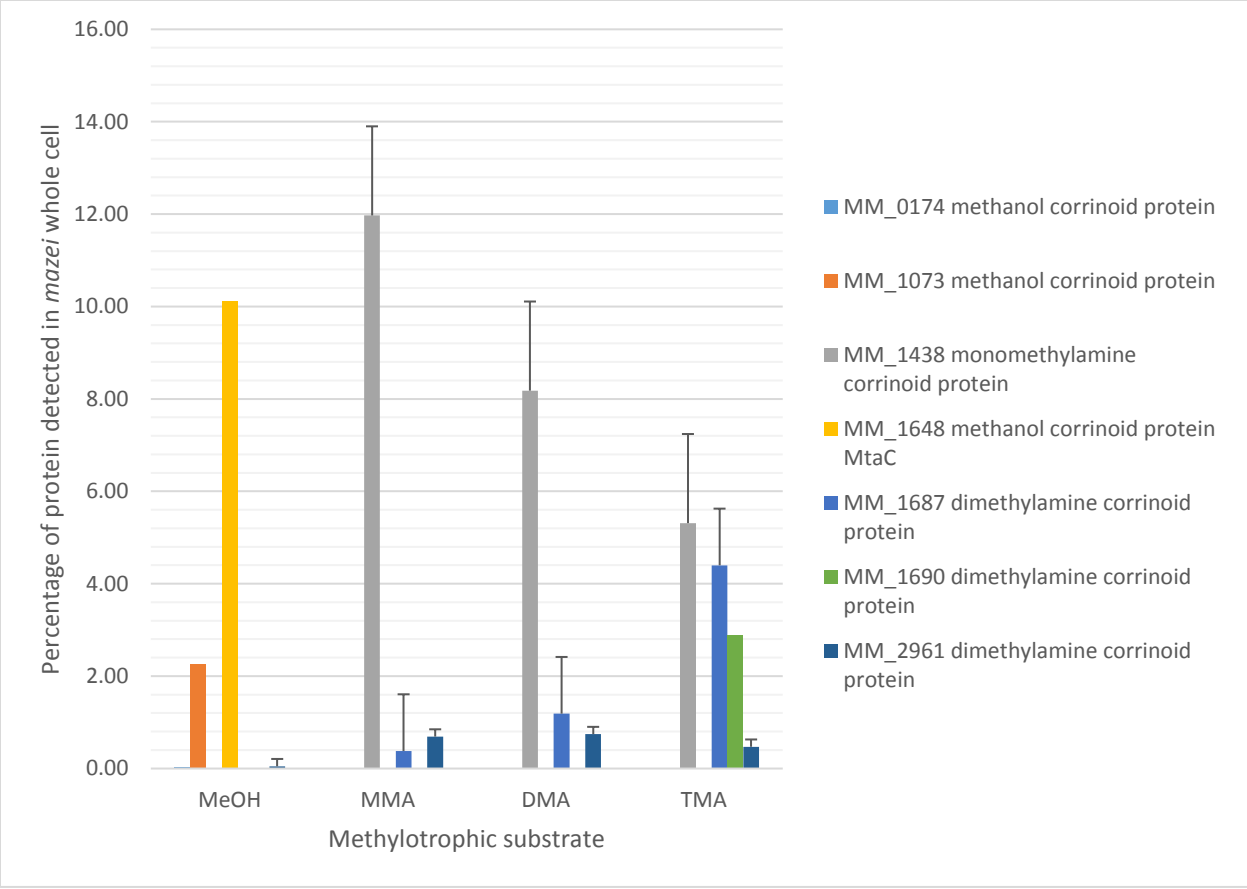

Figure 2.9 Methanol corrinoid protein and MMA corrinoid protein were in highest abundance in MeOH and MMA-grown cells, respectively

Comparative analysis of methanol to C1-methylotrophic substrates

Comparing methanol to monomethylamine grown cells harvested at mid-log growth phase

Out of the nearly 400 proteins that were quantified by data-independent acquisition using MS^E on the hybrid Q-Tof mass spectrometer and that met our requirements (false discovery rate of 1%, protein appears in at least 3 out of 4 technical replicates), 264 proteins were shown to have 2.5-fold higher or 2.5-fold lower amount of protein in cells grown in MMA compared to those in MeOH. The methanol-specific proteins such as MM_0174 (methanol corrinoid protein), MM_1073 (methanol corrinoird protein), MM_1074 (methanol:corrinoid methyltransferase), MM_1647 (methanol:corrinoid methyltransferase MtaB), and MM_1648 (methanol: corrinoid protein MtaC) were not detected in the monomethylamine grown cells. On the other hand, monomethylamine-specific proteins, such as MM_3335 (monomethylamine methyltransferase) and MM_1436 (monomethylamine:corrinoid methyltransferase) were detected in methanol grown cells; however, they were upregulated in monomethylamine grown cells 129-fold and 589-fold, respectively.

Proteins, such as MM_2961 (dimethylamine corrinoid protein) and MM_1689 (trimethylamine: corrinoid methyltransferase, MttB), which are dimethylamine- and trimethylamine-specific proteins, respectively, were upregulated in monomethylamine-grown cells. Furthermore, the V-type ATP synthases (MM_0778 to MM_0783) and the F_{420} nonreducing hydrogenases (MM_2313 and MM_2314) were all upregulated in MMA-grown cell by at least 3-fold when compared to cells grown in MeOH. Highlighted proteins were selected based upon their participation in the methanogenic process, and can be either soluble or membrane bound proteins. Regulation of proteins grown in MMA vs MeOH substrates, harvested during mid-log growth phase are depicted in Table 2.1. Proteins highlighted in green are upregulated in MMA, and those highlighted in pink are down regulated in MMA.

Comparing methanol to dimethylamine grown cells harvested at mid-log growth phase

For cells grown in dimethylamine, nearly 400 proteins were quantified, and approximately 230 proteins were found to have at least 2.5-fold higher or 2.5-fold lower levels when compared to cells grown in methanol. When compared to cells grown in methanol, methanol-specific proteins, such as the methyltransferases and the corrinoid proteins were absent from the DMA grown cells. For example, MM_0174 and MM_1073 (methanol: corrinoid protein), MM_0175 and MM_1074 (methanol: corrinoid protein methyltransferase), MM_1647 (methanol: corrinoid protein methyltransferase MtaB), and MM_1648 (methanol corrinoid protein MtaC) were all absent from the DMA grown cells.

Nonetheless, DMA-specific proteins, such as MM_2961 (dimethylamine corrinoid protein) were detected in methanol grown cells; however, it was upregulated in DMA grown cells by 116-fold. While the aforementioned results are expected, and further support our hypothesis that substrate-specific proteins are either upregulated or only found in cells that were grown in its respective medium, one result that was not expected was that the S-layer protein (MM_1976) was quantified in both methanol and DMA grown cells; however, its protein levels were increased almost 3-fold in DMA-grown cells. One might expect for the S-layer protein levels to remain constant throughout the growth in different medium.

The highlighted proteins were selected based upon their participation in the methanogenic process, and can be either soluble or membrane bound proteins. Regulation of proteins grown in DMA versus MeOH substrates, harvested during mid-log growth phase are depicted in Table 2.2. Proteins highlighted in green are upregulated in DMA, and those highlighted in pink are down regulated in DMA.

Comparing methanol to trimethylamine grown cells harvested at mid-log growth phase

As for cells grown in trimethylamine medium, the results are as follows:

1. The methanol-specific proteins such as MM_0174 (methanol corrinoid protein), MM_0175 (methanol: corrinoid methyltransferase), MM_1073 (methanol corrinoird protein), MM_1074 (methanol:corrinoid methyltransferase), MM_1647 (methanol:corrinoid methyltransferase MtaB), and MM_1648 (methanol: corrinoid protein MtaC) were not detected in the trimethylamine grown cells, as expected.
2. The trimethylamine-specific protein MM_1689 (trimethylamine:corrinoid methyltransferase MttB) was detected in methanol grown cells; however it was upregulated by almost a 3-order of magnitude (882-fold) in the trimethylamine grown cells.
3. Furthermore, MM_1436 (monomethylamine: corrinoid methyltransferase) was upregulated 34-fold, while MM_2961 (dimethylamine corrinoid protein) and MM_3335 (monomethylamine methyltransferase) were upregulated 17-fold and 39-fold in TMA grown cells, respectively.

The highlighted proteins were selected based upon their participation in the methanogenic process (see Table 2.4), and can be either soluble or membrane bound proteins. Regulation of proteins grown in TMA versus MeOH substrates, harvested during mid-log growth phase are depicted in Table 2.3. Proteins highlighted in green are upregulated in TMA; those highlighted in pink are down regulated in TMA.

Table 2.1 Regulation of proteins grown in MMA versus MeOH substrates, harvested during mid-log growth phase (relevant proteins highlighted in green are upregulated in MMA; pink are down regulated in MMA)

	MeOH	MMA	MMA/ MeOH	Upregulated in MMA	Downregulated in MMA
Protein Name	**fmol of protein**	**fmol of protein**		**2.5-fold higher**	**2.5-fold lower**
MM_0011 hypothetical protein	0.46		0.00	FALSE	TRUE
MM_0037 argininosuccinate synthase mazei	1.83	9.78	5.33	TRUE	FALSE
MM_0042 glycine betaine transporter_ substrate-binding	2.18	11.01	5.05	TRUE	FALSE
MM_0074 aspartyl-tRNA synthetase mazei	3.20	14.39	4.50	TRUE	FALSE
MM_0123 universal stress protein	1.53	7.21	4.70	TRUE	FALSE
MM_0125 universal stress protein	8.88	26.18	2.95	TRUE	FALSE
MM_0142 orotate phosphoribosyltransferase mazei	0.44	2.69	6.11	TRUE	FALSE
MM_0174 methanol corrinoid protein	1.19		0.00	FALSE	TRUE
MM_0184 30S ribosomal protein S3	10.59	39.15	3.70	TRUE	FALSE
MM_0243 aspartate aminotransferase mazei	1.54		0.00	FALSE	TRUE
MM_0263 hypothetical protein	0.35		0.00	FALSE	TRUE
MM_0282 threonine synthase mazei	1.67	6.25	3.73	TRUE	FALSE
MM_0293 replication factor A	1.10		0.00	FALSE	TRUE
MM_0305 hypothetical protein	3.73		0.00	FALSE	TRUE
MM_0307 uroporphyrin-III C-methyltransferase mazei	1.42	4.45	3.14	TRUE	FALSE
MM_0337 tryptophan synthase subunit beta	1.64	10.12	6.16	TRUE	FALSE
MM_0339 small nuclear ribonucleoprotein	3.36	20.10	5.99	TRUE	FALSE
MM_0363 hypothetical protein	0.80	2.19	2.75	TRUE	FALSE
MM_0382 peptidyl-prolyl cis-trans isomerase	2.36	10.84	4.60	TRUE	FALSE
MM_0410 hypothetical protein	1.09	6.28	5.74	TRUE	FALSE
MM_0436 thioredoxin mazei Go1]	4.96	16.03	3.23	TRUE	FALSE
MM_0441 bifunctional 5_10-methylene-tetrahydrofolate dehydrogenase	3.68	11.12	3.02	TRUE	FALSE
MM_0448 hypothetical protein	2.78	9.27	3.34	TRUE	FALSE
MM_0495 acetate kinase mazei	4.60	13.58	2.95	TRUE	FALSE
MM_0496 phosphate acetyltransferase mazei	5.68	30.25	5.32	TRUE	FALSE
MM_0517 sirohydrochlorin cobaltochelatase mazei	9.23	40.41	4.38	TRUE	FALSE
MM_0537 hypothetical protein	3.72		0.00	FALSE	TRUE
MM_0593 5-formaminoimidazole-4-carboxamide-1-(beta)-D-ribofuranosyl	1.24	4.44	3.58	TRUE	FALSE
MM_0594 translation initiation factor IF-2	2.49	10.18	4.08	TRUE	FALSE
MM_0599 30S ribosomal protein S24	4.07		0.00	FALSE	TRUE

Protein Name	MeOH fmol of protein	MMA fmol of protein	MMA/ MeOH	Upregulated in MMA 2.5-fold higher	Downregulated in MMA 2.5-fold lower
MM_0627 F420H2 dehydrogenase subunit F	**3.05**		**0.00**	**FALSE**	**TRUE**
MM_0628 methylenetetrahydromethanopterin reductase mazei	95.07	363.72	3.83	TRUE	FALSE
MM_0629 Zinc finger protein	2.22	8.50	3.84	TRUE	FALSE
MM_0631 hypothetical protein	2.60		0.00	FALSE	TRUE
MM_0635 flavoprotein mazei Go1]	2.03		0.00	FALSE	TRUE
MM_0664 oxidoreductase mazei Go1]	1.37	5.31	3.88	TRUE	FALSE
MM_0668 ketol-acid reductoisomerase mazei	10.86	55.94	5.15	TRUE	FALSE
MM_0669 acetolactate synthase 3 regulatory	4.27	27.94	6.55	TRUE	FALSE
MM_0670 acetolactate synthase 3 catalytic	3.94	27.91	7.08	TRUE	FALSE
MM_0684 acetyl-CoA decarbonylase/synthase complex subunit	31.99	146.50	4.58	TRUE	FALSE
MM_0685 acetyl-CoA decarbonylase/synthase complex subunit	26.96	125.76	4.67	TRUE	FALSE
MM_0686 acetyl-CoA decarbonylase/synthase complex subunit	60.86		0.00	FALSE	TRUE
MM_0687 nitrogenase iron protein	13.04	52.21	4.01	TRUE	FALSE
MM_0688 acetyl-CoA decarbonylase/synthase complex subunit	18.51	121.51	6.56	TRUE	FALSE
MM_0689 acetyl-CoA decarbonylase/synthase complex subunit	25.55	157.06	6.15	TRUE	FALSE
MM_0694 proteasome subunit beta	4.75	13.55	2.85	TRUE	FALSE
MM_0705 hypothetical protein	2.87		0.00	FALSE	TRUE
MM_0707 prolyl-tRNA synthetase mazei	1.20	5.42	4.52	TRUE	FALSE
MM_0714 aldolase mazei Go1]	1.84		0.00	FALSE	TRUE
MM_0747 ATP-dependent RNA helicase	3.12	5.54	1.77	FALSE	FALSE
MM_0757 NifB protein mazei	1.83	8.56	4.68	TRUE	FALSE
MM_0767 hypothetical protein	4.16	24.11	5.79	TRUE	FALSE
MM_0774 hypothetical protein	9.33	43.98	4.71	TRUE	FALSE
MM_0778 V-type ATP synthase subunit	2.62	8.65	3.30	TRUE	FALSE
MM_0779 V-type ATP synthase subunit	20.12	72.38	3.60	TRUE	FALSE
MM_0780 V-type ATP synthase subunit	18.01	69.89	3.88	TRUE	FALSE
MM_0781 V-type ATP synthase subunit	2.98	9.26	3.10	TRUE	FALSE
MM_0782 V-type ATP synthase subunit	4.78	17.84	3.73	TRUE	FALSE
MM_0783 V-type ATP synthase subunit	8.69	27.92	3.21	TRUE	FALSE
MM_0786 A1AO H+ ATPase subunit H	**5.13**		**0.00**	**FALSE**	**TRUE**
MM_0801 adenylosuccinate synthetase mazei	2.42	8.09	3.34	TRUE	FALSE
MM_0806 50S ribosomal protein L31	4.79	12.93	2.70	TRUE	FALSE
MM_0808 50S ribosomal protein LX	2.30		0.00	FALSE	TRUE
MM_0814 peroxiredoxin mazei Go1]	4.50		0.00	FALSE	TRUE
MM_0817 pyrroline-5-carboxylate reductase mazei	1.55	5.86	3.78	TRUE	FALSE

Protein Name	MeOH fmol of protein	MMA fmol of protein	MMA/ MeOH	Upregulated in MMA 2.5-fold higher	Downregulated in MMA 2.5-fold lower
MM_0825 hypothetical protein	2.79	12.06	4.32	TRUE	FALSE
MM_0842 nickel responsive regulator	7.10	18.61	2.62	TRUE	FALSE
MM_0855 phosphoribosylaminoimidazole-succinocarboxamide synthase	1.51	4.92	3.25	TRUE	FALSE
MM_0858 translation initiation factor Sui1	1.95		0.00	FALSE	TRUE
MM_0860 phosphoribosylformylglycinamidine synthase II	1.49	7.09	4.77	TRUE	FALSE
MM_0867 methionyl-tRNA synthetase mazei	1.28	4.64	3.61	TRUE	FALSE
MM_0869 hypothetical protein	0.72		0.00	FALSE	TRUE
MM_0871 hypothetical protein	1.43		0.00	FALSE	TRUE
MM_0898 IMP cyclohydrolase mazei	1.24		0.00	FALSE	TRUE
MM_0911 ABC transporter ATP-binding protein	2.42	14.46	5.98	TRUE	FALSE
MM_0944 methyl coenzyme M reductase	1.57		0.00	FALSE	TRUE
MM_0967 glutamate synthase_ large chain	2.12	7.00	3.30	TRUE	FALSE
MM_0968 glutamate synthase_ large chain	1.88	8.86	4.71	TRUE	FALSE
MM_0969 coenzyme F420 hydrogenase subunit	3.16	10.47	3.31	TRUE	FALSE
MM_0977 F420-dependent NADP reductase	1.30	5.96	4.57	TRUE	FALSE
MM_0990 nucleotide-binding protein mazei	3.18	9.34	2.94	TRUE	FALSE
MM_0994 precorrin-8X methylmutase mazei	1.37		0.00	FALSE	TRUE
MM_0998 precorrin-4 C11-methyltransferase mazei	1.31	5.24	4.01	TRUE	FALSE
MM_1003 isocitrate dehydrogenase	2.68	10.91	4.06	TRUE	FALSE
MM_1005 Zinc finger protein	1.44		0.00	FALSE	TRUE
MM_1008 cell division protein FtsZ	3.11	16.30	5.24	TRUE	FALSE
MM_1012 50S ribosomal protein L1	5.28	21.77	4.12	TRUE	FALSE
MM_1013 acidic ribosomal protein P0	13.77	39.76	2.89	TRUE	FALSE
MM_1014 50S ribosomal protein L12	16.93		0.00	FALSE	TRUE
MM_1025 thiamine biosynthesis protein ThiC	17.71	62.88	3.55	TRUE	FALSE
MM_1028 transcription factor mazei	2.10	10.67	5.09	TRUE	FALSE
MM_1045 branched-chain amino acid aminotransferase	3.95		0.00	FALSE	TRUE
MM_1051 chromosomal protein mazei	1.32	4.31	3.26	TRUE	FALSE
MM_1073 methanol corrinoid protein	89.48		0.00	FALSE	TRUE
MM_1074 methanol:corrinoid methyltransferase mazei	25.51		0.00	FALSE	TRUE
MM_1098 hypothetical protein	1.76	11.80	6.70	TRUE	FALSE
MM_1106 phosphoserine phosphatase mazei	8.34	22.05	2.64	TRUE	FALSE
MM_1108 F420-dependent methylenetetrahydromethanopterin dehydrogenase	38.60	121.97	3.16	TRUE	FALSE
MM_1114 hypothetical protein	5.05	21.57	4.27	TRUE	FALSE
MM_1152 aspartate aminotransferase mazei	1.98	5.93	3.00	TRUE	FALSE
MM_1154 NDP-N-acetyl-D-galactosaminuronic acid dehydrogenase	3.51		0.00	FALSE	TRUE
MM_1200 30S ribosomal protein S17	12.46	42.51	3.41	TRUE	FALSE

Protein Name	MeOH fmol of protein	MMA fmol of protein	MMA/ MeOH	Upregulated in MMA 2.5-fold higher	Downregulated in MMA 2.5-fold lower
MM_1201 dihydrodipicolinate synthase mazei	3.85	10.39	2.70	TRUE	FALSE
MM_1221 chromosomal protein mazei	6.89	26.93	3.91	TRUE	FALSE
MM_1240 methyl-coenzyme M reductase subunit	261.36	1090.53	4.17	TRUE	FALSE
MM_1241 methyl-coenzyme M reductase subunit	162.18	779.82	4.81	TRUE	FALSE
MM_1244 methyl-coenzyme M reductase subunit	241.12	1251.30	5.19	TRUE	FALSE
MM_1271 fructose-bisphosphate aldolase mazei	3.75	10.27	2.74	TRUE	FALSE
MM_1272 3-dehydroquinate synthase mazei	2.81	11.46	4.08	TRUE	FALSE
MM_1279 bifunctional formaldehyde-activating enzyme/3-hexulose-6-phosphate	4.00	13.17	3.29	TRUE	FALSE
MM_1284 2-isopropylmalate synthase mazei	3.86		0.00	FALSE	TRUE
MM_1295 DNA primase mazei	2.16		0.00	FALSE	TRUE
MM_1303 hypothetical protein	3.20	12.72	3.98	TRUE	FALSE
MM_1304 hypothetical protein	5.37		0.00	FALSE	TRUE
MM_1305 hypothetical protein	5.15	20.05	3.89	TRUE	FALSE
MM_1321 formylmethanofuran--tetrahydromethanopterin formyltransferase	15.86	43.71	2.76	TRUE	FALSE
MM_1341 pyruvate synthase subunit delta	2.45	11.23	4.58	TRUE	FALSE
MM_1342 pyruvate ferredoxin oxidoreductase subunit	5.15	15.88	3.08	TRUE	FALSE
MM_1353 5-methyltetrahydropteroyltriglutamate--homocysteine S-methyltransferase	1.33		0.00	FALSE	TRUE
MM_1356 hypothetical protein	24.66	86.48	3.51	TRUE	FALSE
MM_1357 hypothetical protein	83.74	210.17	2.51	TRUE	FALSE
MM_1358 methyltransferase	13.09	45.16	3.45	TRUE	FALSE
MM_1362 aliphatic sulfonate binding protein	1.90	9.29	4.89	TRUE	FALSE
MM_1368 glutaredoxin-like protein mazei	0.74		0.00	FALSE	TRUE
MM_1370 myo-inositol-1-phosphate synthase mazei	1.58	6.00	3.79	TRUE	FALSE
MM_1379 thermosome subunit alpha	63.66	189.96	2.98	TRUE	FALSE
MM_1385 hypothetical protein	3.56	26.04	7.31	TRUE	FALSE
MM_1397 DNA polymerase sliding clamp	2.56	11.42	4.47	TRUE	FALSE
MM_1419 small heat shock protein	0.95	6.72	7.04	TRUE	FALSE
MM_1436 monomethylamine:corrinoid methyltransferase mazei	5.08	589.12	115.89	TRUE	FALSE
MM_1439 methylcobalamin:coenzyme M methyltransferase	4.30	223.47	51.91	TRUE	FALSE
MM_1456 universal stress protein	9.14	37.51	4.11	TRUE	FALSE
MM_1475 translation initiation factor IF-2	2.30	6.42	2.79	TRUE	FALSE
MM_1476 50S ribosomal protein L10	4.45	11.34	2.55	TRUE	FALSE
MM_1489 3-isopropylmalate dehydrogenase mazei	2.90	13.93	4.80	TRUE	FALSE
MM_1490 3-isopropylmalate dehydratase small subunit	2.31	6.65	2.87	TRUE	FALSE
MM_1502 S-adenosylmethionine synthetase mazei	3.00	9.09	3.03	TRUE	FALSE
MM_1528 aconitate hydratase mazei	1.57	8.72	5.57	TRUE	FALSE

	MeOH	MMA	MMA/ MeOH	Upregulated in MMA	Downregulated in MMA
Protein Name	**fmol of protein**	**fmol of protein**		**2.5-fold higher**	**2.5-fold lower**
MM_1540 tetrahydromethanopterin S-methyltransferase subunit H	33.11		0.00	FALSE	TRUE
MM_1541 tetrahydromethanopterin S-methyltransferase subunit G	11.80		0.00	FALSE	TRUE
MM_1542 tetrahydromethanopterin S-methyltransferase subunit F	1.85		0.00	FALSE	TRUE
MM_1543 tetrahydromethanopterin S-methyltransferase subunit A	9.65	38.87	4.03	TRUE	FALSE
MM_1544 tetrahydromethanopterin S-methyltransferase subunit B	5.48	14.02	2.56	TRUE	FALSE
MM_1545 tetrahydromethanopterin S-methyltransferase subunit C	6.60		0.00	FALSE	TRUE
MM_1547 tetrahydromethanopterin S-methyltransferase subunit E	3.78	12.49	3.30	TRUE	FALSE
MM_1585 iron-sulfur flavoprotein mazei	1.23	6.90	5.59	TRUE	FALSE
MM_1590 hypothetical protein	1.27	9.37	7.36	TRUE	FALSE
MM_1604 tungsten formylmethanofuran dehydrogenase subunit	4.30	16.73	3.89	TRUE	FALSE
MM_1619 ferredoxin mazei Go1]	4.37	24.60	5.63	TRUE	FALSE
MM_1647 methanol:corrinoid methyltransferase MtaB	522.10		0.00	FALSE	TRUE
MM_1648 methanol corrinoid protein MtaC	400.16		0.00	FALSE	TRUE
MM_1689 trimethylamine:corrinoid methyltransferase MttB	0.60	50.34	83.47	TRUE	FALSE
MM_1702 hypothetical protein	2.17	8.59	3.96	TRUE	FALSE
MM_1743 glutamate-1-semialdehyde aminotransferase mazei	1.12		0.00	FALSE	TRUE
MM_1753 D-3-phosphoglycerate dehydrogenase mazei	7.38	21.49	2.91	TRUE	FALSE
MM_1755 50S ribosomal protein L18	5.08	15.17	2.98	TRUE	FALSE
MM_1757 30S ribosomal protein S9	8.53	24.56	2.88	TRUE	FALSE
MM_1759 DNA-directed RNA polymerase subunit	0.46		0.00	FALSE	TRUE
MM_1760 30S ribosomal protein S2	13.30	38.56	2.90	TRUE	FALSE
MM_1770 pyruvate phosphate dikinase	4.96	18.38	3.70	TRUE	FALSE
MM_1797 co-chaperonin GroES mazei	1.99	6.84	3.44	TRUE	FALSE
MM_1798 molecular chaperone GroEL	5.39	26.35	4.89	TRUE	FALSE
MM_1804 rubrerythrin mazei Go1]	3.47	23.39	6.74	TRUE	FALSE
MM_1807 translation initiation factor IF-2	1.83	7.25	3.96	TRUE	FALSE
MM_1808 30S ribosomal protein S27	3.45	16.53	4.79	TRUE	FALSE
MM_1824 ferredoxin mazei Go1]	2.94		0.00	FALSE	TRUE
MM_1843 heterodisulfide reductase subunit	6.12	30.85	5.04	TRUE	FALSE
MM_1844 heterodisulfide reductase subunit	8.02	27.08	3.38	TRUE	FALSE
MM_1851 hypothetical protein	2.50	9.21	3.69	TRUE	FALSE
MM_1879 RNA-binding protein mazei	2.04		0.00	FALSE	TRUE
MM_1880 DNA-directed RNA polymerase subunit	5.94	18.30	3.08	TRUE	FALSE
MM_1881 Sep-tRNA:Cys-tRNA synthetase mazei	0.77	4.21	5.45	TRUE	FALSE

Protein Name	MeOH fmol of protein	MMA fmol of protein	MMA/ MeOH	Upregulated in MMA 2.5-fold higher	Downregulated in MMA 2.5-fold lower
MM_1916 lysyl-tRNA synthetase mazei	0.89		0.00	FALSE	TRUE
MM_1939 glutamine-binding protein mazei	2.44	18.81	7.71	TRUE	FALSE
MM_1963 tyrosyl-tRNA synthetase mazei	2.17	10.95	5.04	TRUE	FALSE
MM_1976 hypothetical protein MM_1976	177.44	419.63	2.36	FALSE	FALSE
MM_1978 tungsten formylmethanofuran dehydrogenase subunit	5.75	19.13	3.33	TRUE	FALSE
MM_1979 tungsten formylmethanofuran dehydrogenase subunit	4.50	22.74	5.05	TRUE	FALSE
MM_1980 tungsten formylmethanofuran dehydrogenase subunit	6.88	20.82	3.03	TRUE	FALSE
MM_2015 nascent polypeptide-associated complex	1.97		0.00	FALSE	TRUE
MM_2016 HesB protein mazei	9.53	24.56	2.58	TRUE	FALSE
MM_2035 orotate phosphoribosyltransferase-like protein	1.97	6.88	3.50	TRUE	FALSE
MM_2037 hypothetical protein	2.99	13.31	4.44	TRUE	FALSE
MM_2039 30S ribosomal protein S8	13.87	34.96	2.52	TRUE	FALSE
MM_2040 AsnC family transcriptional regulator	2.47	8.23	3.33	TRUE	FALSE
MM_2066 30S ribosomal protein S15	10.21	35.33	3.46	TRUE	FALSE
MM_2069 Iron(III) dicitrate-binding protein	1.91	11.02	5.78	TRUE	FALSE
MM_2089 acetyl-CoA decarbonylase/synthase	1.97	8.93	4.53	TRUE	FALSE
MM_2124 50S ribosomal protein L3P	9.93	47.58	4.79	TRUE	FALSE
MM_2125 50S ribosomal protein L4	11.39	53.52	4.70	TRUE	FALSE
MM_2129 50S ribosomal protein L22	4.93	13.81	2.80	TRUE	FALSE
MM_2131 50S ribosomal protein L29	7.11	28.25	3.97	TRUE	FALSE
MM_2133 30S ribosomal protein S17	8.82	40.48	4.59	TRUE	FALSE
MM_2134 50S ribosomal protein L14	6.88	18.77	2.73	TRUE	FALSE
MM_2135 50S ribosomal protein L24	5.68	18.40	3.24	TRUE	FALSE
MM_2136 30S ribosomal protein S4	7.75	26.67	3.44	TRUE	FALSE
MM_2137 50S ribosomal protein L5	5.04	19.60	3.89	TRUE	FALSE
MM_2139 30S ribosomal protein S8	14.20	66.27	4.67	TRUE	FALSE
MM_2142 50S ribosomal protein L19	10.07	47.22	4.69	TRUE	FALSE
MM_2143 50S ribosomal protein L18	7.47	27.96	3.74	TRUE	FALSE
MM_2146 50S ribosomal protein L15	11.08		0.00	FALSE	TRUE
MM_2148 adenylate kinase mazei	5.52	24.14	4.37	TRUE	FALSE
MM_2155 30S ribosomal protein S13	11.85	33.47	2.82	TRUE	FALSE
MM_2157 30S ribosomal protein S11	10.14	49.62	4.89	TRUE	FALSE
MM_2158 DNA-directed RNA polymerase subunit	1.91	6.93	3.62	TRUE	FALSE
MM_2169 F420-nonreducing hydrogenase II	2.75	9.84	3.58	TRUE	FALSE
MM_2170 F420-nonreducing hydrogenase II_ large	7.97		0.00	FALSE	TRUE
MM_2181 fructose 1_6-bisphosphatase II	1.68		0.00	FALSE	TRUE
MM_2263 30S ribosomal protein S10	10.17	26.30	2.59	TRUE	FALSE

Protein Name	MeOH fmol of protein	MMA fmol of protein	MMA/ MeOH	Upregulated in MMA 2.5-fold higher	Downregulated in MMA 2.5-fold lower
MM_2264 elongation factor 1-alpha	63.61	174.70	2.75	TRUE	FALSE
MM_2265 elongation factor EF-2	10.38	33.93	3.27	TRUE	FALSE
MM_2266 30S ribosomal protein S7	10.60	28.12	2.65	TRUE	FALSE
MM_2267 30S ribosomal protein S12	5.69	23.77	4.18	TRUE	FALSE
MM_2270 DNA-directed RNA polymerase subunit	1.38		0.00	FALSE	TRUE
MM_2271 DNA-directed RNA polymerase subunit	2.62	7.81	2.99	TRUE	FALSE
MM_2273 DNA-directed RNA polymerase subunit	2.08		0.00	FALSE	TRUE
MM_2278 S-adenosyl-L-homocysteine hydrolase mazei	1.99	6.39	3.21	TRUE	FALSE
MM_2313 F420-nonreducing hydrogenase I_ large	2.48	9.94	4.00	TRUE	FALSE
MM_2314 F420-nonreducing hydrogenase I	1.42	4.69	3.29	TRUE	FALSE
MM_2324 ech hydrogenase subunit	2.61		0.00	FALSE	TRUE
MM_2336 translation initiation factor IF-1A	2.22	10.60	4.78	TRUE	FALSE
MM_2352 hypothetical protein	1.33	5.95	4.49	TRUE	FALSE
MM_2357 hypothetical protein	1.31		0.00	FALSE	TRUE
MM_2371 hypothetical protein	3.03	10.73	3.54	TRUE	FALSE
MM_2383 small nuclear riboprotein-like protein	2.66		0.00	FALSE	TRUE
MM_2432 pyridoxal biosynthesis lyase PdxS	5.67	15.58	2.75	TRUE	FALSE
MM_2462 30S ribosomal protein S6	14.67	45.73	3.12	TRUE	FALSE
MM_2464 nucleoside diphosphate kinase	3.73		0.00	FALSE	TRUE
MM_2465 50S ribosomal protein L24	1.05	3.93	3.72	TRUE	FALSE
MM_2466 30S ribosomal protein S28	3.11	19.90	6.40	TRUE	FALSE
MM_2489 NADH dehydrogenase subunit C	2.36	10.66	4.52	TRUE	FALSE
MM_2505 molecular chaperone DnaK	13.02	60.26	4.63	TRUE	FALSE
MM_2506 heat shock protein GrpE	2.07	7.49	3.61	TRUE	FALSE
MM_2513 hypothetical protein	4.47	19.57	4.38	TRUE	FALSE
MM_2514 elongation factor 1-beta	9.26		0.00	FALSE	TRUE
MM_2516 transcriptional regulator mazei	0.69		0.00	FALSE	TRUE
MM_2536 50S ribosomal protein L21	3.25	9.93	3.06	TRUE	FALSE
MM_2616 50S ribosomal protein L15	3.47		0.00	FALSE	TRUE
MM_2620 proteasome subunit alpha	5.65	18.77	3.32	TRUE	FALSE
MM_2623 exosome complex exonuclease 1	3.29	13.34	4.06	TRUE	FALSE
MM_2624 exosome complex RNA-binding protein	1.78		0.00	FALSE	TRUE
MM_2649 LL-diaminopimelate aminotransferase mazei	1.92	14.49	7.54	TRUE	FALSE
MM_2653 N(5)_N(10)-methenyltetrahydromethanopterin cyclohydrolase	2.72		0.00	FALSE	TRUE
MM_2656 peptidyl-prolyl cis-trans isomerase	9.15	24.78	2.71	TRUE	FALSE
MM_2721 hypothetical protein	1.57	15.45	9.87	TRUE	FALSE
MM_2772 hypothetical protein	4.03	16.07	3.99	TRUE	FALSE
MM_2782 glyceraldehyde-3-phosphate dehydrogenase mazei	2.92	12.79	4.38	TRUE	FALSE

Protein Name	MeOH fmol of protein	MMA fmol of protein	MMA/ MeOH	Upregulated in MMA 2.5-fold higher	Downregulated in MMA 2.5-fold lower
MM_2836 phosphopyruvate hydratase mazei	3.21	9.98	3.11	TRUE	FALSE
MM_2860 hypothetical protein	3.28		0.00	FALSE	TRUE
MM_2867 coenzyme F390 synthetase/phenylacetyl-CoA ligase	4.17	18.73	4.49	TRUE	FALSE
MM_2961 dimethylamine corrinoid protein	1.94	92.87	47.76	TRUE	FALSE
MM_2967 isoleucyl-tRNA synthetase mazei	1.88	6.32	3.37	TRUE	FALSE
MM_3179 transcriptional regulator mazei	2.09	9.45	4.51	TRUE	FALSE
MM_3180 acetyl-CoA synthetase mazei	3.70	14.84	4.01	TRUE	FALSE
MM_3182 2-ketoisovalerate ferredoxin reductase	3.54	13.42	3.79	TRUE	FALSE
MM_3183 ketoisovalerate oxidoreductase subunit	3.11	11.66	3.75	TRUE	FALSE
MM_3188 glutamine synthetase mazei	22.77	70.34	3.09	TRUE	FALSE
MM_3335 monomethylamine methyltransferase mazei	5.60	721.45	128.92	TRUE	FALSE

Table 2.2 Regulation of proteins grown in DMA versus MeOH substrates, harvested during mid-log growth phase (relevant proteins highlighted in green are upregulated in DMA; pink are down regulated in DMA)

	MeOH	DMA	DMA/ MeOH	Upregulated in DMA	Downregulated in MMA
Protein Name	**fmol of protein**	**fmol of protein**	**fmol of protein**	**2.5-fold higher**	**2.5-fold lower**
MM_0011 hypothetical protein MM_0011	0.46		0.00	FALSE	TRUE
MM_0037 argininosuccinate synthase	1.83	5.52	3.01	TRUE	FALSE
MM_0042 glycine betaine transporter_ substrate-binding protein	2.18		0.00	FALSE	TRUE
MM_0072 thermosome subunit	8.37	42.10	5.03	TRUE	FALSE
MM_0074 aspartyl-tRNA synthetase	3.20		0.00	FALSE	TRUE
MM_0123 universal stress protein	1.53		0.00	FALSE	TRUE
MM_0125 universal stress protein	8.88	23.08	2.60	TRUE	FALSE
MM_0142 orotate phosphoribosyltransferase	0.44		0.00	FALSE	TRUE
MM_0174 methanol corrinoid protein	1.19		0.00	FALSE	TRUE
MM_0175 methanol:corrinoid methyltransferase	5.51		0.00	FALSE	TRUE
MM_0263 hypothetical protein MM_0263	0.35		0.00	FALSE	TRUE
MM_0282 threonine synthase	1.67		0.00	FALSE	TRUE
MM_0293 replication factor A	1.10		0.00	FALSE	TRUE
MM_0305 hypothetical protein MM_0305	3.73		0.00	FALSE	TRUE
MM_0307 uroporphyrin-III C-methyltransferase	1.42		0.00	FALSE	TRUE
MM_0337 tryptophan synthase subunit beta	1.64		0.00	FALSE	TRUE
MM_0339 small nuclear ribonucleoprotein	3.36	10.61	3.16	TRUE	FALSE
MM_0363 hypothetical protein MM_0363	0.80		0.00	FALSE	TRUE
MM_0410 hypothetical protein MM_0410	1.09		0.00	FALSE	TRUE
MM_0448 hypothetical protein MM_0448	2.78		0.00	FALSE	TRUE
MM_0495 acetate kinase	4.60	11.81	2.57	TRUE	FALSE
MM_0496 phosphate acetyltransferase	5.68	21.56	3.79	TRUE	FALSE
MM_0517 sirohydrochlorin cobaltochelatase	9.23	41.14	4.46	TRUE	FALSE
MM_0537 hypothetical protein MM_0537	3.72		0.00	FALSE	TRUE
MM_0593 5-formaminoimidazole-4-carboxamide-1-(beta)-D-ribofuranosyl	1.24		0.00	FALSE	TRUE
MM_0594 translation initiation factor IF-2 subunit gamma	2.49		0.00	FALSE	TRUE
MM_0599 30S ribosomal protein S24	4.07	19.76	4.86	TRUE	FALSE
MM_0627 F420H2 dehydrogenase subunit F	**3.05**	**9.53**	**3.13**	**TRUE**	**FALSE**
MM_0628 methylenetetrahydromethanopterin reductase	95.07		0.00	FALSE	TRUE
MM_0631 hypothetical protein MM_0631	2.60		0.00	FALSE	TRUE
MM_0635 flavoprotein	2.03		0.00	FALSE	TRUE
MM_0664 oxidoreductase	1.37		0.00	FALSE	TRUE

	MeOH	DMA	DMA/ MeOH	Upregulated in DMA	Downregulated in MMA
Protein Name	**fmol of protein**	**fmol of protein**	**fmol of protein**	**2.5-fold higher**	**2.5-fold lower**
MM_0668 ketol-acid reductoisomerase	10.86	36.30	3.34	TRUE	FALSE
MM_0669 acetolactate synthase 3 regulatory subunit	4.27	16.63	3.89	TRUE	FALSE
MM_0670 acetolactate synthase 3 catalytic subunit	3.94		0.00	FALSE	TRUE
MM_0674 prefoldin subunit beta	3.61	12.62	3.49	TRUE	FALSE
MM_0684 acetyl-CoA decarbonylase/synthase complex subunit alpha	31.99	135.82	4.25	TRUE	FALSE
MM_0685 acetyl-CoA decarbonylase/synthase complex subunit epsilon	26.96		0.00	FALSE	TRUE
MM_0686 acetyl-CoA decarbonylase/synthase complex subunit beta	60.86	254.80	4.19	TRUE	FALSE
MM_0687 nitrogenase iron protein	13.04		0.00	FALSE	TRUE
MM_0688 acetyl-CoA decarbonylase/synthase complex subunit delta	18.51		0.00	FALSE	TRUE
MM_0689 acetyl-CoA decarbonylase/synthase complex subunit gamma	25.55	84.90	3.32	TRUE	FALSE
MM_0694 proteasome subunit beta	4.75		0.00	FALSE	TRUE
MM_0707 prolyl-tRNA synthetase	1.20		0.00	FALSE	TRUE
MM_0714 aldolase	1.84		0.00	FALSE	TRUE
MM_0747 ATP-dependent RNA helicase	3.12		0.00	FALSE	TRUE
MM_0757 NifB protein	1.83		0.00	FALSE	TRUE
MM_0767 hypothetical protein MM_0767	4.16	16.82	4.04	TRUE	FALSE
MM_0774 hypothetical protein MM_0774	9.33		0.00	FALSE	TRUE
MM_0778 V-type ATP synthase subunit D	2.62		0.00	FALSE	TRUE
MM_0780 V-type ATP synthase subunit A	18.01	45.78	2.54	TRUE	FALSE
MM_0784 A1AO H+ ATPase subunit K	**41.36**		**0.00**	**FALSE**	**TRUE**
MM_0786 A1AO H+ ATPase subunit H	**5.13**		**0.00**	**FALSE**	**TRUE**
MM_0801 adenylosuccinate synthetase	2.42		0.00	FALSE	TRUE
MM_0817 pyrroline-5-carboxylate reductase	1.55		0.00	FALSE	TRUE
MM_0824 universal stress protein	1.82		0.00	FALSE	TRUE
MM_0825 hypothetical protein MM_0825	2.79		0.00	FALSE	TRUE
MM_0842 nickel responsive regulator	7.10	25.69	3.62	TRUE	FALSE
MM_0855 phosphoribosylaminoimidazole-succinocarboxamide synthase	1.51		0.00	FALSE	TRUE
MM_0858 translation initiation factor Sui1	1.95		0.00	FALSE	TRUE
MM_0860 phosphoribosylformylglycinamidine synthase II	1.49		0.00	FALSE	TRUE
MM_0867 methionyl-tRNA synthetase	1.28		0.00	FALSE	TRUE
MM_0869 hypothetical protein MM_0869	0.72		0.00	FALSE	TRUE
MM_0871 hypothetical protein MM_0871	1.43		0.00	FALSE	TRUE
MM_0898 IMP cyclohydrolase	1.24		0.00	FALSE	TRUE
MM_0911 ABC transporter ATP-binding protein	2.42		0.00	FALSE	TRUE
MM_0922 translation initiation factor IF-5A	5.64		0.00	FALSE	TRUE

Protein Name	MeOH fmol of protein	DMA fmol of protein	DMA/ MeOH fmol of protein	Upregulated in DMA 2.5-fold higher	Downregulated in MMA 2.5-fold lower
MM_0944 methyl coenzyme M reductase system_ component A2	1.57		0.00	FALSE	TRUE
MM_0967 glutamate synthase_ large chain	2.12		0.00	FALSE	TRUE
MM_0968 glutamate synthase_ large chain	1.88		0.00	FALSE	TRUE
MM_0969 coenzyme F420 hydrogenase subunit beta	3.16		0.00	FALSE	TRUE
MM_0977 F420-dependent NADP reductase	1.30		0.00	FALSE	TRUE
MM_0990 nucleotide-binding protein	3.18		0.00	FALSE	TRUE
MM_0994 precorrin-8X methylmutase	1.37		0.00	FALSE	TRUE
MM_0998 precorrin-4 C11-methyltransferase	1.31		0.00	FALSE	TRUE
MM_1003 isocitrate dehydrogenase	2.68	7.08	2.64	TRUE	FALSE
MM_1005 Zinc finger protein	1.44		0.00	FALSE	TRUE
MM_1008 cell division protein FtsZ	3.11	11.11	3.57	TRUE	FALSE
MM_1011 50S ribosomal protein L17	7.92		0.00	FALSE	TRUE
MM_1013 acidic ribosomal protein P0	13.77		0.00	FALSE	TRUE
MM_1014 50S ribosomal protein L12	16.93		0.00	FALSE	TRUE
MM_1025 thiamine biosynthesis protein ThiC	17.71	67.30	3.80	TRUE	FALSE
MM_1045 branched-chain amino acid aminotransferase	3.95		0.00	FALSE	TRUE
MM_1051 chromosomal protein	1.32		0.00	FALSE	TRUE
MM_1070 methylcobalamin:coenzyme M methyltransferase	142.31		0.00	FALSE	TRUE
MM_1071 hypothetical protein MM_1071	5.68		0.00	FALSE	TRUE
MM_1073 methanol corrinoid protein	89.48		0.00	FALSE	TRUE
MM_1074 methanol:corrinoid methyltransferase	25.51		0.00	FALSE	TRUE
MM_1098 hypothetical protein MM_1098	1.76		0.00	FALSE	TRUE
MM_1106 phosphoserine phosphatase	8.34	24.34	2.92	TRUE	FALSE
MM_1108 F420-dependent methylenetetrahydromethanopterin dehydrogenase	38.60		0.00	FALSE	TRUE
MM_1152 aspartate aminotransferase	1.98		0.00	FALSE	TRUE
MM_1154 NDP-N-acetyl-D-galactosaminuronic acid dehydrogenase	3.51		0.00	FALSE	TRUE
MM_1200 30S ribosomal protein S17	12.46		0.00	FALSE	TRUE
MM_1201 dihydrodipicolinate synthase	3.85		0.00	FALSE	TRUE
MM_1221 chromosomal protein	6.89		0.00	FALSE	TRUE
MM_1240 methyl-coenzyme M reductase subunit alpha	261.36		0.00	FALSE	TRUE
MM_1241 methyl-coenzyme M reductase subunit gamma	162.18	761.31	4.69	TRUE	FALSE
MM_1244 methyl-coenzyme M reductase subunit beta	241.12	776.07	3.22	TRUE	FALSE
MM_1271 fructose-bisphosphate aldolase	3.75	11.70	3.12	TRUE	FALSE
MM_1272 3-dehydroquinate synthase	2.81		0.00	FALSE	TRUE
MM_1279 bifunctional formaldehyde-activating enzyme/3-hexulose-6-phosphate	4.00		0.00	FALSE	TRUE
MM_1284 2-isopropylmalate synthase	3.86	13.12	3.40	TRUE	FALSE

Protein Name	MeOH fmol of protein	DMA fmol of protein	DMA/ MeOH fmol of protein	Upregulated in DMA 2.5-fold higher	Downregulated in MMA 2.5-fold lower
MM_1295 DNA primase	2.16		0.00	FALSE	TRUE
MM_1303 hypothetical protein MM_1303	3.20		0.00	FALSE	TRUE
MM_1304 hypothetical protein MM_1304	5.37	13.70	2.55	TRUE	FALSE
MM_1305 hypothetical protein MM_1305	5.15	17.03	3.30	TRUE	FALSE
MM_1321 formylmethanofuran--tetrahydromethanopterin formyltransferase	15.86	46.28	2.92	TRUE	FALSE
MM_1341 pyruvate synthase subunit delta	2.45		0.00	FALSE	TRUE
MM_1342 pyruvate ferredoxin oxidoreductase subunit gamma	5.15	13.14	2.55	TRUE	FALSE
MM_1353 5-methyltetrahydropteroyltriglutamate--homocysteine S-methyltransfe	1.33		0.00	FALSE	TRUE
MM_1356 hypothetical protein MM_1356	24.66		0.00	FALSE	TRUE
MM_1357 hypothetical protein MM_1357	83.74		0.00	FALSE	TRUE
MM_1358 methyltransferase	13.09		0.00	FALSE	TRUE
MM_1362 aliphatic sulfonate binding protein	1.90		0.00	FALSE	TRUE
MM_1368 glutaredoxin-like protein	0.74		0.00	FALSE	TRUE
MM_1370 myo-inositol-1-phosphate synthase	1.58		0.00	FALSE	TRUE
MM_1379 thermosome subunit alpha	63.66	168.48	2.65	TRUE	FALSE
MM_1385 hypothetical protein MM_1385	3.56	10.26	2.88	TRUE	FALSE
MM_1419 small heat shock protein	0.95		0.00	FALSE	TRUE
MM_1436 monomethylamine:corrinoid methyltransferase	5.08		0.00	FALSE	TRUE
MM_1439 methylcobalamin:coenzyme M methyltransferase	4.30	303.65	70.54	TRUE	FALSE
MM_1456 universal stress protein	9.14	32.26	3.53	TRUE	FALSE
MM_1475 translation initiation factor IF-2 subunit beta	2.30		0.00	FALSE	TRUE
MM_1489 3-isopropylmalate dehydrogenase	2.90	9.55	3.29	TRUE	FALSE
MM_1490 3-isopropylmalate dehydratase small subunit	2.31		0.00	FALSE	TRUE
MM_1502 S-adenosylmethionine synthetase	3.00		0.00	FALSE	TRUE
MM_1528 aconitate hydratase	1.57		0.00	FALSE	TRUE
MM_1540 tetrahydromethanopterin S-methyltransferase subunit H	33.11		0.00	FALSE	TRUE
MM_1541 tetrahydromethanopterin S-methyltransferase subunit G	11.80	41.92	3.55	TRUE	FALSE
MM_1542 tetrahydromethanopterin S-methyltransferase subunit F	1.85		0.00	FALSE	TRUE
MM_1543 tetrahydromethanopterin S-methyltransferase subunit A	9.65		0.00	FALSE	TRUE
MM_1544 tetrahydromethanopterin S-methyltransferase subunit B	5.48		0.00	FALSE	TRUE
MM_1545 tetrahydromethanopterin S-methyltransferase subunit C	6.60		0.00	FALSE	TRUE
MM_1547 tetrahydromethanopterin S-methyltransferase subunit E	3.78		0.00	FALSE	TRUE
MM_1585 iron-sulfur flavoprotein	1.23		0.00	FALSE	TRUE

Protein Name	MeOH fmol of protein	DMA fmol of protein	DMA/ MeOH fmol of protein	Upregulated in DMA 2.5-fold higher	Downregulated in MMA 2.5-fold lower
MM_1590 hypothetical protein MM_1590	1.27		0.00	FALSE	TRUE
MM_1604 tungsten formylmethanofuran dehydrogenase subunit E	4.30	16.32	3.79	TRUE	FALSE
MM_1619 ferredoxin	4.37		0.00	FALSE	TRUE
MM_1627 fructose-bisphosphate aldolase	2.73		0.00	FALSE	TRUE
MM_1647 methanol:corrinoid methyltransferase MtaB	522.10		0.00	FALSE	TRUE
MM_1648 methanol corrinoid protein MtaC	400.16		0.00	FALSE	TRUE
MM_1689 trimethylamine:corrinoid methyltransferase MttB	0.60		0.00	FALSE	TRUE
MM_1743 glutamate-1-semialdehyde aminotransferase	1.12		0.00	FALSE	TRUE
MM_1755 50S ribosomal protein L18	5.08	15.78	3.11	TRUE	FALSE
MM_1759 DNA-directed RNA polymerase subunit K	0.46		0.00	FALSE	TRUE
MM_1760 30S ribosomal protein S2	13.30	35.24	2.65	TRUE	FALSE
MM_1770 pyruvate phosphate dikinase	4.96	14.92	3.00	TRUE	FALSE
MM_1797 co-chaperonin GroES	1.99		0.00	FALSE	TRUE
MM_1804 rubrerythrin	3.47	11.72	3.38	TRUE	FALSE
MM_1807 translation initiation factor IF-2 subunit alpha	1.83		0.00	FALSE	TRUE
MM_1808 30S ribosomal protein S27	3.45		0.00	FALSE	TRUE
MM_1824 ferredoxin	2.94	8.62	2.93	TRUE	FALSE
MM_1843 heterodisulfide reductase subunit	6.12		0.00	FALSE	TRUE
MM_1844 heterodisulfide reductase subunit	8.02	28.74	3.58	TRUE	FALSE
MM_1879 RNA-binding protein	2.04		0.00	FALSE	TRUE
MM_1880 DNA-directed RNA polymerase subunit L	5.94		0.00	FALSE	TRUE
MM_1881 Sep-tRNA:Cys-tRNA synthetase	0.77		0.00	FALSE	TRUE
MM_1916 lysyl-tRNA synthetase	0.89		0.00	FALSE	TRUE
MM_1939 glutamine-binding protein	2.44		0.00	FALSE	TRUE
MM_1963 tyrosyl-tRNA synthetase	2.17		0.00	FALSE	TRUE
MM_1976 hypothetical protein MM_1976	177.44	521.56	2.94	TRUE	FALSE
MM_1979 tungsten formylmethanofuran dehydrogenase subunit A	4.50	12.46	2.77	TRUE	FALSE
MM_2015 nascent polypeptide-associated complex protein	1.97		0.00	FALSE	TRUE
MM_2016 HesB protein	9.53	31.94	3.35	TRUE	FALSE
MM_2035 orotate phosphoribosyltransferase-like protein	1.97	5.67	2.88	TRUE	FALSE
MM_2037 hypothetical protein MM_2037	2.99	7.56	2.52	TRUE	FALSE
MM_2040 AsnC family transcriptional regulator	2.47		0.00	FALSE	TRUE
MM_2069 Iron(III) dicitrate-binding protein	1.91		0.00	FALSE	TRUE
MM_2089 acetyl-CoA decarbonylase/synthase complex subunit alpha	1.97		0.00	FALSE	TRUE
MM_2124 50S ribosomal protein L3P	9.93		0.00	FALSE	TRUE
MM_2125 50S ribosomal protein L4	11.39		0.00	FALSE	TRUE
MM_2130 30S ribosomal protein S3	16.16	43.50	2.69	TRUE	FALSE

Protein Name	MeOH fmol of protein	DMA fmol of protein	DMA/ MeOH fmol of protein	Upregulated in DMA 2.5-fold higher	Downregulated in MMA 2.5-fold lower
MM_2131 50S ribosomal protein L29	7.11	22.87	3.22	TRUE	FALSE
MM_2133 30S ribosomal protein S17	8.82	30.82	3.49	TRUE	FALSE
MM_2135 50S ribosomal protein L24	5.68	14.77	2.60	TRUE	FALSE
MM_2136 30S ribosomal protein S4	7.75	23.54	3.04	TRUE	FALSE
MM_2137 50S ribosomal protein L5	5.04		0.00	FALSE	TRUE
MM_2139 30S ribosomal protein S8	14.20		0.00	FALSE	TRUE
MM_2141 50S ribosomal protein L32	4.29	13.40	3.12	TRUE	FALSE
MM_2142 50S ribosomal protein L19	10.07		0.00	FALSE	TRUE
MM_2146 50S ribosomal protein L15	11.08		0.00	FALSE	TRUE
MM_2155 30S ribosomal protein S13	11.85		0.00	FALSE	TRUE
MM_2157 30S ribosomal protein S11	10.14	43.23	4.26	TRUE	FALSE
MM_2169 F420-nonreducing hydrogenase II	2.75	8.34	3.03	TRUE	FALSE
MM_2170 F420-nonreducing hydrogenase II_ large subunit	7.97		0.00	FALSE	TRUE
MM_2181 fructose 1_6-bisphosphatase II	1.68		0.00	FALSE	TRUE
MM_2264 elongation factor 1-alpha	63.61		0.00	FALSE	TRUE
MM_2265 elongation factor EF-2	10.38	27.09	2.61	TRUE	FALSE
MM_2267 30S ribosomal protein S12	5.69		0.00	FALSE	TRUE
MM_2270 DNA-directed RNA polymerase subunit A''	1.38		0.00	FALSE	TRUE
MM_2271 DNA-directed RNA polymerase subunit A'	2.62		0.00	FALSE	TRUE
MM_2273 DNA-directed RNA polymerase subunit beta''	2.08		0.00	FALSE	TRUE
MM_2278 S-adenosyl-L-homocysteine hydrolase	1.99		0.00	FALSE	TRUE
MM_2313 F420-nonreducing hydrogenase I_ large subunit	2.48		0.00	FALSE	TRUE
MM_2324 ech hydrogenase subunit	2.61	7.70	2.95	TRUE	FALSE
MM_2352 hypothetical protein MM_2352	1.33		0.00	FALSE	TRUE
MM_2357 hypothetical protein MM_2357	1.31		0.00	FALSE	TRUE
MM_2371 hypothetical protein MM_2371	3.03	10.48	3.46	TRUE	FALSE
MM_2394 MerR family transcriptional regulator	3.21		0.00	FALSE	TRUE
MM_2464 nucleoside diphosphate kinase	3.73	13.28	3.56	TRUE	FALSE
MM_2465 50S ribosomal protein L24	1.05		0.00	FALSE	TRUE
MM_2466 30S ribosomal protein S28	3.11		0.00	FALSE	TRUE
MM_2489 NADH dehydrogenase subunit C	2.36		0.00	FALSE	TRUE
MM_2505 molecular chaperone DnaK	13.02	46.60	3.58	TRUE	FALSE
MM_2506 heat shock protein GrpE	2.07		0.00	FALSE	TRUE
MM_2513 hypothetical protein MM_2513	4.47		0.00	FALSE	TRUE
MM_2514 elongation factor 1-beta	9.26		0.00	FALSE	TRUE
MM_2516 transcriptional regulator	0.69		0.00	FALSE	TRUE
MM_2536 50S ribosomal protein L21	3.25	9.13	2.81	TRUE	FALSE
MM_2623 exosome complex exonuclease 1	3.29		0.00	FALSE	TRUE
MM_2624 exosome complex RNA-binding protein Rrp42	1.78		0.00	FALSE	TRUE

Protein Name	MeOH fmol of protein	DMA fmol of protein	DMA/ MeOH fmol of protein	Upregulated in DMA 2.5-fold higher	Downregulated in MMA 2.5-fold lower
MM_2649 LL-diaminopimelate aminotransferase	1.92		0.00	FALSE	TRUE
MM_2653 N(5)_N(10)-methenyltetrahydromethanopterin cyclohydrolase	2.72	10.46	3.85	TRUE	FALSE
MM_2656 peptidyl-prolyl cis-trans isomerase	9.15	24.95	2.73	TRUE	FALSE
MM_2772 hypothetical protein MM_2772	4.03		0.00	FALSE	TRUE
MM_2782 glyceraldehyde-3-phosphate dehydrogenase	2.92		0.00	FALSE	TRUE
MM_2829 peptidyl-prolyl cis-trans isomerase	3.05		0.00	FALSE	TRUE
MM_2860 hypothetical protein MM_2860	3.28		0.00	FALSE	TRUE
MM_2867 coenzyme F390 synthetase/phenylacetyl-CoA ligase	4.17		0.00	FALSE	TRUE
MM_2961 dimethylamine corrinoid protein	1.94	226.90	116.68	TRUE	FALSE
MM_2967 isoleucyl-tRNA synthetase	1.88		0.00	FALSE	TRUE
MM_3045 coenzyme F420 hydrogenase subunit alpha	3.15		0.00	FALSE	TRUE
MM_3179 transcriptional regulator	2.09		0.00	FALSE	TRUE
MM_3180 acetyl-CoA synthetase	3.70		0.00	FALSE	TRUE
MM_3182 2-ketoisovalerate ferredoxin reductase	3.54		0.00	FALSE	TRUE
MM_3183 ketoisovalerate oxidoreductase subunit	3.11		0.00	FALSE	TRUE
MM_3188 glutamine synthetase	22.77	76.44	3.36	TRUE	FALSE
MM_3335 monomethylamine methyltransferase	5.60		0.00	FALSE	TRUE

Table 2.3 Regulation of proteins grown in TMA versus MeOH substrates

	MeOH	TMA	TMA/ MeOH	Upregulated in TMA	Downregulated in TMA
Protein Name	**fmol of protein**	**fmol of protein**	**fmol of protein**	**2.5-fold higher**	**2.5-fold lower**
MM_0142 orotate phosphoribosyltransferase	0.44		0.00	FALSE	TRUE
MM_0174 methanol corrinoid protein	1.19		0.00	FALSE	TRUE
MM_0175 methanol:corrinoid methyltransferase	5.51		0.00	FALSE	TRUE
MM_0263 hypothetical protein MM_0263	0.35		0.00	FALSE	TRUE
MM_0293 replication factor A	1.10		0.00	FALSE	TRUE
MM_0363 hypothetical protein MM_0363	0.80		0.00	FALSE	TRUE
MM_0410 hypothetical protein MM_0410	1.09		0.00	FALSE	TRUE
MM_0436 thioredoxin	4.96		0.00	FALSE	TRUE
MM_0495 acetate kinase	4.60		0.00	FALSE	TRUE
MM_0593 5-formaminoimidazole-4-carboxamide-1-(beta)-D-ribofuranosyl	1.24		0.00	FALSE	TRUE
MM_0686 acetyl-CoA decarbonylase/synthase complex subunit beta	60.86		0.00	FALSE	TRUE
MM_0786 A1AO H+ ATPase subunit H	**5.13**		**0.00**	**FALSE**	**TRUE**
MM_0801 adenylosuccinate synthetase	2.42		0.00	FALSE	TRUE
MM_0855 phosphoribosylaminoimidazole-succinocarboxamide synthase	1.51		0.00	FALSE	TRUE
MM_0869 hypothetical protein MM_0869	0.72		0.00	FALSE	TRUE
MM_0871 hypothetical protein MM_0871	1.43		0.00	FALSE	TRUE
MM_0944 methyl coenzyme M reductase system_ component A2	1.57		0.00	FALSE	TRUE
MM_1005 Zinc finger protein	1.44		0.00	FALSE	TRUE
MM_1028 transcription factor	2.10		0.00	FALSE	TRUE
MM_1045 branched-chain amino acid aminotransferase	3.95		0.00	FALSE	TRUE
MM_1071 hypothetical protein MM_1071	5.68	1.69	0.30	FALSE	TRUE
MM_1073 methanol corrinoid protein	89.48		0.00	FALSE	TRUE
MM_1074 methanol:corrinoid methyltransferase	25.51		0.00	FALSE	TRUE
MM_1098 hypothetical protein MM_1098	1.76		0.00	FALSE	TRUE
MM_1108 F420-dependent methylenetetrahydromethanopterin dehydrogenase	38.60		0.00	FALSE	TRUE
MM_1368 glutaredoxin-like protein	0.74		0.00	FALSE	TRUE
MM_1385 hypothetical protein MM_1385	3.56	11.05	3.10	TRUE	FALSE
MM_1436 monomethylamine:corrinoid methyltransferase	5.08	174.23	34.27	TRUE	FALSE
MM_1439 methylcobalamin:coenzyme M methyltransferase	4.30	108.10	25.11	TRUE	FALSE
MM_1456 universal stress protein	9.14	12.21	1.34	FALSE	FALSE
MM_1545 tetrahydromethanopterin S-methyltransferase subunit C	6.60		0.00	FALSE	TRUE
MM_1585 iron-sulfur flavoprotein	1.23		0.00	FALSE	TRUE
MM_1590 hypothetical protein MM_1590	1.27		0.00	FALSE	TRUE
MM_1647 methanol:corrinoid methyltransferase MtaB	522.10		0.00	FALSE	TRUE
MM_1648 methanol corrinoid protein MtaC	400.16		0.00	FALSE	TRUE
MM_1689 trimethylamine:corrinoid methyltransferase MttB	0.60	531.76	881.82	TRUE	FALSE
MM_1743 glutamate-1-semialdehyde aminotransferase	1.12		0.00	FALSE	TRUE

Protein Name	MeOH fmol of protein	TMA fmol of protein	TMA/ MeOH fmol of protein	Upregulated in TMA 2.5-fold higher	Downregulated in TMA 2.5-fold lower
MM_1759 DNA-directed RNA polymerase subunit K	0.46		0.00	FALSE	TRUE
MM_1879 RNA-binding protein	2.04		0.00	FALSE	TRUE
MM_1916 lysyl-tRNA synthetase	0.89		0.00	FALSE	TRUE
MM_1976 hypothetical protein MM_1976	177.44	220.03	1.24	FALSE	FALSE
MM_2015 nascent polypeptide-associated complex protein	1.97		0.00	FALSE	TRUE
MM_2040 AsnC family transcriptional regulator	2.47		0.00	FALSE	TRUE
MM_2089 acetyl-CoA decarbonylase/synthase complex subunit alpha	1.97		0.00	FALSE	TRUE
MM_2146 50S ribosomal protein L15	11.08	4.27	0.39	FALSE	TRUE
MM_2465 50S ribosomal protein L24	1.05		0.00	FALSE	TRUE
MM_2516 transcriptional regulator	0.69		0.00	FALSE	TRUE
MM_2624 exosome complex RNA-binding protein Rrp42	1.78		0.00	FALSE	TRUE
MM_2653 N(5)_N(10)-methenyltetrahydromethanopterin cyclohydrolase	2.72	7.55	2.78	TRUE	FALSE
MM_2860 hypothetical protein MM_2860	3.28		0.00	FALSE	TRUE
MM_2961 dimethylamine corrinoid protein	1.94	34.01	17.49	TRUE	FALSE
MM_3335 monomethylamine methyltransferase	5.60	223.74	39.98	TRUE	FALSE

Table 2.4 List of proteins involved in the methanogenic process for *Methanosarcina mazei*. Note that mtmB1 (MM_1436/ MM_1437) and mtmB2 (MM_3335/ MM_3336) were annotated and counted as distinct methyltransferases in the collection of this data, even though they could have also been combined.

Corrinoid Protein Subunits			**UniProt**	
Methanol Corrinoid Protein	MM0174		MtaC_METMA	Q8Q0G2
Methanol Corrinoid Protein	MM1073		MtaC_METMA	Q8PXZ3
Methanol Corrinoid Protein	MM1648		MtaC_METMA	Q8PWE1
Monomethylamine Corrinoid Protein 1	MM1438		MtmC1_METMA	P58977
Monomethylamine Corrinoid Protein 2	MM3334		MtmC2_METMA	P58978
Dimethylamine Corrinoid Protein 3	MM1687		MtbC3_METMA	P58981
Dimethylamine Corrinoid Protein 1	MM2052		MtbC1_METMA	P58979
Dimethylamine Corrinoid Protein 2	MM2961		MtbC2_METMA	P58980
Trimethylamine Corrinoid Protein	MM1055		MttC_METMA	Q8PY11
Trimethylamine Corrinoid Protein 1	MM1690		MttC1_METMA	P58982
Trimethylamine Corrinoid Protein 2	MM2047		MttC2_METMA	P58983
Substrate binding subunits				
Methanol:corrinoid methyltransferase	MM0175		MtaB_METMA	Q8Q0G1
Methanol:corrinoid methyltransferase	MM1074		MtaB_METMA	Q8PXZ2
Methanol:corrinoid methyltransferase	MM1647		MtaB_METMA	Q8PWE2
Monomethylamine:corrinoid methyltransferase	MM1437*	*N-term domain*	MtmB_METMA	P58969
Monomethylamine:corrinoid methyltransferase	MM1436*	*C-term domain*	MtmB_METMA	P58969
Monomethylamine:corrinoid methyltransferase	MM3335*	*N-term domain*	MtmB_METMA	P58969
Monomethylamine:corrinoid methyltransferase	MM3336*	*C-term domain*	MtmB_METMA	P58969
Dimethylamine:corrinoid methyltransferase	MM2962	*N-term domain*	MtbB2_METMA	P58971
Dimethylamine:corrinoid methyltransferase	MM2963	*C-term domain*	MtbB2_METMA	P58971
Dimethylamine:corrinoid methyltransferase	MM1693	*N-term domain*	MtbB3_METMA	P58972
Dimethylamine:corrinoid methyltransferase	MM1694	*C-term domain*	MtbB3_METMA	P58972
Dimethylamine:corrinoid methyltransferase	MM2050	*C-term domain*	MtbB1_METMA	P58970
Dimethylamine:corrinoid methyltransferase	MM2051	*N-term domain*	MtbB1_METMA	P58970
Trimethylamine:corrinoid methyltransferase	MM2048	*N-term domain*	MttB2_METMA	P58974
Trimethylamine:corrinoid methyltransferase	MM2049	*C-term domain*	MttB2_METMA	P58974
Trimethylamine:corrinoid methyltransferase	MM1688	*N-term domain*	MttB1_METMA	P58973
Trimethylamine:corrinoid methyltransferase	MM1689	*C-term domain*	MttB1_METMA	P58973

Coenzyme M-Binding Subunits				
Methylcobalamin-coenzyme M methyltransferase	MM1070		MtaA_METMA	Q8PXZ6
Methylcobamide:CoM methyltransferase	MM1439		MtbA_METMA	P58984
Methylcobalamin:coenzyme M methyltransferase	MM1932		MtbA_METMA	Q8PVN1
Methylcobalamin:coenzyme M methyltransferase	MM0176		MtaA_METMA	Q8Q0G0
Methylcobalamin:coenzyme M methyltransferase	MM0505		MtbA_METMA	Q8PZI7

Discussion

When compared to the genome-wide transcriptional profiling study performed by Krazter and colleagues, our whole cell proteomic studies reflect high levels of correlation for the comparison of protein levels in trimethylamine- versus methanol-grown cells in *Methanosarcina mazei* microorganism (see Table 2.5). For example, the genes in Krazter's study and the proteins from our study, such as MM_1436 (monomethylamine:corrinoid methyltransferase mtmB1), MM_1439 (methylcobalamin:coenzyme M methyltransferase mtbA2), and MM_3335 (monomethylamine: corrinoid methyltransferase mtmB2) were all upregulated in TMA-grown cells. Furthermore, while MM_1689 (trimethylamind:corrinoid methyltransferase mttB1 – C-terminal domain) was upregulated in both our proteomics and the genome-wide transcriptional profiling study, the protein levels were considerably upregulated by 881-fold versus 22.30-fold in transcript levels. Nonetheless, even though the transcript levels for MM_0175 (methanol:corrinoid methyltransferase mtaB3), MM_1073 (methanol:corrinod protein mtaC2), and MM_1074 (methanol:corrinoid methyltransferase mtaB2) were all downregulated in TMA-grown cells, the protein levels for these genes were not even detected in our quantitative proteomic study. However, as depicted with the transcript profiling study, protein levels for MM_1071 (hypothetical protein) was downregulated. Therefore, our proteomic studies are in accordance with the transcript profiling study for the comparison of genes grown in TMA versus MeOH substrates for *mazei* cells.

As proposed by Kratzer and colleagues from their transcriptional profiling study, it is possible that the proteins in our study that showed significant fold change in abundance when grown in TMA versus MeOH may be also be tightly regulated. Therefore, we postulate that steps in the methanogenic pathway where proteins were upregulated more than 2.5-fold in TMA-grown *mazei* cells, specifically for the methylotrophic branch of the pathway, are rate- limiting steps that are considerably thermodynamically favorable in the forward, product-forming direction. The

novelty of our research is that we provide a comprehensive whole-cell proteomic study of *Methanosarcina mazei* and its differential regulation in monomethylamine, dimethylamine, and trimethylamine substrates as compared to cells grown in methanol. Few transcript profiling studies have performed such a comparative analysis study in *M. mazei*, and few to no proteomic studies have been performed on this scale. Therefore, our work can complement existing transcript-profiling studies on methylotrophic substrate-specific regulation in *Methanosarcina mazei*.

Methanosarcina mazei Gö1 exhibit precise substrate flexibility and can efficiently switch carbon sources by producing substrate-specific enzymes in the mid-log stage of growth, in an effort to conserve energy. To summarize, the key findings that are significant from this study are:

1. Methanol-grown *M. mazei* cells contained the A_1A_O H^+ ATPase subunit H (MM_0786), and the protein level of the ATPase was downregulated (or not found in significant abundance) in cells grown in MMA, DMA, or TMA.
2. The $F_{420}H_2$ dehydrogenase (MM_0627) was only upregulated in DMA-grown *M. mazei* cells when compared to methanol-grown cells, at approximately 3-fold greater.
3. Substrate-specific methyltransferases accounted for >20% of the total protein content identified, while the methylconezyme M reductases accounted for an additional ~20% of the total protein content
4. The methylotrophic growth media dictates which substrate-specific protein is present in highest abundance. For instance the methanol-specific methyltransferases were in highest abundance in cells grown in methanol growth media.
5. When comparing protein levels to transcript levels, most of the data was in agreement with each other. For instance the substrate-specific corrinoid methyltransferases, which are responsible for transferring the methyl groups from their respective C1 methylotrophic substrate to the corrinoid protein, were all upregulated when *M. mazei*

cells were grown in TMA versus MeOH. The only noticeable difference was that the transcript study did not show any upregulation or down regulation of DMA-corrinoid methymtransferase MtbC3 (MM_2961), while our proteomic study did show a 17.5 fold increase in this protein when cells were grown in TMA. Furthermore, protein levels showed a much greater fold-change than transcript levels. This greater fold change for most of the proteins was approximately one-order of magnitude greater.

Table 2.5 Comparison of transcriptomics data with proteomics data by noting the fold change in the gene or protein, respectively

Gene annotation	Gene no.	Gene Fold change[a]	Protein Fold change[b]	Putative operon
Methanol corrinoid protein MtaC3	MM0174		0	0174-0175
Methanol:corrinoid methyltransferase MtaB3	MM0175	0.25	0	0174-0175
Hypothetical protein	MM0312	0.36	-	0311-0312
Hypothetical protein	MM0408	0.34	-	Single gene
Hypothetical protein	MM0479	0.37	-	Single gene
Hypothetical protein	MM0924	0.28	-	Single gene
Hypothetical protein	MM1071	0.42	0.3	Single gene
Methanol corrinoid protein MtaC2	MM1073	0.005	0	1073-1075
Methanol:corrinoid methyltransferase MtaB2	MM1074	0.006	0	1073-1075
Putative regulatory protein	MM1075	0.07	-	1073-1075
Hypothetical protein	MM1112	0.15	-	Single gene
2-Dehydro-3-desoxyphosphoheptanote aldolase	MM1271	0.18	-	1271-1275
3-Dehydroquinate synthase	MM1272	0.24	-	1271-1275
3-Dehydroquinate dehydratase	MM1273	0.22	-	1271-1275
Shikimate 5-dehydrogenase	MM1274	0.30	-	1271-1275
Prephenate dehydrogenase	MM1275	0.33	-	1271-1275
Methanol:corrinoid methyltransferase MtaB1	MM1647	0.16	0	1647-1648
Methanol corrinoid protein MtaC1	MM1648	0.07	0	1647-1648
Hypothetical protein	MM1761	0.35	-	1760-1764
Mevalonate kinase	MM1762	0.32	-	1760-1764
Hypothetical protein	MM1977	0.38	-	1976-1977
Hypothetical protein	MM2882	0.23	-	2882-2884
Hypothetical protein	MM2933	0.30	-	Single gene
Hypothetical protein	MM3197	0.28	-	Single gene
Hypothetical protein	MM0011	2.38	-	Single gene
Cobyric acid synthase CbiP	MM0093	2.28	-	Single gene
Phosphate acetyltransferase	MM0496	2.25	-	0495-0496
Hypothetical protein	MM0583	3.83	-	Single gene
2-Isopropylmalate synthase	MM0671	3.04	-	Single gene
Hypothetical protein	MM0772	3.53	-	Single gene
Hypothetical protein	MM0869	3.96	0	0869-0872
Beta-ketoacyl synthase/thiolase	MM0870	5.86	-	0869-0872
Hydroxymethylglutaryl-CoA synthase	MM0871	5.27	0	0869-0872
Putative transcriptional regulator	MM0872	5.10	-	0869-0872

Gene annotation	Gene no.	Gene Fold change[a]	Protein Fold change[b]	Putative operon
Thiamine biosynthesis protein ThiC	MM1025	3.34	-	Single gene
2-Isopropylmalate synthase	MM1284	5.26	-	1284-1287
Hypothetical protein	MM1304	2.94	-	Single gene
Formylmethanofuran H_4MPT formyltransferase	MM1321	2.25	-	Single gene
Monomethylamine:corrinoid methyltransferase MtmB1	MM1436	2.26	32.3	1436-1438
Monomethylamine corrinoid protein MtmC1	MM1438	3.42	-	1436-1438
Methylcobalamin:coenzyme M methyltransferase MtbA2	MM1439	3.46	25.1	Single gene
Hypothetical protein	MM1488	2.93	-	1487-1488
Cobalamin biosynthesis protein CobN	MM1601	3.19	-	1601-1602
Cobalamin biosynthesis protein CobN	MM1602	5.40	-	1601-1602
Hypothetical protein	MM1612	6.15	-	Single gene
Dimethylamine corrinoid protein MtbC1	MM1687	32.89	-	1687-1694
Trimethylamine:corrinoid methyltransferase MttB1 (N-terminal domain)	MM1688	40.59	-	1687-1694
Trimethylamine:corrinoid methyltransferase MttB1 (C-terminal domain)	MM1689	22.30	882	1687-1694
Trimethylamine corrionid protein MttC1	MM1690	16.76	-	1687-1694
Trimethylamine permease MttP1	MM1691	4.93	-	1687-1694
Conserved protein	MM1692	2.90	-	1687-1694
Dimethylamine:corrinoid methyltransferase MtbB1	MM1693	3.11	-	1687-1694
Dimethylamine:corrinoid methyltransferase MtbB1 (C-terminal domain)	MM1694	15.21	-	1687-1694
Catalase	MM1950	4.31	-	Single gene
Hypothetical protein	MM1951	12.89	-	Single gene
Alkyl sulfatase	MM1982	4.39	-	Single gene
Hypothetical protein	MM1988	18.36	-	Single gene
Trimethylamine corrionid protein MttC2	MM2047	2.86	-	2047-2052
Trimethylamine:corrinoid methyltransferase MttB2	MM2049	3.45	-	2047-2052
Dimethylamine:corrinoid methyltransferase MtbB2	MM2051	3.51	-	2047-2052
Dimethylamine corrionid protein MtbC2	MM2052		-	2047-2052
Hypothetical protein	MM2338	2.33	-	Single gene
Cobalt transport ATP-binding protein CbiO	MM2387	2.32	-	2386-2388
Anthranilate synthase component I	MM2818	2.51	-	2817-2823

Gene annotation	Gene no.	Gene Fold change[a]	Protein Fold change[b]	Putative operon
Tryptophan synthase, alpha chain	MM2821	2.39	-	2817-2823
Tryptophan synthase subunit beta	MM2822	4.51	-	2817-2823
Hypothetical protein	MM2843	2.89	-	Single gene
Dimethylamine corrinoid protein MtbC3	MM2961		17.5	2961-2963
Dimethylamine:corrinoid methyltransferase MtbB3	MM2962	6.33	-	2961-2963
Dimethylamine:corrinoid methyltransferase MtbB3 (C-terminal domain)	MM2963	11.54	-	2961-2963
Hypothetical protein	MM3011	2.52	-	Single gene
Hypothetical protein	MM3108	3.32	-	Single gene
Monomethylamine corrinoid protein MtmC2	MM3334	2.60	-	3334-3336
Monomethylamine:corrinoid methyltransferase MtmB2	MM3335	2.50	39.9	3334-3336
Monomethylamine:corrinoid methyltransferase MtmB2 (C-terminal domain)	MM3336	2.31	-	3334-3336

[a] Data originally appeared in Kratzer, C.; Carini, P.; Hovey, R.; Deppenmeier, U. Transcriptional Profiling of Methyltransferase Gene during Growth of *Methanosarcina mazei* on Trimethylamine. *Journal of Bacteriology.* **2009**, 191 (16), 5108-5115

[b] Data is from this thesis document

- Indicates that the protein was not on our proteomic list

0 Indicates that the information of the specified protein is not applicable, primarily because the protein was not detected and/ or did not meet error limit criteria outlined in the Methods section in Chapter 2

Conclusion

Based upon our results, *Methanosarcina mazei* are able to use different methyltransferases in a substrate dependent approach. This occurs possibly because the substrates can repress the transcription or translation of other methylotrophic methyltransferases. Furthermore, methyltransferases and methyl-CoM reductases account for ~40% of protein abundance in *Methanosarcina mazei*. According to Galagan and colleagues (Galagan et al. 2002), the 4th largest multigene family in *Methanosarcina acetivorans* is the methyltransferases, which have 46 proteins. Furthermore, out of the 30 largest multigene families that are found in *M. acetivorans*, the 46 proteins belonging to the methyltransferases account for ~7% of the total number of proteins found in the 30 aforementioned multigene families, as opposed to ~20% of the total amount of proteins in our study. The methylcoenzyme M reductases were not among the top 30 multigene families found in *M. acetivorans*, which is different from our findings in *M. mazei,* in which the reductases accounted for ~20% of the total amount of proteins identified. Additionally the reductases resided in the top 10 most abundant proteins regardless of the substrate within which the cells were grown for the *mazei* cell.

The greater relative abundance of methyltransferases indicates that they may play a constitutive role in methanogens (indispensable enzymes) and/or they may be rate-limiting enzymes. Likewise, the S-layer protein MM_1976 was among the membrane-bound proteins in high abundance. The surface protein in *M. acetivorans* was the 2nd largest multigene family and has 62 proteins, which accounts for greater than 9% of the total number of proteins found in the 30 largest multigene families. This is somewhat consistent with our results showing that the surface layer protein in *M. mazei* (MM_1976) accounts for 3% - 7% of the total amount of proteins identified. Consequently, our study on *Methanosarcina mazei* elucidates significant roles of methyltransferases, methyl-coenzyme reductases, and the SLP MM_1976 in methanogenesis;

each can be targeted in future genetic studies for knock down experiments to modulate the production of methane.

The enzyme switching mechanism, in which the substrate-specific methyltransferases found in each specific substrate-grown cell, should be duely noted; as well as the possible cause of the high abundance of the methyltransferases being that the enzymes have a low turnover rate. The low turnover rate is a possible feature of the enzyme Ribulose-1,5-bisphosphate carboxylase/oxygenase (RuBisCO), which is involved in the first major step of the Calvin Cycle of photosynthesis, whereby carbon dioxide is converted to sugar. RuBisCO makes up half of the soluble protein found in the leaves of plants and its slow rate of catalysis is compensated for by having a greater abundance in the cell. The phenomenon observed with the enzyme RuBisCO may also be present in the *mazei* cells with the methyltransferases.

To summarize, the research performed on *M. mazei* grown in different substrates that allowed the quantitative and qualitative analysis of proteins in this methane-producing microorganism at the mid-log stage of growth, has improved our our understanding in:

1. The proteins that are crucial to methanogenesis in *M. mazei*
2. The specific gene protducts involved in methanogenesis and
3. The function of those gene products

Furthermore, it is possible that the transcriptomics data, which coincides with our proteomic data, shows lower quantities of the mRNA because they have a shorter half-life than the proteins.

References

1. Abken, H-J.; Deppenmeier, U. Purification and properties of an F420H2 dehydrogenase from *Methanosarcina mazei* Go1 *Federation of European Microbiological Societies Microbiology Letters.* **1997,** 154, 231-237.
2. Aggeler, R.; Capaldi, R.A. Nucleotide-dependent movement of the epsilon subunit between alpha and beta subunits in the Escherichia coli F1Fo-type ATPase *J. Biol. Chem.* **1996,** *271,* 13888-13891.
3. Basak, S.; Lim, J.; Manimekalai, M.S.S.; Balakrishna, A.M.; Gruber, G.; Crystal- and NMR structures give insights into the role and dynamics of subunit F of the eukaryotic V-ATPase from *Saccharomyces cerevisiae J. Biol. Chem.* **2013,** *288,* 11930-11939.
4. Baumer, S.; Ide, T.;Jacobi, C.; Johann, A.; Gottschalk, G. The F420H2 Dehydrogenase from *Methanosarcina mazei* Is a Redox-driven Proton pump closed related to NADH Dehydrogenases *The Journal of Biological Chemistry.* **2000,** 275:24, 17968-17973.
5. Boekema, E.J.; van Breemen, J.F.; Brisson, A.; Ubbink-Kok, T.; Konings, W.N.; Lolkema, J.S. Connecting stalks in V-type ATPase *Nature.* **1993,** *401,* 37-38.
6. Browne, P.D.; Cadillo-Quiroz, H. Contribution of Transcriptomics to Systems-Level Understanding of Methanogenic Archaea *Archaea.* **2013,** 1-11.
7. Buckhardt, B.C.; Thelen, P. Effect of primary, secondary and tertiary amines on membrane potential and intracellular pH in *Xenopus laevis* oocytes *Arch. Eur. J. Physiol.* **1995,** 429, 306-312.
8. Coskun, U.; Chaban, Y.L.; Singl, A.; Muller, V.; Keegstra, Boekema, E.J.; Gruber, G. Structure and subunit arrangement of the A-type ATP synthase comlex from the archaeon Methanococcus jannaschii visualized by electron microscopy *J. Biol. Chem.* **2004,** *279,* 38644-38648.

9. Coskun, U.; Radermacher, M.; Muller, V.; Ruiz, T.; Gruber, G. Three-dimensional organization of the archaeal A1-ATPase from *Methanosarcina mazei* Go1 *J. Biol. Chem.* **2004,** 279, 22759-22764.
10. Cross, R.L.; Muller, V. The evolution of A-, F-, and V-type ATP synthases and ATPases:reversals in function and changesin the H+/ ATP stoichiometry *FEBS Lett.* **2004,** *576,* 1-4.
11. Culley, D.E.; Kovacik, W.P.; Brockman, F.J.; Zhang, W. Optimization of RNA isolation from the archaebacterium *Methanosarcina barkeri* and validation for oligonucleotide microarray analysis *Journal of Microbiological Methods.* **2006,** 67:1, 36-43.
12. Deckers-Hebestreit, G.; Altendorf, K. The FoF1-type ATP synthases of bacteria: structure and function of the Fo complex *Annu. Rev. Microbiol.* **1996,** 50, 791-824.
13. Deppenmeier, U. The membrane-bound electron transport system of Methanosarcina species *J. Bioenerg Biomembr.* **2004,** *36,* 55-64.
14. Deppenmeier, U.; Blaut, M.; Mahmann, A.; Gottschalk, G. Reduced coenzyme F420: heterodisulfide oxidoreductase, a proton-translocating redox system in methanogenic bacteria *Proceedings for the National Academy of Sciences of the United States of America.* **1990,** 87, 9449-9453.
15. Deppenmeier, U.; Muller, V. Life Close to the Thermodynamic Limit: How Methanogenic Archaea Conserve Energy *Results Probl Cell Differ.* **2007,** 45, 143-152.
16. Dutton, P.L.; Moser, C.C.; Sled, V.; Daldal, F.; Ohnishi, T. *Biochimica et Biophysica Acta.* **1999,** 1364, 245-257.
17. Erde, J.; Loo, R.R.; Loo, J.A. Enhanced FASP (eFASP) to increase proteome coverage and sample recovery for quantitative proteomic experiments. *Journal fo Proteome Research.* **2014,** 13:4, 1885-95.

18. Esteban, O.; Bernal, R.A.; Donohoe, M.; Videler, H.; Sharon, M.; Robinson, C.V.; Stock, D. Stoichiometry and localization of the stator subunits E and G in *Thermus thermophiles* H+-ATPase/ synthase *J. Biolo. Chem.* **2008,** 283, 2595-2603.
19. Feder, M.E.; Walser, J.-C. The biological limitations in transcriptomics in elucidating stress and stress responses *J. Evol. Biol.* **2005,** *18,* 901-910.
20. Ferry, J.G. Biochemistry of Methanogenesis *Critical Reviews in Biochemistry and Molecular Biology.* **1992,** 27:6, 473-503.
21. Fillingame, R.H. H+ transport and coupling by the Fo sector of the ATP-synthase – insights into the molecular mechanism of function *J. Bioenerg. Biomembr.* **1992,** 24, 485-491.
22. Gayen, S.; Vivekanandan, S.; Biukovic, G.; Gruber, G.; Yoon, H.S. NMR solution structure of subunit F of the methanogenic A1Ao adenosine triphosphate synthase and its interaction with the nucleotide-binding subunit B *Biochemistry.* **2007,** *46,* 11684-11694.
23. Gloger, C.; Born, A-K.; Antosch, M.; Muller. The a subunit of the A1Ao ATP synthase of *Methanosarcina mazei* Go1 contains two conserved arginine residues that are crucial for ATP synthesis *Biochimica et Biophysica Acta.* **2015,** 1847, 505-513.
24. Gruber, G.; Manimekalai, M.S.S.; Mayer, F.; Muller, V. ATP synthases from archaea: the beauty of a molecular motor *Biochimica et Biophysica Acta Bioenergetics.* **2014,** *1837,* 940-952.
25. Gruber, G.; Svergun, D.I.; Coskun, U.; Lemker, T.; Koch, M.H.; Schagger, H.; Muller, V. Structural Insights into the A1-ATPase from the archaeon *Methanosarcina mazei* Go1 *Biochemistry.* **2001,** 40, 1890-1896.
26. Hovey, R.; Lentes, S.; Ehrenreich, A.; Salmon, K.; Saba, K.; Gottschalk, G.; Gunsalus, R.P.; Deppenmeier, U. DNA microarray analysis of *Methanosarcina mazei* Go1 reveals

adaptation to different methanogenic substrates *Molecular Genetics and Genomics.* **2005,** 273:3, 225-239.

27. Jager, D.; Pernitzsch, S.R.; Richter, A.S.; Backofen, R.; Sharma, C.M.; Schmitz, R.A. An archaeal sRNA targeting cis and trans-encoded mRNAs via two distinct domains *Nucleic Acids Research.* **2012,** 40:21, 10964-10979.
28. Kratzer, C.; Carini, P.; Hovey, R.; Deppenmeier, U. Transcriptional Profiling of Methyltransferase Gene during Growth of *Methanosarcina mazei* on Trimethylamine *Journal of Bacteriology.* **2009,**191:16, 5108-5115.
29. Lange, C.; Zaigler, M.; Hammelmann, M.; Twellmeyer, J.; Raddatz, G.; Schuster, S.C.; Oesterhelt, D.; Soppa, J. Genome-wide analysis of growth phase-dependent translational and transcriptional regulation in halophilic archaea *BMC Genomics.* **2007,** 8:415, 1-16.
30. Lau, W.C.; Rubinstein, J.L. Subnanometre-resolution structure of the intact *Thermus thermophiles* H+-driven ATP synthase *Nature.* **2012,** 481, 214-218.
31. Li, L.; Li, Q.; Rohlin, L.; Kim, U.; Salmon, K.; Rejtar, T.; Gunsalus, R.P.; Karger, B.L.; Ferry, J.G. Quantitative proteomics and microarray analysis of the archaeon *Methanosarcina acetivorans* grown in acetate vs methanol *Journal of Proteome Research.* **2007,** 6:2, 759-771.
32. Liu, Y.; Boone, D.R.; Sleat, R.; Mah, R.A.. *Methanosarcina mazei* LYC, a new methanogenic isolate which produces a disaggregating enzyme. *Appl Environ Miocrobiol.* **1985,** 49:3, 608-13.
33. Marshansky, V.; Rubinstein, J.; Gruber, G. Eukaryotic V-ATPases: novel structural findings and functional insights *Biochimica et Biophysica Acta Bioenergetics.* **2014,** *1837,* 857-879.
34. Maestrojuan, G.M.; Boone, J.E.; Mah, R.A.; Menaia, J.A.G.F.; Sachs, M.S.; Boone, D.R. Taxonomy and Halotolerance of mesophilic *Methanosarcina* strains, Assignment of

strains to species, and synonomy of *Mehtanosarcina mazei* and *Methanosarcina frisia. International Journal of Systematic and Evolutionary Microbiology*. **1992,** 42:4, 561-567.

35. Muller, V. Energy Conservation of Acetogenic bacteria. *Appl Environ Microbiol.* **2003,** 69:11, 6345-6353.
36. Noji, H.; Yasuda, R.; Yoshida, M.; Jr Kinosita, K. Direct observation of the rotation of F1-ATPase *Nature.* **1997,** *386,* 299-302.
37. Portnoy, V.; Schuster, G. RNA polyadenylation and degradation in different Archaea; roles of the exosome and RNase R *Nucleic Acids Research.* **2006,** 34:20, 5923-5931.
38. Schlegel, K.; Muller, V. Evolution of Na(+) and H(+) Bionergetics in methanogenic archaea. *Biochem Soc Trans.* **2013,** 41:1, 421-426.
39. Schafer,I.; Rossle, M.; Biukovic, G.; Muller, V.; Gruber, G. Structural and functional analysis of the coupling subunit F in solution and topological arrangement of the stalk domains of methanogenic A1Ao ATPsynthase *J. Bioenerg. Biomembr.* **2006,** *38,* 83-92.
40. Singh, D.; Sielaff, H.; Sundararaman, L.; Bhushan, S.; Gruber, G. The stimulating role of subunit F in ATPase activity inside the A1-complex of the *Methanosarcina mazei* Go1 A1Ao ATP synthase *Biochimica et Biophysica Acta.* **2016,** 1857, 177-187.
41. Sonnleitner, E.; Abdou, L.; Hass, D. Small RNA as global regulator of carbon catabolite repression in *Pseudomonas aeruginosa Proceedings for the National Academy of Sciences of the United States of America.* **2009,** 106:51, 21866-21871.
42. van der Meijden, P.; Heythuysen, H.J.; Pouwels, A.; Houwen, F.; van der Drift, C.; Vogels, G.D. Methyltransferases involved in methanol conversion by *Methanosarcina barkeri Arch. Microbiol.* **1983,** *134:3,* 238-42.
43. van der Meijden, P.; te Brommelstroet, B.W.; Poirot, C.M.; van der Drift, C.; Vogels, G.D. Purification and properties of methanol:5 hydroxy-benzimidazolyl cobamide methyltransferase from *Methanosarcina barkeri J. Bacteriol.* **1984,** 160, 629-635.

44. Vogels, G.D.; Keltjens, J.T.; van der Drift, C. Biochemistry of methane production *Biology of Anaerobic Microorganisms,* Zehnder, A.J.B., Ed., Wiley, New York, **1988,** 707.

45. Vonck, J.; Pisa, K.Y., Morgner, N.; Brutschy, B.; Muller, V. Three-dimensional structure of A1Ao ATP synthase from the hyperthermophilic archaeon *Pyrococcus furiosus* by electron microscopy *J. Biolo. Chem.* **2009,** 284, 10110-13406.

46. Xia, Q.; Henderickson, E.L.; Zhang, Y.; Wang, T.; Taub, F.; Moore, B.C.; Porat, I.; Whitman, W.B.; Hackett, M.; Leigh, J.A. Quantitative proteomics of the archaeon *Mehtanococcus maripaludis* validated by microarray analysis and real time PCR *Molecular and Cellular Proteomics.* **2006,** 5:5, 868-881.

47. Kratzer, C.; Carini, P.; Hovery, R.; Deppenmeier, U. Transcriptional Profiling of Methyltransferase genes during growth of *Methanosarcina mazei* on Trimethylamine. *Journal of Bacteriology*. **2009,** 191:16, 5108-5115.

48. Galagan et al. The genome of *M. acetivorans* reveals extensive metabolic and physiological diversity. *Genome research.* **2002,** 532-542.

CHAPTER 3

Methanosarcina mazei Gö1 Stationary Phase Proteomic Analysis

Introduction: The 4 Growth Phases

The four stages of growth in microorganisms such as *Methanosarcina mazei* are the lag, exponential, stationary and death phase, with each stage being associated with distinct physiology. During the lag phase of growth, laboratory cells adapt to the growth culture, a process that requires time to transcribe mRNA and translate proteins. During this phase of growth, cells recognize and synthesize the appropriate enzymes for glucose catabolism. Archaea, such as *Methanosarcina barkeri,* can participate in either the classical glycolytic pathway or the modified route of the Entner–Doudoroff pathway, which uses different enzymes. When exogenous hexose is not available as the carbon source for cell growth, gluconeogenesis becomes the pathway for the generation of polysaccharides. The growth of the cells during all four phases can be measured by determining the colony forming units (CFU) per volume as a function of time or the optical density. Next, the exponential phase is characterized by rapid growth on the order of 2^n cell divisions, whereby each cell division results in a doubling of the cell number, and n is equal to the number of cell divisions. More accurately, if the initial cell number is X_o, then the number of cells after n cell divisions is $2^n X_o$. Other factors, such as generation time, can be taken into consideration to determine the number of cells or cell mass (X). The transition between the lag and the exponential phases is determined after the population of the first colony has doubled.

After the exponential growth phase is complete, the third phase of growth is the stationary phase, which is one of the two phases analyzed in our proteomic analysis of *M. mazei*; the second being the mid-log (also known as the mid-exponential phase of growth; see Chapter 2). At stationary phase, the number of cells that grow and the number of cells that die are equal per unit time, and hence there exists no net growth of cells. Both the carbon and energy sources are depleted during the stationary phase. Nonetheless, even though the carbon and energy sources are depleted, the dead cells can lyse and provide a source of nutrients. Growth on dead cells is

called endogenous metabolism, which occurs throughout the entire growth cycle; however, it is more pronounced during the stationary phase. This third phase is also characterized by a buildup of waste products, whereby they inhibit cell growth and can be toxic. During the death phase there is a net loss of viable cells for culture.

When cells are cultured in a lab they can be grown continuously or batched; the difference being that continuous culture is an open system that has a continuous feed of nutrients and substrates, while batch culture uses a fixed amount of the substrate that is added at the outset of growth. During the growth cycle of microorganisms, an increase in cell mass occurs and this phenomenon corresponds to the cells metabolizing the substrates under various growth conditions. Under the circumstances that new cells are not produced, then the cell is using the energy of the substrate for maintenance. Therefore the cell yield is dependent upon the substrate, and the more reduced is a substrate and more energy is obtainable through oxidation. According to Santiago-Martinez and colleagues, 90% of the carbon source in *Methanosarcina* is devoted towards ATP production via the methanogenic pathway, while the other 10% is used for biomass production (Santiago-Martinez et al. 2016). Therefore efficient carbon assimilation is essential for cell survival (Santiago-Martinez et al. 2016). Because *M. mazei* cells were cultured under anaerobic conditions, the transformation of organic matter into methane is characterized by a process known as disproportionation, in which organic carbon is both fully oxidized to carbon dioxide and fully reduced to methane.

Schultz (Schultz et al. 2013) cited the work of Dekel and colleagues (Dekel et al. 2005) who demonstrated that during the lag phase of growth and before accumulating biomass, microorganisms devote their primary energies to produce the “bottleneck” enzymes responsible for carbon utilization. According to Schultz (Schultz et al. 2013), the lag phase is associated with the cells’ goal of surviving in a new environment when cell numbers are small, and some do so

by remaining dormant or maximizing growth in a minimal amount of time. On the other hand the exponential and stationary phases correspond to the accumulation of growth and stress genes, respectively.

Even though the exponential phase of growth in often studied experimentally, the stationary phase is the most dominant in nature, primarily because nutrient resources are limited for many microorganisms. Furthermore, while the stationary phase is often associated with growth-arrest and a constant optical density (OD), Gefen and colleagues (Gefen et al. 2014) demonstrated that protein production can still occur at a constant rate in *E. coli* bacteria. Via the use of microfluidic devices, in which batch cultures of bacteria were established under starvation conditions, it was shown that most cells arrested their growth versus a minority of cells that showed extremely slow growth, thereby contributing to the observed constant OD. In order to determine whether the non -growing (arrested-growth) cells were responsible for the production of proteins during the stationary phase, protein concentration was measured after the promoter for a green fluorescent protein (GFP) gene was induced by IPTG. This experiment resulted in >90% of the starved bacteria responding to promoter signal. It was further shown that the non-growing bacteria were able to produce proteins over more than 60 hours of starvation, thereby existing in a “constant-activity stationary phase” (CASP), which is distinct from starvation conditions that reduce cell viability. In additional experiments the fitness of the constant-activity stationary phase bacteria was determined by re-growth in diluted fresh medium and it was demonstrated that the CASP cells grown with and without inducers had the same regrowth time. Therefore the fitness of the cells was not compromised by CASP, otherwise, the CASP cells without an inducer would not have been able to regrow. The information espoused by Gefen and colleagues (Gefen at al. 2014) is applicable to our proteomic study of *M. mazei*, which was analyzed after growth in both the mid-exponential and stationary phases; however, *M. mazei* showed no immediate distinctions in the the type of proteins that exist in high abundance, i.e.,

methyltransferases and methyl coenzyme M reductases. Principally, even though the stationary phase can be characterized by an equal rate of cells growing and dying, the rate of protein production is not significantly reduced.

Results and Discussion

Using the proteomics methods described in Chpater 2, out of the 220 proteins identified by label-free quantitative proteomics for stationary phase cells grown in methanol, the ten most abundant proteins accounted for 63% of the total protein amount **(Figure 3.1)**. Furthermore, the methyltransferases MtaA-C, and methyl coenzyme M reductases McrA-C comprise 34% and 18% of the total amount of proteins detected, respectively. The most abundant methyltransferases were the methanol-specific methyltransferase subunits. On the other hand, the monomethylamine corrinoid protein, MM_1438, accounted for only 0.02% of the total amount of proteins identified, and no di- or tri-methylamine-specific methyltransferases were identified in methanol-grown cells during the stationary phase. The S-layer protein, MM_1976, is among the top five most abundant proteins, further indicating its significance in the maintenance and structure of *M. mazei* cells specifically during methanogenesis. Interestingly enough, MM_1379, a thermosome subunit is among the ten most abundant proteins found in *M. mazei*. The thermosome is a Group II chaperonin that facilitates the proper folding of proteins in archaea via ATP hydrolysis. The other two thermosomes that were identified in the methanol-grown cells were MM_1096 (thermosome subunit alpha) and MM_0072 (thermosome subunit), each of which accounted for 0.6% and 0.2% of the total amound of proteins on column, respectively. Similar results are present for cells grown in monomethylamine and trimethylamine, except that MM_1379 (thermosome subunit alpha) is the sixteenth most abundant protein found in *M. mazei* cells grown in trimethylamine. Furthermore, all of the three thermosome proteins (MM_1379, MM_1096, and MM_0072) were also identified in the MeOH, MMA, DMA, and TMA grown cells during the mid-log analysis, in the specified order from most

abundant to least abundant. Additionally the hypothetical protein MM_1357 has 100% identity with translational initiation factor 2 subunit beta, and 90% identity with the putative methyltransferase MM_1358, which accounted for 0.4%, 0.3%, and 0.2% of the total amount of protein identified in MeOH-, MMA-, and TMA-grown cells, respectively.

Two hundred and fifty nine proteins were identified in *M. mazei* cells that utilized monomethylamine as a carbon source, and 55% of the protein mass comprised the ten most abundant proteins **(Figure 3.2)**. The methyltransferases and methylcoenzyme M reductases accounted for 23% of the total amount of protein mass in *M. mazei*. The most abundant methyltransferase was the monomethylamine methyltransferase (MtbA, MtmB, and MtmC). Again, as observed in *M. mazei* cells grown in methanol during stationary phase, the S-layer protein, MM_1976, is also among the top ten most abundant proteins. Even though MM_1436 and MM_1437 are linked by a pyrrolysine and are actually a single protein, as is the case for MM_3335 and MM_3336, and MM_1436/MM_1437 has an identical sequence to MM_3335/MM_3336, the pie chart below **(Figure 3.2)** would not considerably change, because both MM_1437 and MM_3336 were absent from the list of proteins identified, and did not contribute to the total mass of the proteins.

Two hundred and seventy nine proteins were identified in *M. mazei* cells grown in trimethylamine during the stationary phase, and the ten most abundant proteins accounted for 50% of the total mass of the proteins identified in the cell **(Figure 3.3).** Even though the trimethylamine corrinoid and methyltransferase proteins, MM_1688 and MM_1689, were the two most abundant proteins identified, monomethylamine and dimethylamine corrinoid proteins and methyltransferase were also identified among the top ten proteins, which is consistent with the fact that the TMA substrate is sequentially demethylated to form DMA then MMA. All of the methyltransferases identified accounted for 31% of the total amount of proteins recovered.

Furthermore, the methyl coenzyme M reductase accounts for 15% of the total amount of proteins identified, and the S-layer protein, MM_1976, was found in the ten most abundant proteins.

After determining which proteins were regulated by 2.5-fold or greater in *M. mazei* cells (**Table 3.1)**, we discovered a total of 66 proteins that were either upregulated or downregulated when grown in monomethylamine versus methanol substrates. As expected the methanol:corrinoid methyltransferase (MM_0175) was downregulated in monomethylamine grown cells, and significantly so by 0.06-fold. Neither the methanol:corrinoid protein (MM_1073) nor the methanol:corrinoid methyltransferase (MM_1074) were detected in cells grown in monomethylamine. Furthermore, even though MtaB – methanol:corrinoid methyltransferase (MM_1647) and MtaC – methanol:corrinoid protein (MM_1648) were detected in monomethylamine grown cells, they were significantly downregulated by 0.004-fold and 0.01-fold, respectively.

A total of 23 proteins were upregulated in the *M. mazei* cells grown in monomethylamine versus those grown in methanol. Of those 23 proteins, as expected, the monomethylamine: corrinoid protein (MM_1438) was upregulated and significantly so by 676-fold. Furthermore, tungsten formylmethanofuran dehydrogenase –subunit A (MM_1979), which is a methanogenic enzyme responsible for the reduction of CO_2 and methanofuran via a carbamate to N-methylmethanofuran, was upregulated by 4.4-fold in the monomethylamine substrate. The aforementioned reaction is reversible and allows the formation of CO_2 from C1 substrates, such as monomethylamine, and is therefore significant for energy metabolism in *M. mazei*.

Interestingly, the nitrogenase biosynthesis (NifB) protein (MM_0757) was upregulated in monomethylamine grown cells. One would speculate that NifB is upregulated in MMA-grown

cells in order to increase the amount of ammonia that is produced in the cell when compared to TMA-grown cells, because TMA would cause a greater production of ammonia. The NifB upregulation in MMA-grown cells may be serving a beneficial role to thereby create an environment where the amount of ammonia is sufficient to serve as a precursor for amino acids, such as glutamine, and to stabilize cell growth. NifB was only upregulated in MMA-grown cells, when compared to MeOH-grown cells, and not in TMA grown cells. The NifB protein is purported to be a “radical” S- adenosyl-L-methionine (SAM) enzyme that is responsible for the biosynthesis of the cofactor found in molybdemum nitrogenase *Azotobacter vanlandii* (Fay et al., 2015), and nitrogenases catalyze the conversion of molecular nitrogen to ammonia, and CO to hydrocarbons (Hu et al., 2018). NifB, which functions as a SAM methyltransferase, is also found in *Methanosarcina acetivorans.*

Fourteen proteins were either upregulated or down regulated by 2.5-fold when *M. mazei* cells were grown in trimethylamine versus those grown in methanol **(Table 3.2)**. While the methanol:corrinoid proteins (MM_0174 and MM_1648) and the methanol: corrinoid methyltransferases (MM_0175 and MM_1647) were not detected in the trimethylamine grown cells, neither were any of the trimethylamine/ dimethylamine: corrinoid proteins nor the trimethylamine/ dimethylamine: corrinoid methyltransferases detected in the methanol grown cells. The trimethylamine: corrinoid methyltransferases consisted of MM_1688 (10% of total fmol of proteins identified) and MM_1689 (6.5%); the dimethylamine:corrinoid proteins consisted of MM_1687 and MM_1690; and the dimethylamine:corrinoid methyltransferases consisted of MM_1693 (2.7%) and MM_1694 (0.89%). MM_1688 and MM_1689 are thought to be fused with pyrrolysine, as well as MM_1693 and MM_1694, and their respective levels in the *M. mazei* cells vary. The acetyl-CoA decarbonylase/synthase complex subunit beta (MM_2087), which is involved in the aceticlastic pathway for methanogenesis, was downregulated by 0.03-fold when *M. mazei* cells were grown in trimethylamine versus methanol.

After comparing the number and identity of the proteins detected in the stationary phase samples versus those in the mid-log phase, it was discovered that when *M. mazei* cells were grown in methanol, mid-log samples possessed 82 unique proteins, while stationary samples had 13 unique proteins, and both samples shared 207 identical proteins. As for the monomethylamine grown cells, mid-log samples had 97 unique proteins, stationary samples had 55 unique proteins, and both mid-log and stationary phase samples shared 204 identical proteins. Additionally, trimethylamine grown cells for mid-log samples had 65 unique proteins, while stationary phase samples had 28 unique proteins, and both samples shared 252 identical proteins.

Among the biologically relevant proteins unique to the stationary phase **(Table 3.3)**, MM_1438 (monomethylamine corrinoid protein) was found in methanol grown cells only during the stationary phase, when compared to the mid-log phase; MM_0174 (methanol:corrinoid protein), MM_1647 (methanol corrinoid methyltransferase MtaB), MM_1648 (methanol corrinoid protein MtaC), MM_1690 (dimethylamine corrinoid protein), and MM_2962 (dma:corrinoid methyltransferase) were found in monomethylamine grown cells only during the stationary phase, when compared to the mid-log phase; and MM_1437 (mma:corrinoid methyltransferase) was found in trimethylamine grown cells only during the stationary phase, when compared to the mid-log phase. MM_1438 is a part of the mtmBC1 operon, which is composed of MM_1434 through MM_1438 (Kratzer et al. 2009). Even though MM_1438 was absent from the mid-log stage *M. mazei* cells grown in methanol, MM_1436, which is a part of the aforementioned operon, was present during mid-log stage. Furthermore, all other members of the operon (MM_1434 – MM_1437) were absent from the stationary phase of *M. mazei* cells grown in methanol.

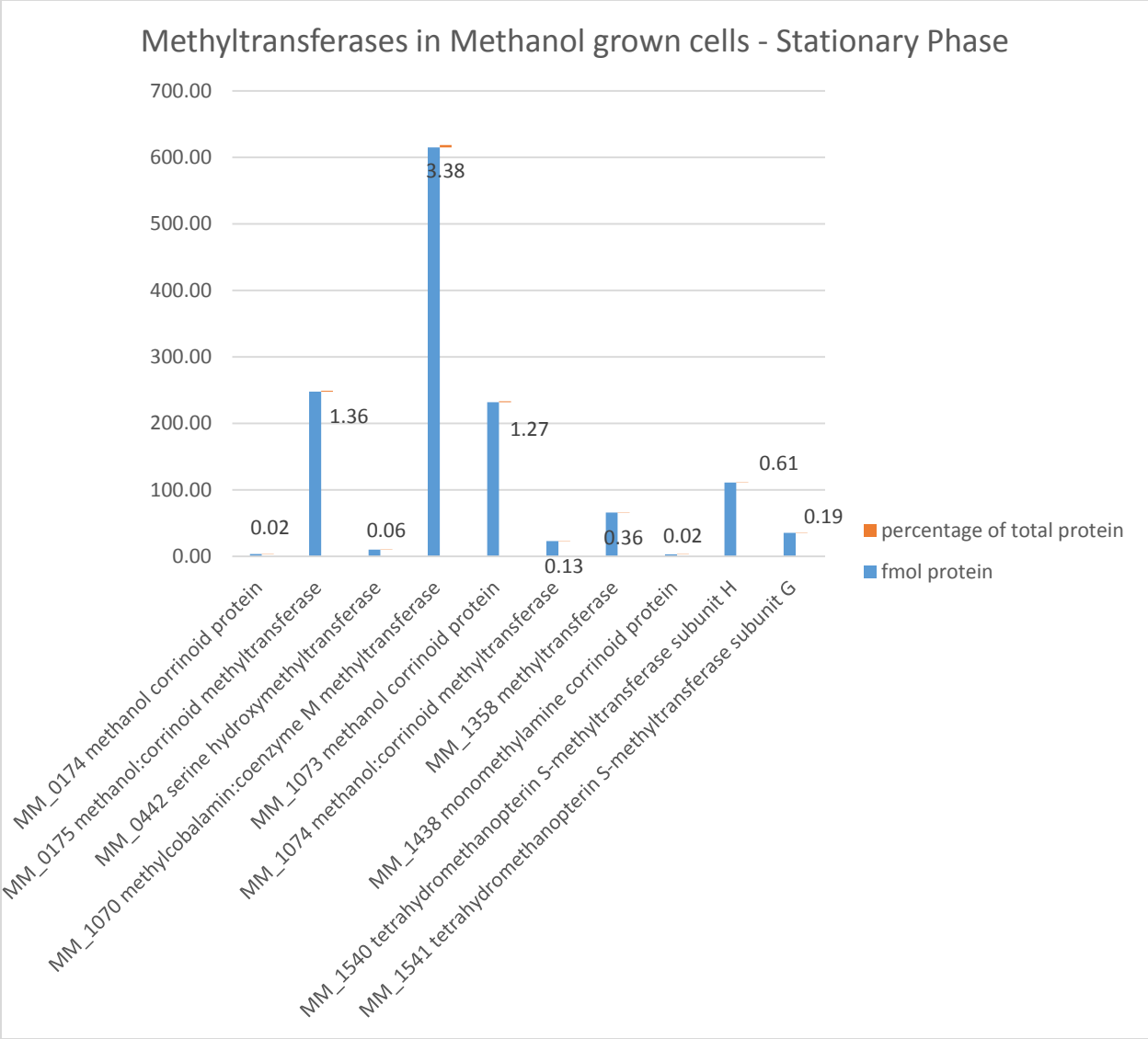

Figure 3.1a Methyltransferases (mtaB, mtaC, and mtaA) account for 34% of total amount of proteins identified in methanol grown cells during stationary phase. (See Figures 3.1b).

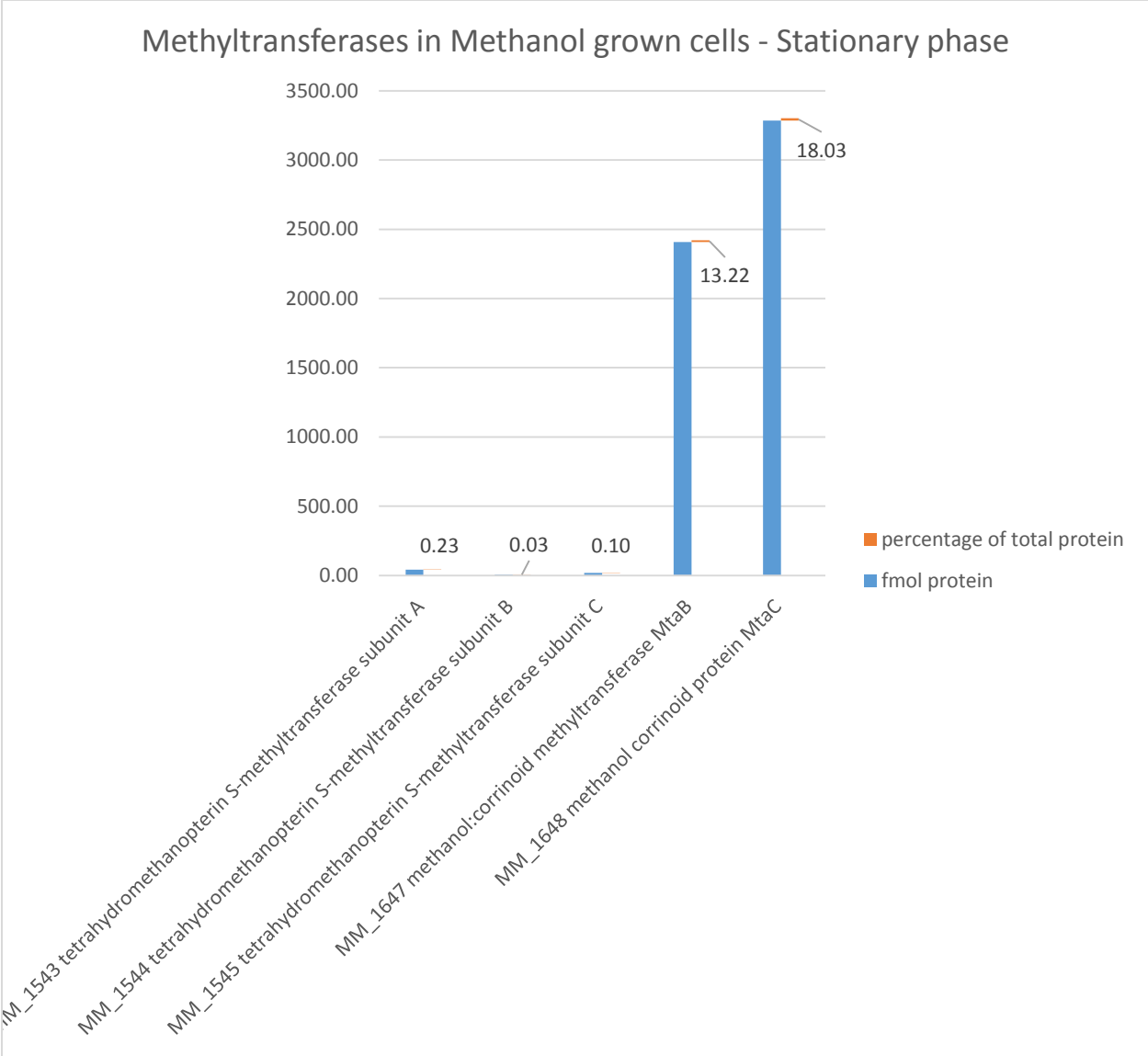

Figure 3.1b Methyltransferases (mtaB, mtaC, and mtaA) account for ~34% of total amount of proteins identified in methanol grown cells during stationary phase. (See Figures 3.1a).

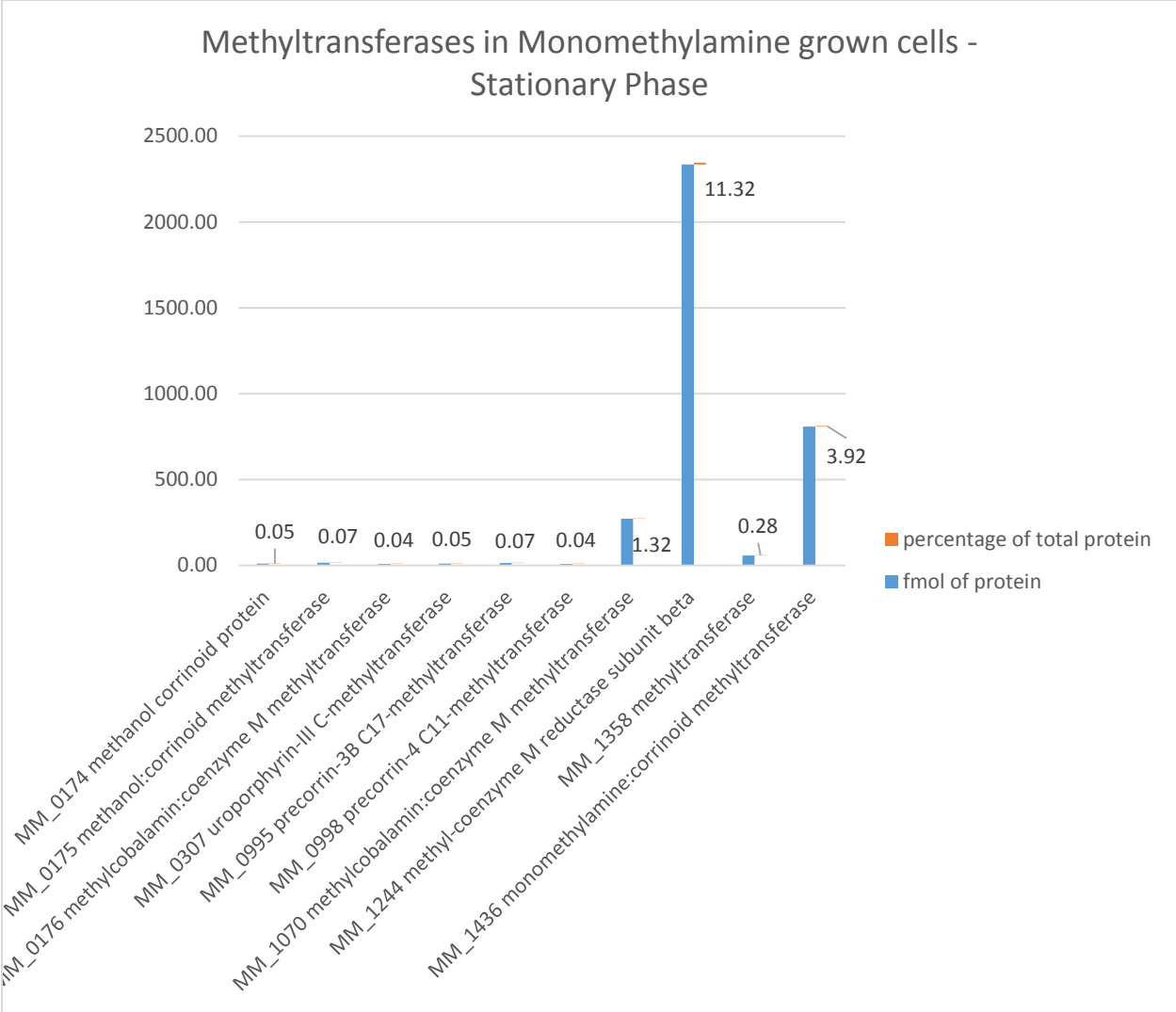

Figure 3.2a Methyltransferases (mtmB, mtmC, and mtmA) account for ~23% of total amount of proteins identified in MMA grown cells during stationary phase. (See Figures 3.2b and 3.2c)

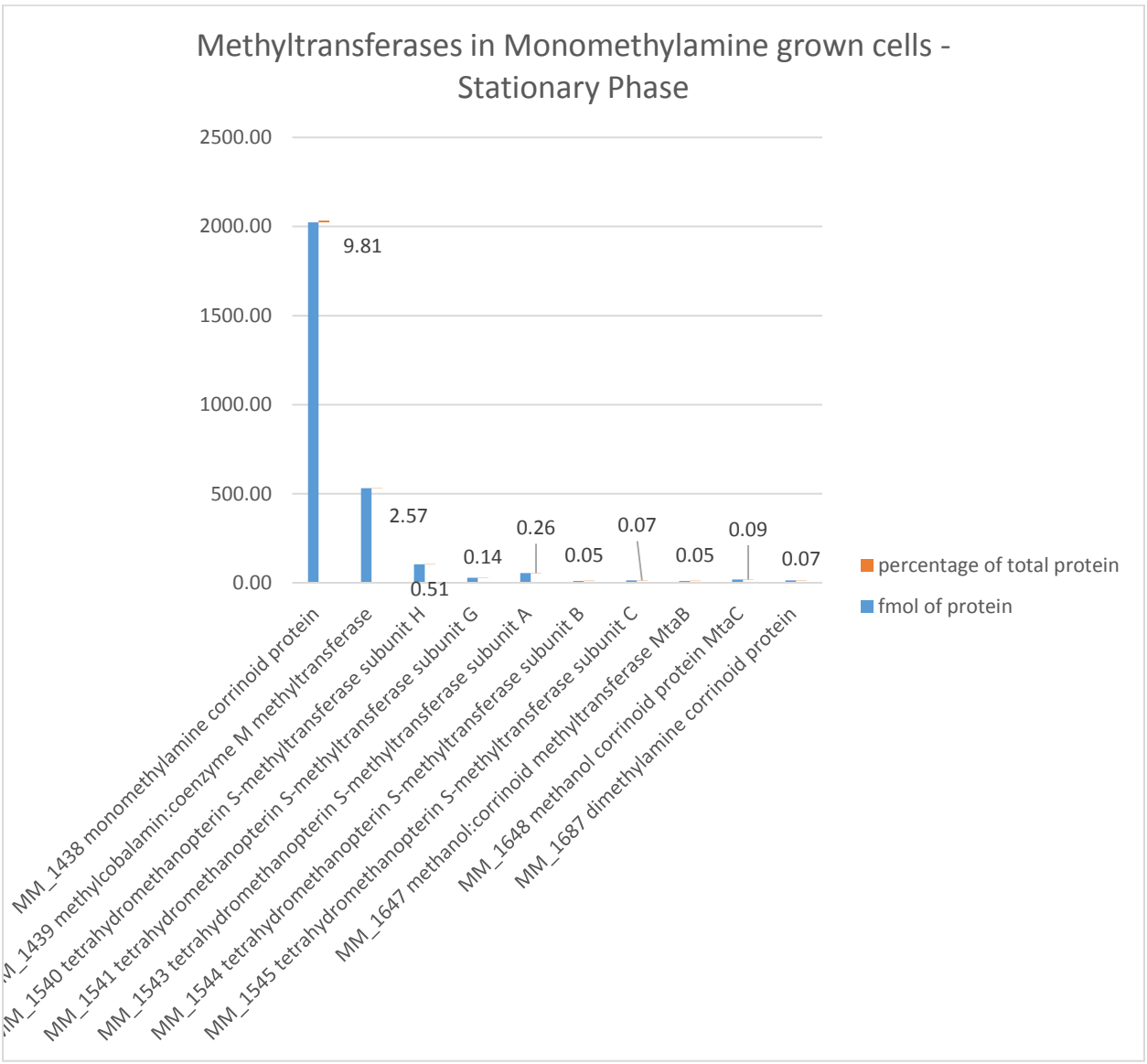

Figure 3.2b Methyltransferases (mtmB, mtmC, and mtmA) account for ~23% of total amount of proteins identified in MMA grown cells during stationary phase. (See Figures 3.2a and 3.2c)

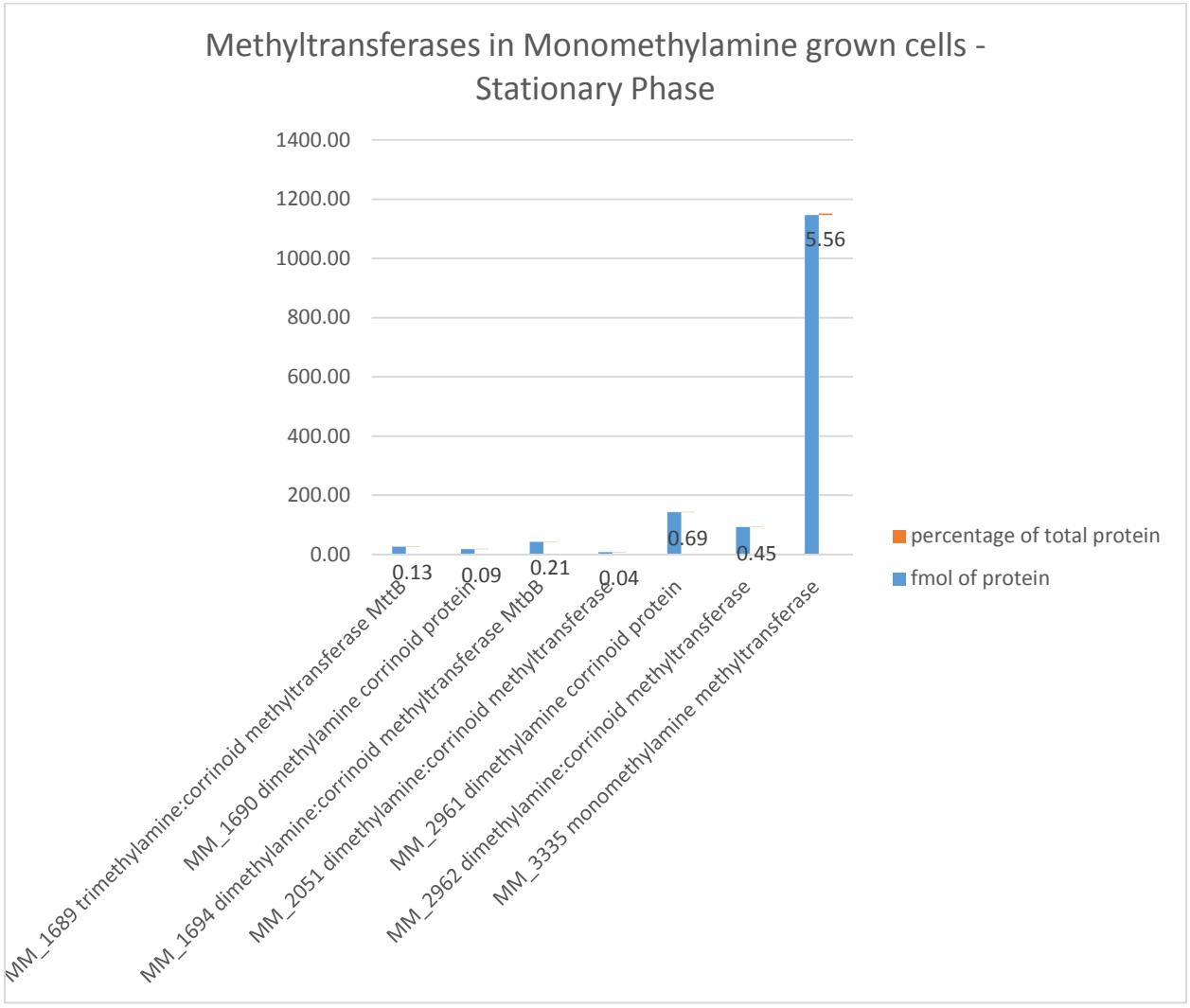

Figure 3.2c Methyltransferases (mtmB, mtmC, and mtmA) account for ~23% of total amount of proteins identified in MMA grown cells during stationary phase (See Figures 3.2a and 3.2b)

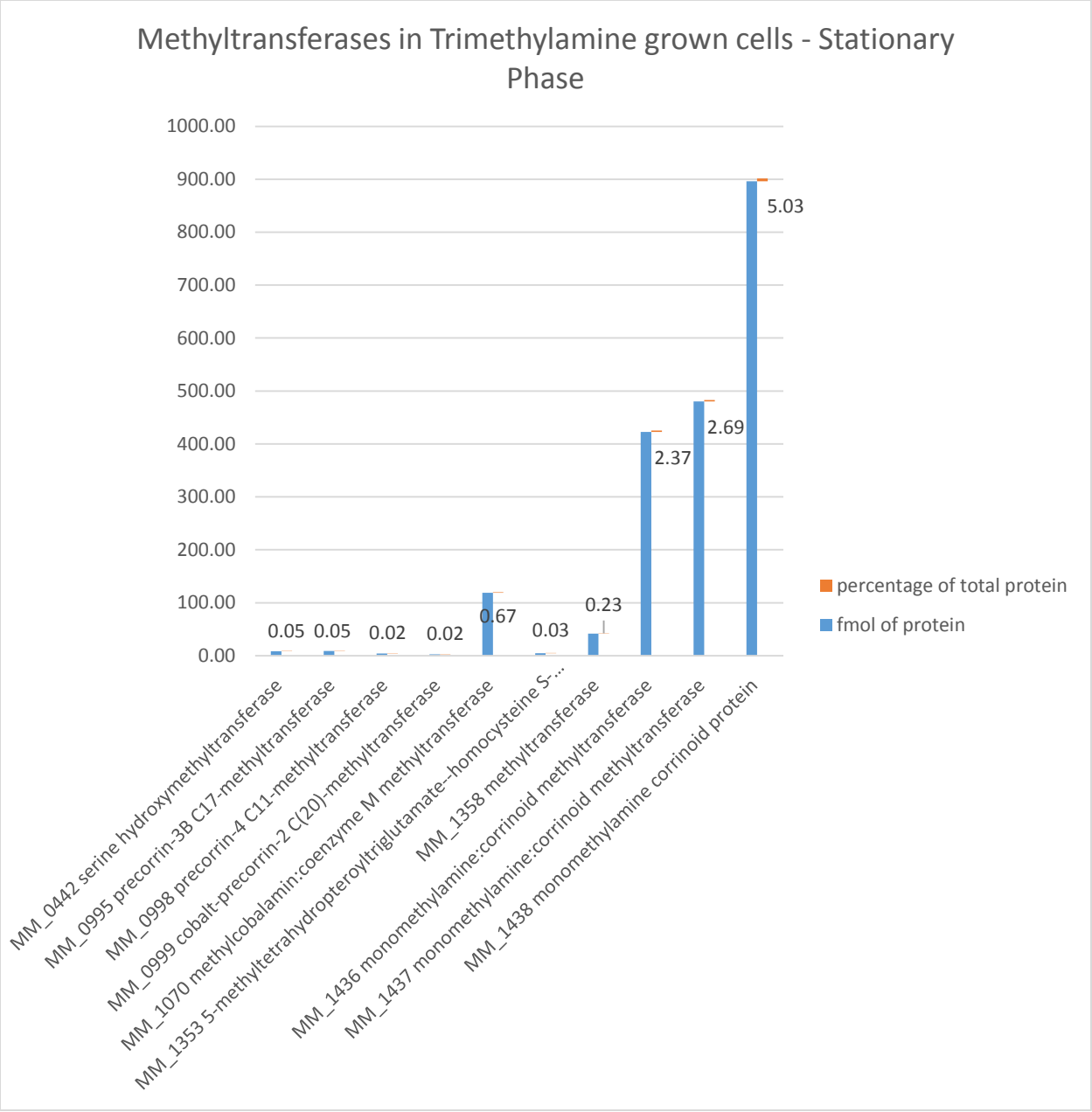

Figure 3.3a Methyltransferases (mttB, mttC, and mttA) account for ~31% of total amount of proteins identified in TMA grown cells during stationary phase. (See Figures 3.3b and 3.3c)

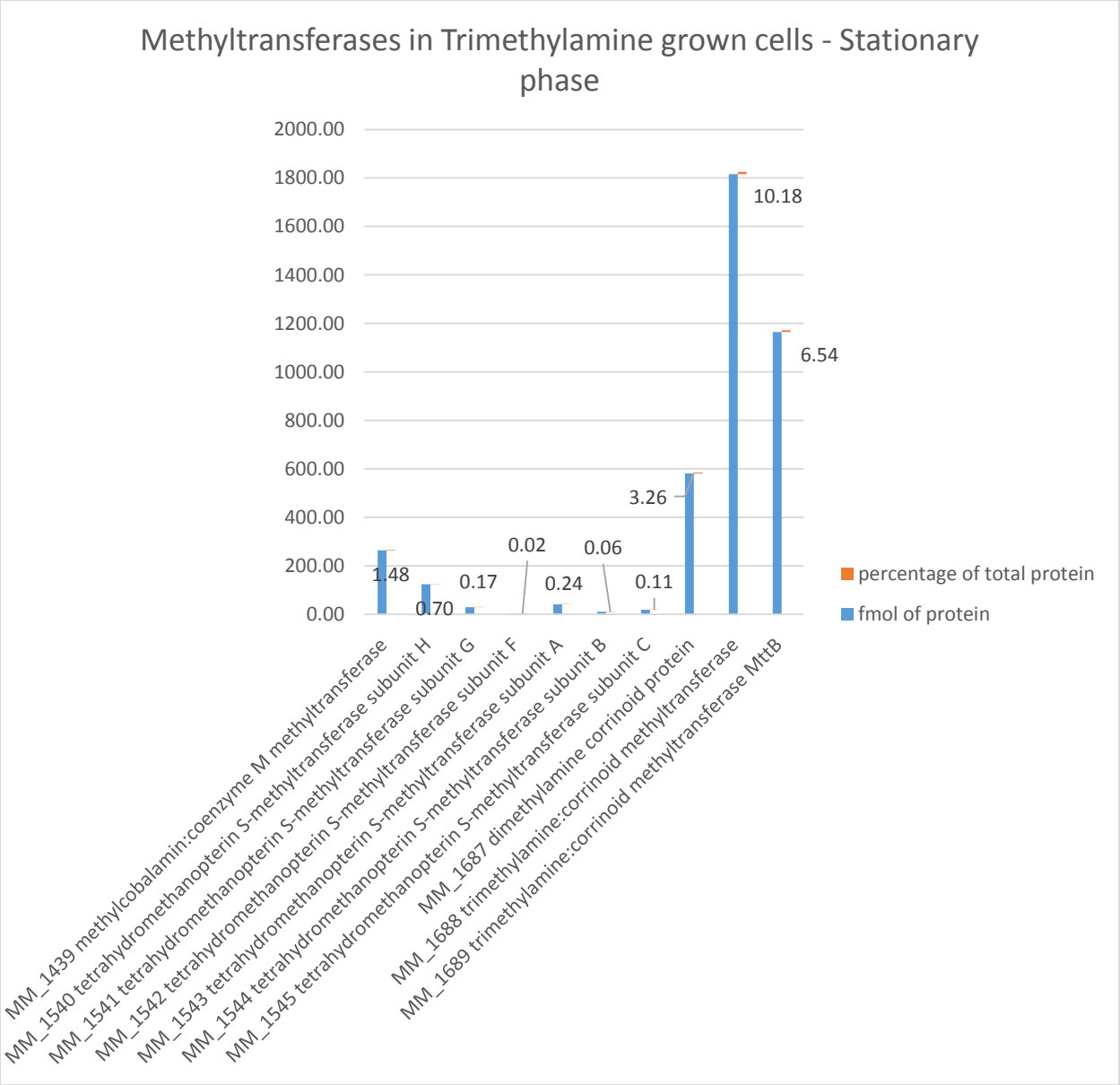

Figure 3.3b Methyltransferases (mttB, mttC, and mttA) account for ~31% of total amount of proteins identified in TMA grown cells during stationary phase. (See Figures 3.3a and 3.3c)

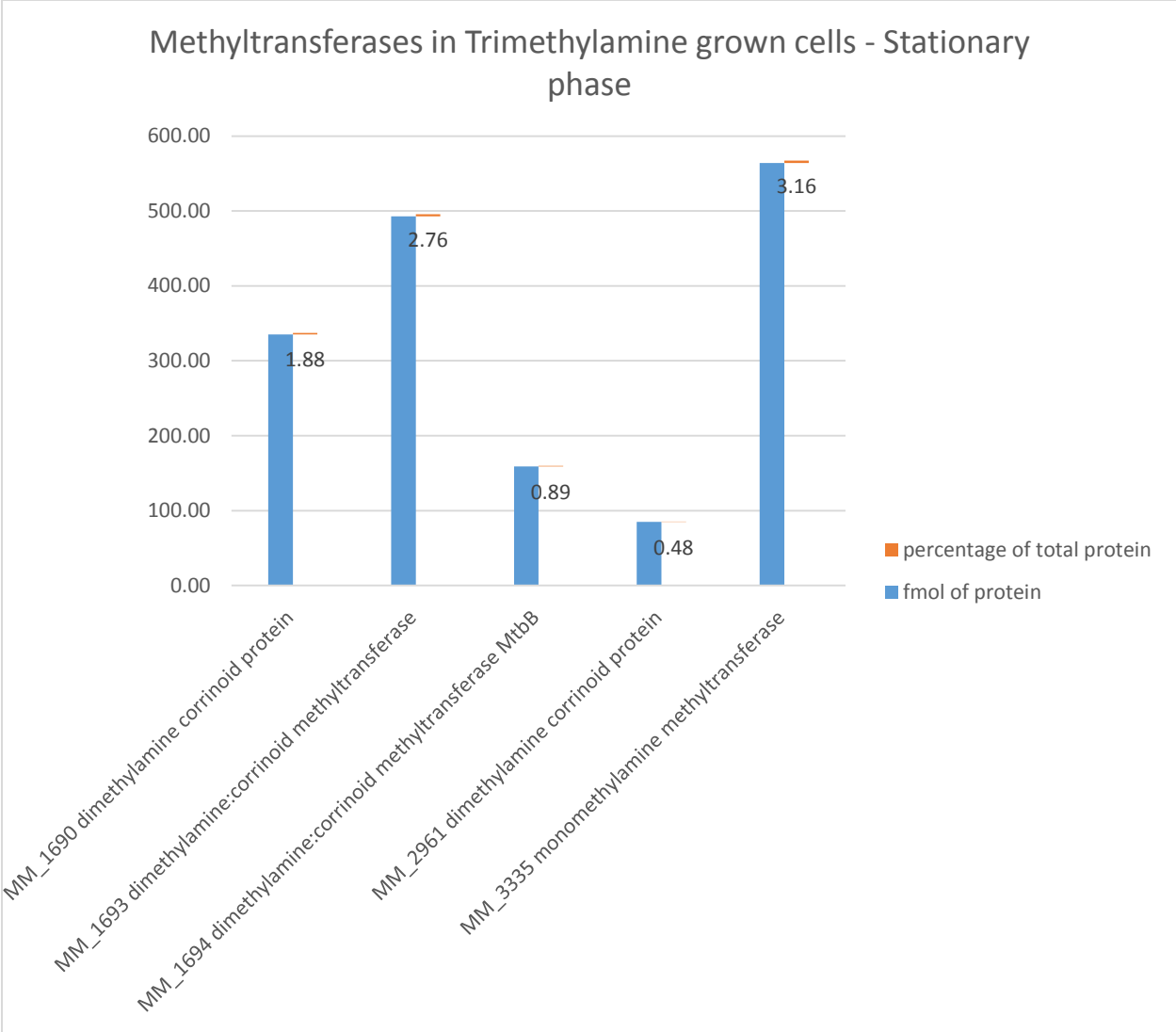

Figure 3.3c Methyltransferases (mttB, mttC, and mttA) account for ~31% of total amount of proteins identified in TMA grown cells during stationary phase. (See Figures 3.3a and 3.3b)

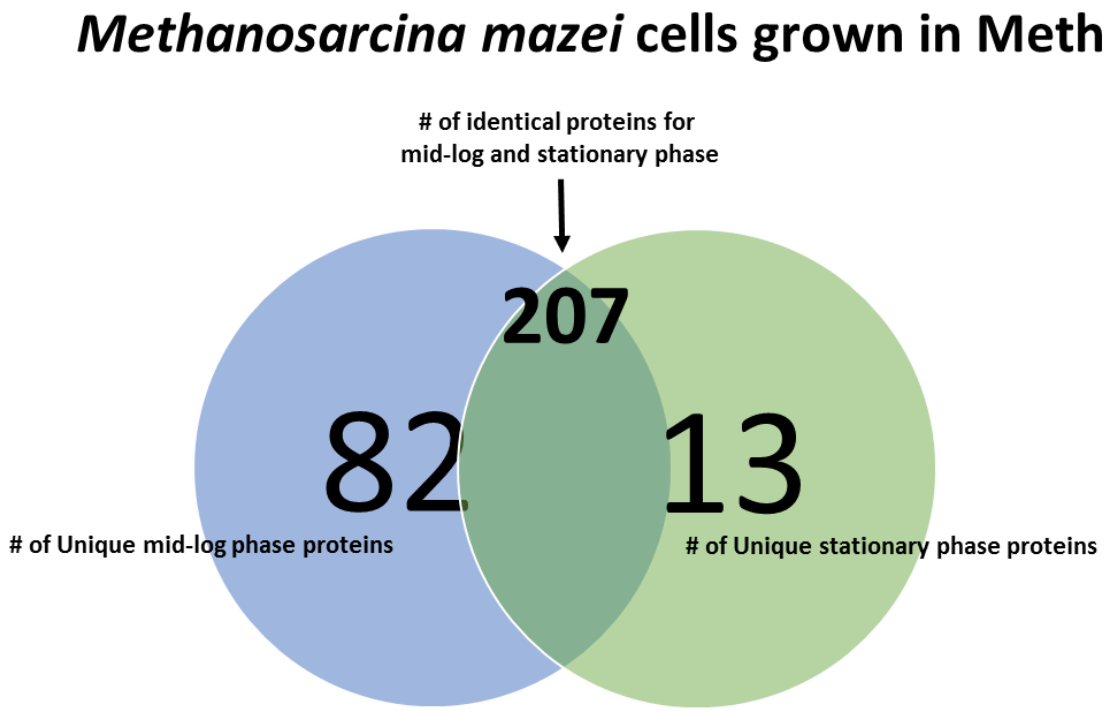

Figure 3.4 Number of Unique Proteins identified during mid-log and stationary phase of growth in methanol

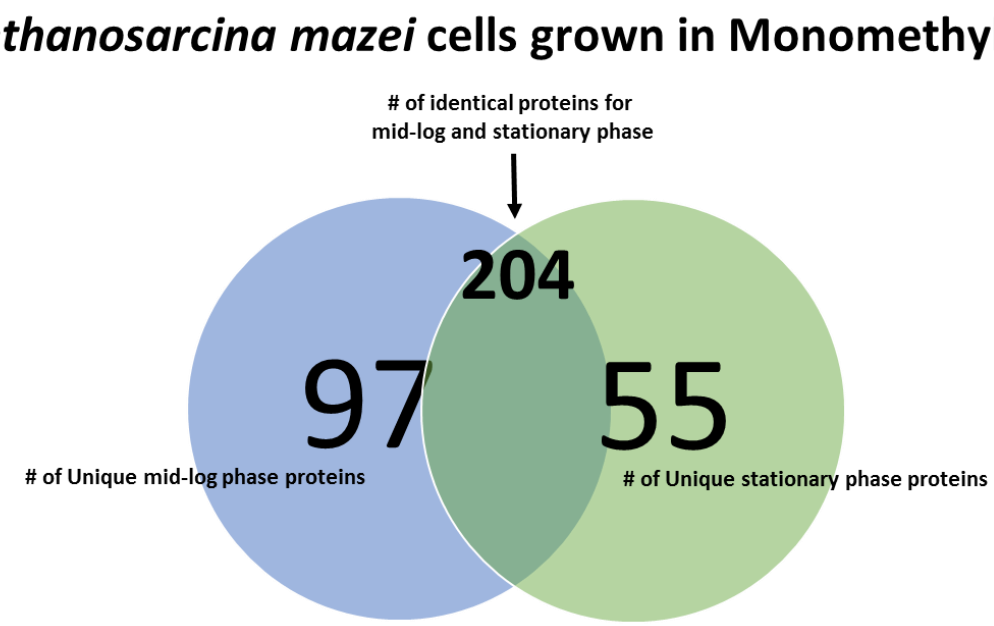

Figure 3.5 Number of Unique Proteins identified during mid-log and stationary phase of growth in MMA

Table 3.1 Protein regulation in cells grown in methanol versus monomethylamine

	MeOH	MMA	MMA/ MeOH	Upregulated in MMA	Downregulated in MMA
	fmol of protein	fmol of protein		2.5-fold higher	2.5-fold lower
MM_0037 argininosuccinate synthase	8.24		0.00	FALSE	TRUE
MM_0174 methanol corrinoid protein	3.80	10.84	2.85	TRUE	FALSE
MM_0175 methanol:corrinoid methyltransferase	247.89	14.81	0.06	FALSE	TRUE
MM_0243 aspartate aminotransferase	3.83		0.00	FALSE	TRUE
MM_0244 6_7-dimethyl-8-ribityllumazine synthase	3.65		0.00	FALSE	TRUE
MM_0442 serine hydroxymethyltransferase	10.48		0.00	FALSE	TRUE
MM_0495 acetate kinase	14.62	40.79	2.79	TRUE	FALSE
MM_0496 phosphate acetyltransferase	28.26	75.68	2.68	TRUE	FALSE
MM_0537 hypothetical protein MM_0537	15.33	52.65	3.43	TRUE	FALSE
MM_0593 5-formaminoimidazole-4-carboxamide-1-(beta)- D-ribofuranosyl 5'-monophosphate synthetase-like protein	3.27		0.00	FALSE	TRUE
MM_0629 Zinc finger protein	4.84	19.60	4.05	TRUE	FALSE
MM_0635 flavoprotein	6.49	19.41	2.99	TRUE	FALSE
MM_0670 acetolactate synthase 3 catalytic subunit	26.70		0.00	FALSE	TRUE
MM_0714 aldolase	8.79		0.00	FALSE	TRUE
MM_0757 NifB protein	5.77	17.77	3.08	TRUE	FALSE
MM_0786 A1AO H+ ATPase subunit H	30.74		0.00	FALSE	TRUE
MM_0808 50S ribosomal protein LX	4.93		0.00	FALSE	TRUE
MM_0814 peroxiredoxin	12.40		0.00	FALSE	TRUE
MM_0858 translation initiation factor Sui1	2.42		0.00	FALSE	TRUE
MM_0871 hypothetical protein MM_0871	3.82		0.00	FALSE	TRUE
MM_0966 glutamate synthase_ large chain	3.61		0.00	FALSE	TRUE
MM_0967 glutamate synthase_ large chain	9.32		0.00	FALSE	TRUE
MM_1071 hypothetical protein MM_1071	21.74		0.00	FALSE	TRUE
MM_1073 methanol corrinoid protein	232.14		0.00	FALSE	TRUE
MM_1074 methanol:corrinoid methyltransferase	23.00		0.00	FALSE	TRUE
MM_1152 aspartate aminotransferase	3.34		0.00	FALSE	TRUE
MM_1201 dihydrodipicolinate synthase	10.48		0.00	FALSE	TRUE
MM_1222 GTP cyclohydrolase	24.88		0.00	FALSE	TRUE
MM_1271 fructose-bisphosphate aldolase	25.24	21.91	0.87	FALSE	FALSE
MM_1284 2-isopropylmalate synthase	21.39	54.83	2.56	TRUE	FALSE

	MeOH	MMA	MMA/ MeOH	Upregulated in MMA	Downregulated in MMA
	fmol of protein	fmol of protein		2.5-fold higher	2.5-fold lower
MM_1362 aliphatic sulfonate binding protein	5.86	21.66	3.69	TRUE	FALSE
MM_1397 DNA polymerase sliding clamp	7.95	22.87	2.88	TRUE	FALSE
MM_1438 monomethylamine corrinoid protein	2.99	2023.35	676.52	TRUE	FALSE
MM_1528 aconitate hydratase	4.07		0.00	FALSE	TRUE
MM_1618 aspartate-semialdehyde dehydrogenase	3.12	13.84	4.44	TRUE	FALSE
MM_1647 methanol:corrinoid methyltransferase MtaB	2408.65	9.99	0.00	FALSE	TRUE
MM_1648 methanol corrinoid protein MtaC	3285.32	18.29	0.01	FALSE	TRUE
MM_1702 hypothetical protein MM_1702	5.80	15.81	2.73	TRUE	FALSE
MM_1788 HTH DNA-binding protein	5.73	16.31	2.85	TRUE	FALSE
MM_1797 co-chaperonin GroES	5.34		0.00	FALSE	TRUE
MM_1804 rubrerythrin	9.93	33.32	3.35	TRUE	FALSE
MM_1879 RNA-binding protein	5.06		0.00	FALSE	TRUE
MM_1963 tyrosyl-tRNA synthetase	8.13	22.64	2.78	TRUE	FALSE
MM_1976 hypothetical protein MM_1976	702.00	662.77	0.94	FALSE	FALSE
MM_1978 tungsten formylmethanofuran dehydrogenase subunit C	5.52	27.43	4.97	TRUE	FALSE
MM_1979 tungsten formylmethanofuran dehydrogenase subunit A	9.45	41.56	4.40	TRUE	FALSE
MM_2016 HesB protein	29.54		0.00	FALSE	TRUE
MM_2037 hypothetical protein MM_2037	8.72	24.73	2.84	TRUE	FALSE
MM_2087 acetyl-CoA decarbonylase/synthase complex subunit beta	268.52		0.00	FALSE	TRUE
MM_2127 50S ribosomal protein L2	26.70		0.00	FALSE	TRUE
MM_2128 30S ribosomal protein S19	12.78		0.00	FALSE	TRUE
MM_2131 50S ribosomal protein L29	20.00		0.00	FALSE	TRUE
MM_2170 F420-nonreducing hydrogenase II_ large subunit	31.96		0.00	FALSE	TRUE
MM_2313 F420-nonreducing hydrogenase I_ large subunit	5.42		0.00	FALSE	TRUE
MM_2336 translation initiation factor IF-1A	5.21		0.00	FALSE	TRUE
MM_2371 hypothetical protein MM_2371	7.24		0.00	FALSE	TRUE
MM_2460 dipeptide/oligopeptide-binding protein	5.69		0.00	FALSE	TRUE
MM_2464 nucleoside diphosphate kinase	9.40		0.00	FALSE	TRUE
MM_2466 30S ribosomal protein S28	11.48		0.00	FALSE	TRUE
MM_2505 molecular chaperone DnaK	57.04	217.76	3.82	TRUE	FALSE
MM_2506 heat shock protein GrpE	5.84	16.03	2.74	TRUE	FALSE

	MeOH	MMA	MMA/ MeOH	Upregulated in MMA	Downregulated in MMA
	fmol of protein	fmol of protein		2.5-fold higher	2.5-fold lower
MM_2563 ferredoxin	5.85		0.00	FALSE	TRUE
MM_2623 exosome complex exonuclease 1	6.40		0.00	FALSE	TRUE
MM_2625 50S ribosomal protein L37	9.07		0.00	FALSE	TRUE
MM_2649 LL-diaminopimelate aminotransferase	7.07	25.01	3.54	TRUE	FALSE
MM_2782 glyceraldehyde-3-phosphate dehydrogenase	6.89	19.10	2.77	TRUE	FALSE
MM_2867 coenzyme F390 synthetase/phenylacetyl-CoA ligase	12.24		0.00	FALSE	TRUE

Table 3.2. Protein regulation in cells grown in methanol versus trimethylamine

	MeOH	TMA	TMA/ MeOH	Upregulated in TMA	Downregulated in TMA
	fmol of protein	fmol of protein		2.5-fold higher	2.5-fold lower
MM_0174 methanol corrinoid protein	3.80		0.00	FALSE	TRUE
MM_0175 methanol:corrinoid methyltransferase	247.89		0.00	FALSE	TRUE
MM_0593 5-formaminoimidazole-4-carboxamide-1-(beta)-D-ribofuranosyl 5'-monophosphate synthetase-like protein	3.27		0.00	FALSE	TRUE
MM_0801 adenylosuccinate synthetase	8.63		0.00	FALSE	TRUE
MM_0858 translation initiation factor Sui1	2.42		0.00	FALSE	TRUE
MM_1355 hypothetical protein MM_1355	102.13	30.96	0.30	FALSE	TRUE
MM_1647 methanol:corrinoid methyltransferase MtaB	2408.65		0.00	FALSE	TRUE
MM_1648 methanol corrinoid protein MtaC	3285.32		0.00	FALSE	TRUE
MM_1687 dimethylamine corrinoid protein		581.686925	N/A	TRUE	FALSE
MM_1688 trimethylamine:corrinoid methyltransferase		1815.4175	N/A	TRUE	FALSE
MM_1689 trimethylamine:corrinoid methyltransferase MttB		1165.4595	N/A	TRUE	FALSE
MM_1690 dimethylamine corrinoid protein		335.149275	N/A	TRUE	FALSE
MM_1693 dimethylamine:corrinoid methyltransferase		492.71325	N/A	TRUE	FALSE
MM_1694 dimethylamine:corrinoid methyltransferase MtbB		158.852975	N/A	TRUE	FALSE
MM_1879 RNA-binding protein	5.06		0.00	FALSE	TRUE
MM_1976 hypothetical protein MM_1976	702.00	673.20	0.96	FALSE	FALSE
MM_2087 acetyl-CoA decarbonylase/synthase complex subunit beta	268.52	7.54	0.03	FALSE	TRUE
MM_2273 DNA-directed RNA polymerase subunit beta"	5.55		0.00	FALSE	TRUE
MM_2460 dipeptide/oligopeptide-binding protein	5.69		0.00	FALSE	TRUE
MM_2721 hypothetical protein MM_2721	7.94	3.14	0.40	FALSE	TRUE

Table 3.3 Partial list of unique proteins identified in stationary phase *M. mazei* cells (methyltransferases including corrinoid proteins are highlighted in green)

Methanol grown cells	Monomethylamine grown cells	Trimethylamine grown cells
MM_0441 bifunctional 5_10-methylene-tetrahydrofolate dehydrogenase/ 5_10-methylene-tetrahydrofolate cyclohydrolase	**MM_2962** dimethylamine:corrinoid methyltransferase	**MM_1437** monomethylamine:corrinoid methyltransferase
MM_0966 glutamate synthase_ large chain	**MM_1355** hypothetical protein MM_1355	**MM_0686** acetyl-CoA decarbonylase/synthase complex subunit beta
MM_1279 bifunctional formaldehyde-activating enzyme/3-hexulose-6-phosphate synthase	**MM_0627** F420H2 dehydrogenase subunit F	**MM_0495** acetate kinase
MM_1355 hypothetical protein MM_1355	**MM_1648** methanol corrinoid protein MtaC	**MM_0786** A1AO H+ ATPase subunit H
MM_1438 monomethylamine corrinoid protein	**MM_1690** dimethylamine corrinoid protein	**MM_1545** tetrahydromethanopterin S-methyltransferase subunit C
MM_2087 acetyl-CoA decarbonylase/synthase complex subunit beta	**MM_0964** glutamine synthetase	**MM_0436** thioredoxin
MM_2563 ferredoxin	**MM_1545** tetrahydromethanopterin S-methyltransferase subunit C	**MM_2087** acetyl-CoA decarbonylase/synthase complex subunit beta
	MM_2423 superoxide dismutase	**MM_0964** glutamine synthetase
	MM_0483 small heat shock protein	**MM_2314** F420-nonreducing hydrogenase I
	MM_0174 methanol corrinoid protein	
	MM_2324 ech hydrogenase subunit	
	MM_1647 methanol:corrinoid methyltransferase MtaB	
	MM_0176 methylcobalamin:coenzyme M methyltransferase	
	MM_2051 dimethylamine:corrinoid methyltransferase	
	MM_2479 F420H2 dehydrogenase subunit	

Conclusion

Similar to cells grown during the mid-log phase, the methyltransferases and methylcoenzyme M reductases combined accounted for ~40% of the total amount of proteins identified in *M. mazei* cells grown in methanol, monomethylamine, and trimethylamine as methylotrophic substrates. Furthermore, even during the stationary phase of growth, the cells switch the methyltransferases in a substrate dependent manner, whereby the most abundant methyltransferases were either methanol-, monomethylamine-, or trimethylamine-specific according to the different substrate conditions. It is interesting to note that a similar pattern arose for regulation of the methyltransferases during the stationary phase for cells grown in methanol versus monomethylamine, or methanol versus trimethylamine, when compared to the mid-log phase. For instance, the monomethylamine: corrinoid methyltransferase MM_1438, was upregulated when grown in monomethylamine by more than 600-fold compared to when the cells were grown in methanol.

The *M. mazei* cells under stationary phase conditions are still able to produce necessary proteins in order to facilitate methanogenesis. These results coincide with what is often observed in nature, where the stationary phase is the most prevalent, due to the shortage of resources for growth, but nonetheless still allowing the cell to perform basic biological functions via the use of pertinent methanogenic proteins, such as the methyltransferases. Furthermore, our results indicate that the constant OD during the stationary phase is likely attributed to cells of arrested growth that are able to still produce proteins vital to their survival (somewhat like an archaeal-Constant Activity Stationary phase), as was demonstrated by Gefen and colleagues (Gefen at al. 2014) with bacteria. In summary, the substrate flexibility and enzyme-switching mechanism exhibited during mid-log stage of growth is also present during the stationary phase, when there is no expected net growth within the cell.

References

1. Dekel, E.; Alon, U. Optimality and evolutionary tuning if the expression level of a protein. *Nature*, **2005**. *436*, 588-592.
2. Fay, A. W; Wiig, J.A.; Lee, C.C.; Hu, Y. Identification and characterization of functional homologs of nitrogenase cofactor biosynthesis protein NifB from methanogens. *PNAS,* **2015.** *112:48*, 14829-14833.
3. Gefen, O.; Fridman, O.; Ronin, I.; Balaban, N.Q. Direct observation of single stationary-phase bacteria reveals a surprisingly long period of constant protein production activity. *PNAS,* **2014.** *11:1*, 556-561.
4. Kratzer, C.; Carini, P.; Hovey, R.; Deppenmeier, U. Transcriptional Profiling of Methyltransferase Genes during growth of *Methanosarcina mazei* on Trimethylamine. *Journal of Bacteriology*, **2009.** *191:16*, 5108-5115.
5. Maier, R.M. Bacterial Growth. In *Environmental Microbiology.* Academic Press, Inc.: 2009: pp 37-54.
6. Santiago-Martinez, M.G.; Encalada, R.; Lira-Silva, E.; Pineda, E.; Gallardo-Perez, J.C.; Reyes-Garcia, M.A.; Saavedra, E.; Moreno-Sanchez, R.; Marin-Hernandez, A.; Jasso-Chavez, R.. The nutritional status of *Methanosarcina acetivorans* regulates glycogen metabolism and gluconeogenesis and glycolysis fluxes. *The FEBS Journal*, **2016**. *283*, 1979-1999.
7. Schultz, D.; Kishony, R. Optimization and control of bacterial Lag phase *BMC Biology.* **2013.** *11:20,* 1-3.

CHAPTER 4

Proteomic Analysis of Salt Adaptation in *Methanosarcina mazei*

Introduction

Salt adaptation in archaea

Evaporation of fluid from soil and rainfall can contribute to changes in environmental osmolarity. High salt conditions in the environment causes a rapid flow of water out of the cell, loss of turgor, shrinkage of the cell, and then cell death via plasmolysis. Alternatively, low salt conditions lead to water rushing into the cells, which increases the cytoplasmic volume of the cell and turgor pressure, thereby resulting in the cell bursting. Cells respond to changes in osmolarity by modifying the concentration of osmolytes inside the organism.

Methanosarcina mazei cells isolated from the sewage sludge of a wastewater treatment plant require 1 mM Na+ in order for the sodium pump methyl tetrahydrosarcinopterin: coenzyme M methyltransferase to function. The significance of the sodium pump is to transport sodium out of the cell, a process that in turn either directly or indirectly drives ATP synthesis (Wagner et al. 2016). The organism can also grow in 400 mM and 800 mM NaCl. Transfer of the *M. mazei* cells from freshwater to saline media increases the lag phase of growth, which indicates that reprogramming of the cell's physiology is a necessary process in salt adaptation.

Microarrary studies were used to examine the effect of elevated salinities on the regulation of gene expression in *M. mazei* Gö1 species. In those studies, cells were grown in 38.5 mM or 800 mM NaCl; the RNA was isolated and transcribed into cDNA, which was then labelled with a fluorescent signal and hybridized to probes for the genome of *M. mazei*. Results demonstrated that *M. mazei* can regulate cellular functions, cell surface landscape, and genetic expression as it adapts to high salt conditions (Pfluger et al. 2007). Nonetheless, microarrary assays necessitate extensive proteomic studies in order to better understand the proteins involved in osmostress relief and the biochemical pathways to such relief. Consequently, our proteomic

studies can be used to elucidate *M. mazei*'s response and adaptation to hypersaline environments.

Salt adaptation in bacteria and archaea and their compatible solutes

Bacteria have been shown to adapt to high salt environments via a series of processes that involve a 1) rapid response with the uptake of potassium ions (K+) from the environment and the de novo synthesis of anions, such as glutamate, inside the cells; 2) slow response via the synthesis of compatible solutes, such as trehalose, inside the cells, while also exporting K+ ions out of the cell. In bacteria, this fast and slow salt adaptation process allows the effects of high salt exposure to be minimized, first by uptake of K+ and charge neutralization via the synthesis of anions, and subsequently by synthesis of compatible solutes to achieve a steady state osmolarity with the high salt environment. Similar behavior is demonstrated in *Methanosarcina mazei*. While further genetic studies are required to fully grasp the means by which methanogens accumulate potassium ions, the *M. mazei* Gö1 genome does encode two homologues of the *E. coli trk*A and *trk*G genes responsible for transporting K+ (Pfluger et al. 2007). Furthermore, *M. mazei* Gö1 has 3 glutathione-regulated potassium-efflux system proteins with similarity to *E. coli*'s cation/ proton antiporter proteins (KefC) that facilitate the cell's response to osmotic pressure changes and that protect from electrophile toxicity. Even though the synthesis of compatible solutes in *M. mazei* Gö1 varies, depending upon the concentration of osmolytes and salt in the extracellular environment, distinctions between solutes are worth mentioning. Under low osmolyte concentrations of 0.3 – 1.0 osmol/ kg, the compatible solutes accumulated in *Methanosarcina* species are potassium and α-glutamate (Sowers and Gunsalus 1995). However, under the high osmolyte concentrations of 2.0 osmol/ kg, N^{ε}-acetyl-β-lysine becomes the predominant compatible solute. Furthermore, under moderate concentrations of 400 mM NaCl, glutamate solutes dominate, while N^{ε}-acetyl-β-lysine solutes dominate under the high salt concentration of 800 mM NaCl in *M. mazei* Gö1 (Pfluger et al. 2003). The biosynthetic

pathway for N^{ε}-acetyl-β-lysine production involves the Abl enzymes and consists of the 1) conversion of α-lysine to β-lysine by lysine-2,3-aminomutase (AblA), and 2) acetylation of β-lysine to N^{ε}-acetyl-β-lysine by β-acetyl transferase (AblB). Both Abl enzymes are encoded by the *abl* operons (*abl*A and *abl*B), a deletion of which has been shown to result in a lack of accumulation of the compatible solute N^{ε}-acetyl-β-lysine and therefore no adaptation of the cells to hypersaline environments (Pfluger et al. 2003).

While *M. mazei* is able to synthesize compatible solutes, it can also transport them from the environment, such as glycine betaine. As with bacteria, archaea have at least one glycine betaine transporter. *Methanosarcina mazei* glycine betaine transporters are similar to those found in bacteria (Ota and Otb). Each of the ATP-driven transporters are composed of 3 subunits: 1) a cytoplasmic ATP-hydrolyzing subunit, 2) a transmembrane transporter subunit, and 3) a substrate binding protein (Spanheimer et al. 2008). Ota concentrations increased with increasing salt concentrations and osmolarity as well, and Ota expression was also regulated by the different phases of growth in *E. coli* (Spanheimer et al.2008). Furthermore, Ota was shown to catalyze glycine betaine transport, which is activated by salinity gradients and is energy-dependent (Schmidt et al. 2007). Genetic studies have also shown that levels of the genes coding MM1598 and MM2587, which are surface layer proteins in *M. mazei*, have increased in salt adapted cells (Pfluger et al. 2007), demonstrating that the cell surface also adjusts to changing saline environments.

Post translational modifications on surface layer proteins in hypersaline environments

Changes in salt concentration in *Hfx. volcanii* from low (1.75 M NaCl) to high (3.4 M NaCl) have an effect on both the glycosylation site of the surface layer glycoprotein, as well as the type of glycan on the residue (Guan et al., 2012). An enzyme is responsible for transferring the glycan from its lipid carrier to the amino acid residue on the surface layer protein, and this enzyme,

AglB, is the only known archaeal oligosaccharyl transferase. SlaA, a surface layer protein found in *S. acidocaldarius*, has a high number of glycosylation sites, perhaps stabilizing the cell wall (Jarrell, 2014). Such a stabilization may also be needed by mesophiles, such as *M. mazei*, when they are exposed to high salt environments and further lack the sugary methanochondroitin outer layer.

The presence of N-linked oligosaccharides on S-layer proteins helps to maintain the *Halobacterium salinarium* rod-like shape, and loss of its N-glycans results in a spherical cell (Mescher and Strominger, 1976). S-layer proteins further promote an understanding of lipid modifications in archaea, specifically the linkage between lipids and proteins/ polypeptides. S-layer proteins that are glycosylated are initially bound to the C-terminal domain with transmembrane-spanning amino acid residues. Afterwards, the enzyme, archaeosortase A (Art), which is an exosortase, cleaves the S-layer glycoprotein and transfers it to a lipid anchor in a magnesium-dependent manner (Kandiba, 2014).

RESULTS

Methanosarcina mazei cells grown under low salt conditions

After trypsin digestion and mass-analyzing (by data-dependant acquisition on a Q-Exactive hybrid Orbitrap mass spectrometer) isolated surface layer proteins from *M. mazei* Gö1 cells grown under low and high salt, we found that the SLP MM_1976 received the highest confidence score for accurate identification. Upon further analysis, 15 peptide fragments were used to identify SLP MM_1976 from *M. mazei* cells grown under low salt conditions, while 14 MM_1976 peptides were found from cells grown under high salt conditions.

In order to determine whether the SLP MM_1976 grown in low salt possessed any glycosylations, which are post-translational modifications that have been shown to be present

on surface layer proteins, the mass spectra for each of the 15 peptide ions were further analyzed. Specifically, oxonium ions were used to verify that saccharides had been released, because collision induced dissociation (CID) was the means of fragmentation. CID shows preferential fragmentation of the glycan moiety from the glycoprotein because it has a lower energy fragmentation pathway, and thereby provides information about the type of glycan rather than the location of the glycan moiety on the amino acid residue.

Based upon our search of oxonium ions present in the mass spectra of the SLP MM_1976 peptide ions, we discovered one peptide ion that possessed a putative oxonium ion with an *m/z* value of 127.08. Because the mass tolerance for the instrument is 0.01 Da, its assignment could be an oxonium ion for Hex-$2H_2O$ (*m/z* = 127.06), which is a hexose sugar such as mannose or galactose that subsequently loses 2 molecules of water. This would be consistent with research performed by Dr. Francoleon from our lab, who demonstrated that SLP MM_1976 is possibly glycosylated with α-D-mannose and α -D-glucose moieties, via a lectin affinity binding study using Concanavalin A (Francoleon 2009). The theoretical $[M+H]^+$ value for the peptide ion that contained the Hex-$2H_2O$ oxonium ion (*m/z* = 127.06), had an *m/z* value of 922.5, with a sequence of VWLEFTK, which unfortunately corresponds to the mass of an unmodified peptide, and therefore this can not be a glycosylated peptide.

***Methanosarcina mazei* cells grown under high salt conditions**

When the *M. mazei* cells, which only contained the S-layer protein, were grown under high salt conditions, SLP MM-1976 achieved the highest confidence score for identification of the protein. Based upon our search of oxonium ions present in the mass spectra of the SLP MM_1976 peptide ions, we again discovered one peptide ion that possessed a putative oxonium ion with an *m/z* value of 186.17. Because the mass tolerance for the instrument is 0.01 Da, its assignment could be an oxonium ion for HexNAc-H_2O (*m/z* = 186.09), which is an *N*-

acetylhexosamine that subsequently lost 1 molecule of water. The theoretical $[M+H]^+$ value for the peptide ion that contained the HexNAc-H_2O oxonium ion (*m/z* = 186.09), had an *m/z* value of 904.5, which again unfortunately is consistent for the unmodified peptide LVLDSDDK, i.e., we found not direct evidence for glycosylation from the mass spectra data.

Discussion and Conclusion

Based upon our findings for the isolated surface layer proteins from cells grown under different salt concentrations, we determined that the most confidently identified S-layer protein was that of MM-1976. This data is consistent with our previous studies in which the most abundant surface layer protein identified in our quantitative proteomic studies was MM_1976 (Francoleon et al. 2009).

Salt adaptation in archaea is essential for the cell's survival. In extreme halophiles, such as *Hfx. volcanii*, the surface-layer protein has been shown to be glycosylated via N-glycosylation patterns, which have been shown to maintain the cell's integrity in structure, shape, and even facilitate lipid modification in a metal-dependent manner. Even though attempts were made to determine the glycosylation status of the peptides that were analyzed under different salt conditions, additional research needs to be performed in order to definitively draw any condlusions. Based upon the precursor masses, the peptides shown appear to be unmodified.

In summary, even though saline environmental conditions can affect the outermost layer of *Methanosarcina mazei* Gö1, our initial stages of proteomic studies on the glycosylation pattern of the surface-layer protein of *M. mazei* showed no distinction between cells grown at low and high salt concentrations.

References

1. Francoleon, D.R.; Boontheung, P.; Yang, Yanan; Kim, U.; Ytterberg, U.K.; Denny, P.A.; Denny, P.C.; Loo, J.A.; Gunsalus, R.P.; Loo, R.O. S-layer Surface-Accessible and Concanavalin A Binding Proteins of *Methanosarcina acetivorans* and *Methanosarcina mazei. J. Proteome Res.* **2009**, *8(4)*, 1972-1982.
2. Guan, Z.; Naparstek, S.; Calo, D.; Eichler, J. Protein glycosylation as an adaptive response in Archaea: growth at different salt concentrations leads to alterations in *Haloferax volcanii* S-layer glycoprotein N-glycosylation. *Environ. Microbiol.* **2012**, *14*, 743-753.
3. Hu, B.; Harris, D.F.; Dean, D.R.; Liu, T.L.; Yang, Z.Y.; Seefeldt, L.C. Electrocatalytic CO_2 reduction catalyzed by Nitrogenase MoFe and FeFe proteins. *Bioelectrochemistry.* **2018,** 120, 104-109.
4. Jarrell, K.F.; Ding, Y.; Meyer, B.H.; Albers, S.V.; Kaminski, L.; Eichler, J. N-linked glycosylation in Archaea: a structural, functional, and genetic analysis. *Microbiol. Mol. Biol. Rev.* **2014**, *78*, 304-341.
5. Kandiba, L.; Eichler, J. Archaeal S-Layer glycoproteins: post-translational modification in the face of extremes. *Frontiers in Microbiology.* **2014**, *5(661)*, 1-5.
6. Mechref, Y. Use of CID/ETD Mass spectrometry to analyze glycopeptides. *Curr Protoc Protein Sci.* **2012**.
7. Mescher, M.F.; Strominger, J.L. Structure (shape-maintaining) role of the cell surface glycoprotein of *Halobacterium salinarium. Proc. Natl. Acad. Sci. U.S.A.* **1976**, *73*, 2687-2691.
8. Pfluger, K.; Baumann, S.; Gottschalk, G.; Lin, W.; Santos, H.; Muller, V. Lysine-2,3-aminomutase and beta-lysine acetyltransferase genes of methanogenic archaea are salt induced and are essential for the biosysnthesis of Nepsilon-acetyl-beta-lysine and growth at high salinity. *Appl Environ, Microbiol.* **2003,** 69:10, 6047-55.

9. Pfluger, K.; Ehrenreich, A.; Salmon, K, Gunsalus, R.P.; Deppenmeier, U.; Gottschalk, G.; Muller, V. Identification of genes involved in salt sadaptation in the archaeon *Methanosarcina mazei* Go1 using genome-wide gene expression profiling. *FEMS Microbiology Letters.* **2007,** 277:1, 79-89.
10. Schmidt, S.; Pfluger, K.; Kogl, S.; Spanheimer, R. ; Muller, V. The salt-induced ABC transporter Ota of the methanogenic archaeon *Methanosarcina mazei* Go1 is a glycine betain transporter. *FEMS Microbiol Lett.* **2007,** 277:1, 44-49.
11. Sowers, K.R.; Gunsalus, R.P. Halotolerance in Methanosarcina spp.: Role of N(sup(epsilon))-Acetyl-(beta)-Lysine, (alpha)-Glutamate, Glycine Betaine, and K(sup+) as Compatible solutes for Osmotic Adaptation. *Appl Environ Microbiol*. **1995,** 61:12, 4382-8.
12. Spanheimer, R.; Muller, V. The molecular basis of salt adaptation in *Methanosarcina mazei* Go1. *Arch Microbiol.* **2008**, *190*, 271-279.
13. Tenchov, B.; Vesico, E. M.; Sprott, G. D.; Zeidel, M.L.; Mathai, J. C. Salt Tolerance of Archael Extremely Halophilic Lipid Membranes. *JBC*. **2006**, *281:15*, 10016-10023.
14. Wagner, R.; Ermler, U.; Shima, S. MtrA of the sodium ion pumping methyltransferase binds cobalamin in a unique mode. *Scientific Reports.* **2016,** 6:28226, 1-10.

APPENDIX

Methanosarcina barkeri's Proteomic Response to Different Methylotrophic Substrates

Introduction

Methanosarcina barkeri Fusaro cells, originally isolated from the freshwater environment of a coastal lagoon in Italy (Kandler and Hippe, 1977), are capable of utilizing all four methanogenic pathways: 1) aceticlastic, 2) methylotrophic, 3) hydrogenotrophic, and 4) methyl reduction with hydrogen. Furthermore, *M. barkeri* is able to grow under hyposaline environments as aggregated cells, while dissociating into individual cells under hypersaline conditions. A methanochondroitin layer, composed of D-galactosamine and D-glucuronic acid (Kreisl and Kandler, 1986), serves as the outermost layer of *M. barkeri* cells grown in a low-saline medium; however, under marine conditions, the methanochondroitin disaggregates and a crystalline proteinaceous material, the surface layer protein becomes the outermost layer (Sowers, 1995). A comparative genome analysis revealed that extensive gene rearrangements had occurred in *M. barkeri,* as compared to *M. mazei* and *M. acetivorans* (Maeder et al., 2006). A study by Maeder and colleagues revealed that *M. barkeri* shows increased transposase activity and the genome distal to the origin of replication is distorted, which is unlike the genome proximal to the origin, having 95% interspecies similarity to *mazei* and *acetivorans* (Maeder et al., 2006).

Methods

Methanosarcina barkeri cells were grown in a similar fashion as *M. mazei* cells. Please refer to the chapter on *M. mazei* growth for further details.

Results

We identified and quantified 112 proteins from *M. barkeri* cells grown on methanol, 68 proteins for cells grown on monomethylamine, 47 proteins from dimethylamine-grown cells and 53 proteins from trimethylamine-grown cells.

Methanol-grown M. barkeri

When *M. barkeri* cells were grown in methanol, the 10 most abundant proteins included the methylcoenzyme M reductases, as well as the methanol-specific methyltransferases and corrinoid protein, all of which accounted for nearly 40% of the total amount of protein quantified **(Figure A.1)**.

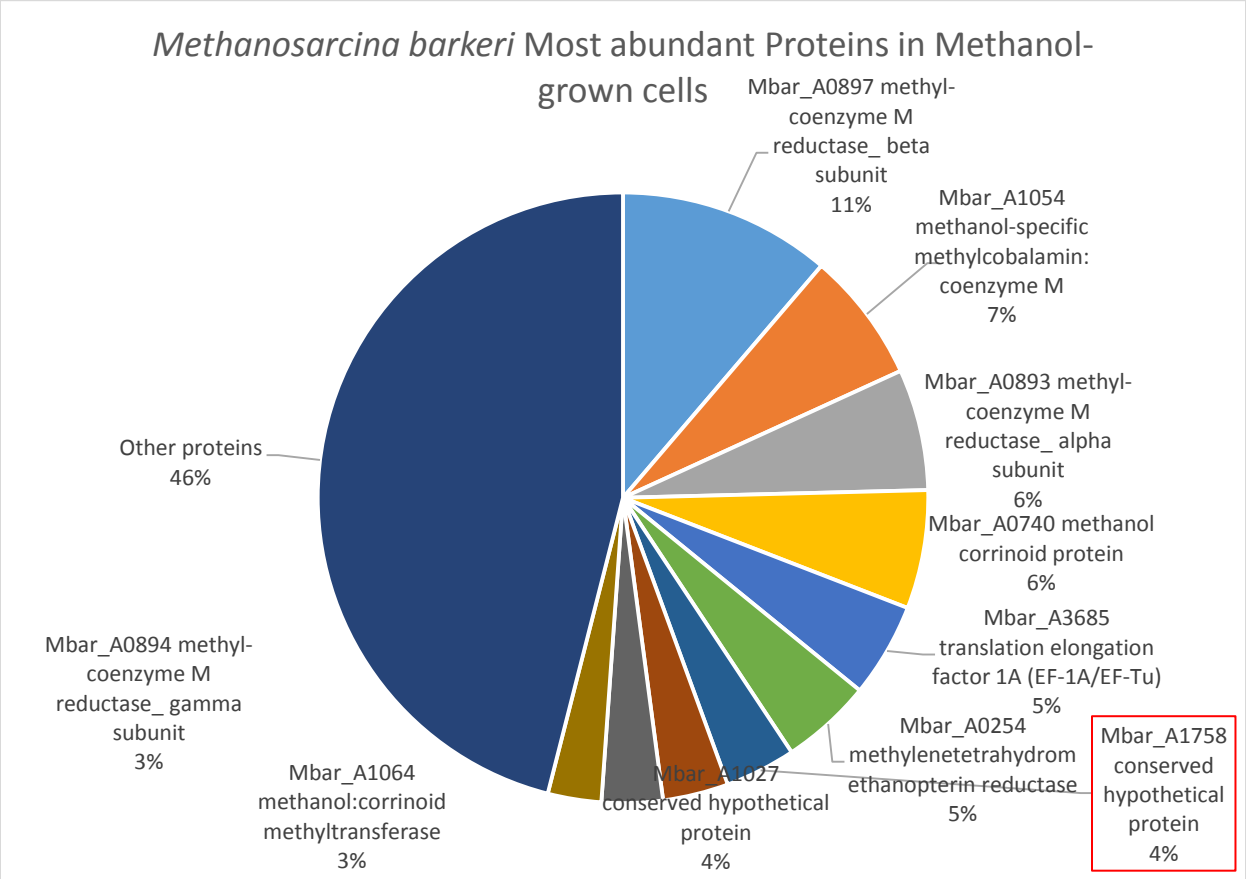

Figure A.1 *Methanosarcina barkeri* produces Mbar_A1758 surface-layer proteins when grown in MeOH

Monomethylamine-grown M. barkeri

When *M. barkeri* cells were grown in the monomethylamine substrate, methylcoenzyme M reductase was among the most abundant protein, as was the case of cells grown in methanol.

However, the methyltransferases are substrate-specific, meaning that among the most abundant methyltransferases was the monomethylamine:corrinoid methyltransferase (Mbar_A0843) at 12% of the total amount of proteins quantified. Nonetheless, the methanol-specific methylcobalamin coenzyme M (Mbar_A1054), accounted for 5% of the protein quantified in *M. barkeri*, making it the sixth most abundant protein from cells grown in monomethylamine. In total, the coenzyme M reductases and methyltransferases with the corrinoid proteins accounted for 44% of the total protein quantified when cells were grown in monomethylamine substrate **(Figure A.2)**.

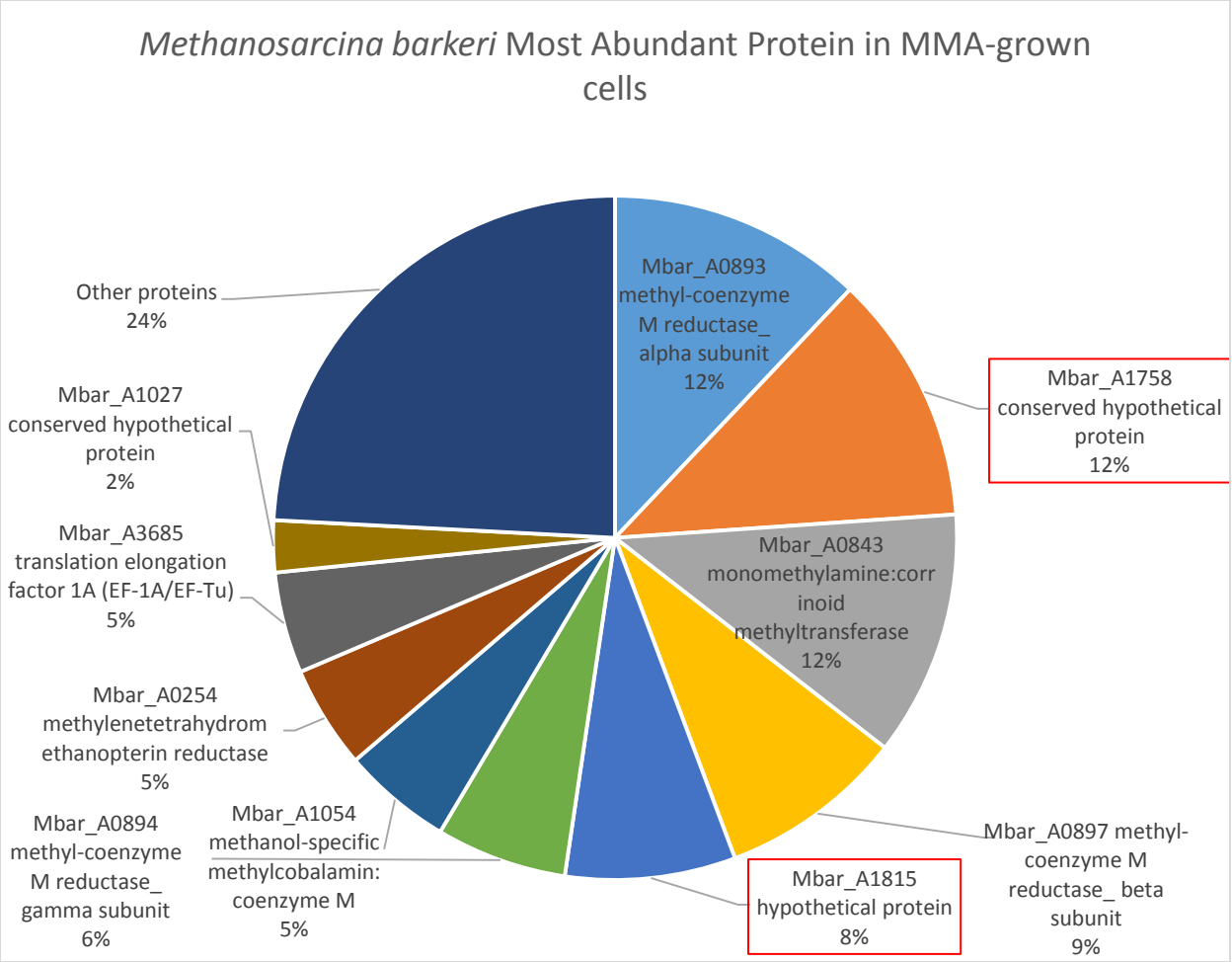

Figure A.2 *Methanosarcina barkeri* produces Mbar_A1815 and Mbar_A1758 surface-layer proteins when grown in MMA

Dimethylamine-grown M. barkeri

For *M. barkeri* cells grown in dimethylamine, a trend similar to those seen from cultivation on methanol and monomethylamine emerged, with the coenzyme M reductases and methyltransferases with the corrinoid proteins accounting for a combined total of nearly 70% of the total amount of proteins quantified. Even though the most abundant proteins were not DMA-specific, *i.e.*, monomethylamine:corrinoid methyltransferase (Mbar_A0843), accounting for 23%

of total protein and methanol-specific methylcobalamin:coenzyme M (Mbar_A1054), accounting for 5%, the DMA-specific dimethylamine corrinoid protein Mbar_A3604 accounted for 3% of the total protein **(Figure A.3)**.

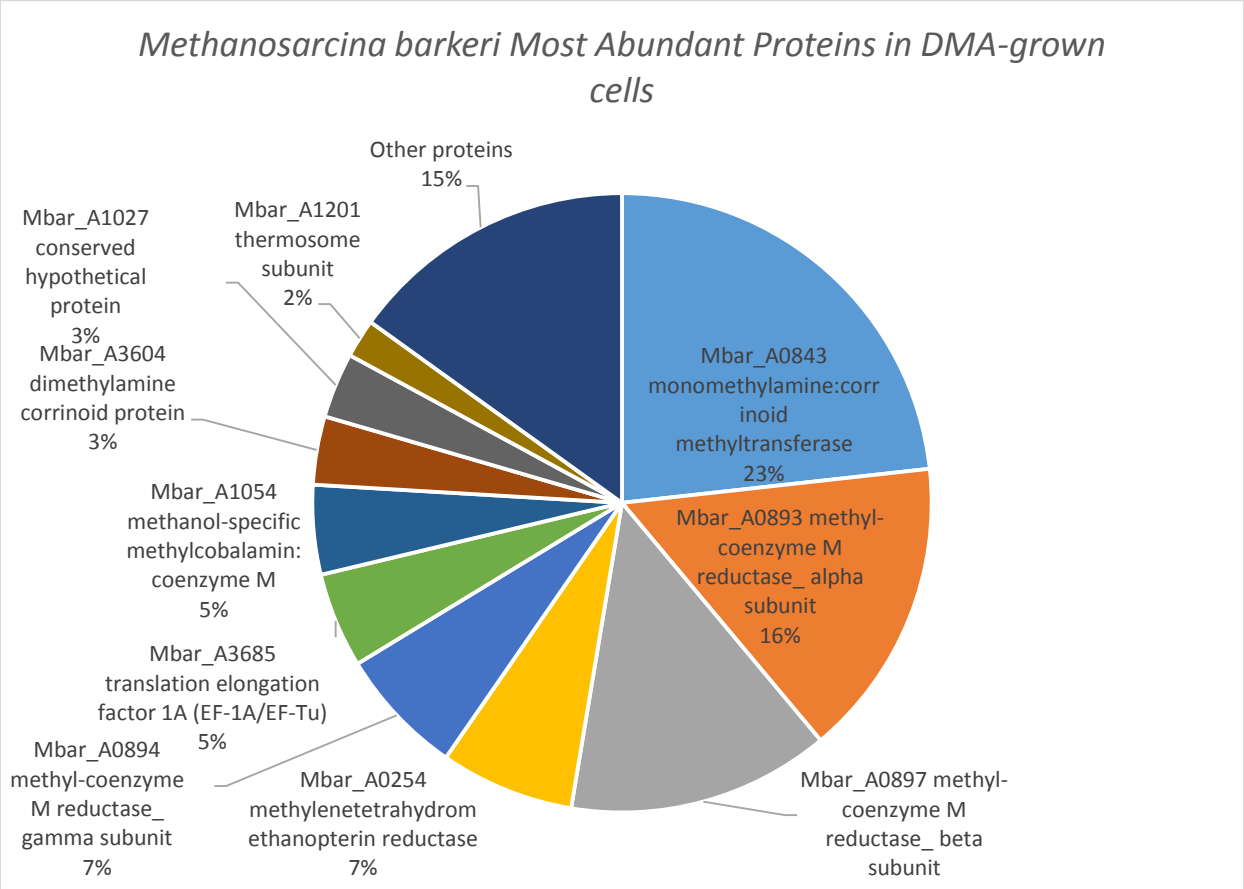

Figure A.3 No surface-layer protein was among the top ten most abundant proteins from *Methanosarcina barkeri* grown in DMA

Trimethylamine-grown M. barkeri

Trimethylamine-grown *M. barkeri* cells also had abundant coenzyme M reductases and methyltransferases with coirrinoid proteins accounting for 60% of the total protein quantified. Nonetheless, non-TMA specific proteins were prevalent, *e.g.*, dimethylamine corrinoid protein (Mbar_A3604) accounting for 5% of protein, monomethylamine:corrinoid methyltransferase

(Mbar_A0843) accounting for 10%, and methanol-specific methylcobalamin coenzyme M (Mbar_A1054) comprising 5% **(Figure A.4)**.

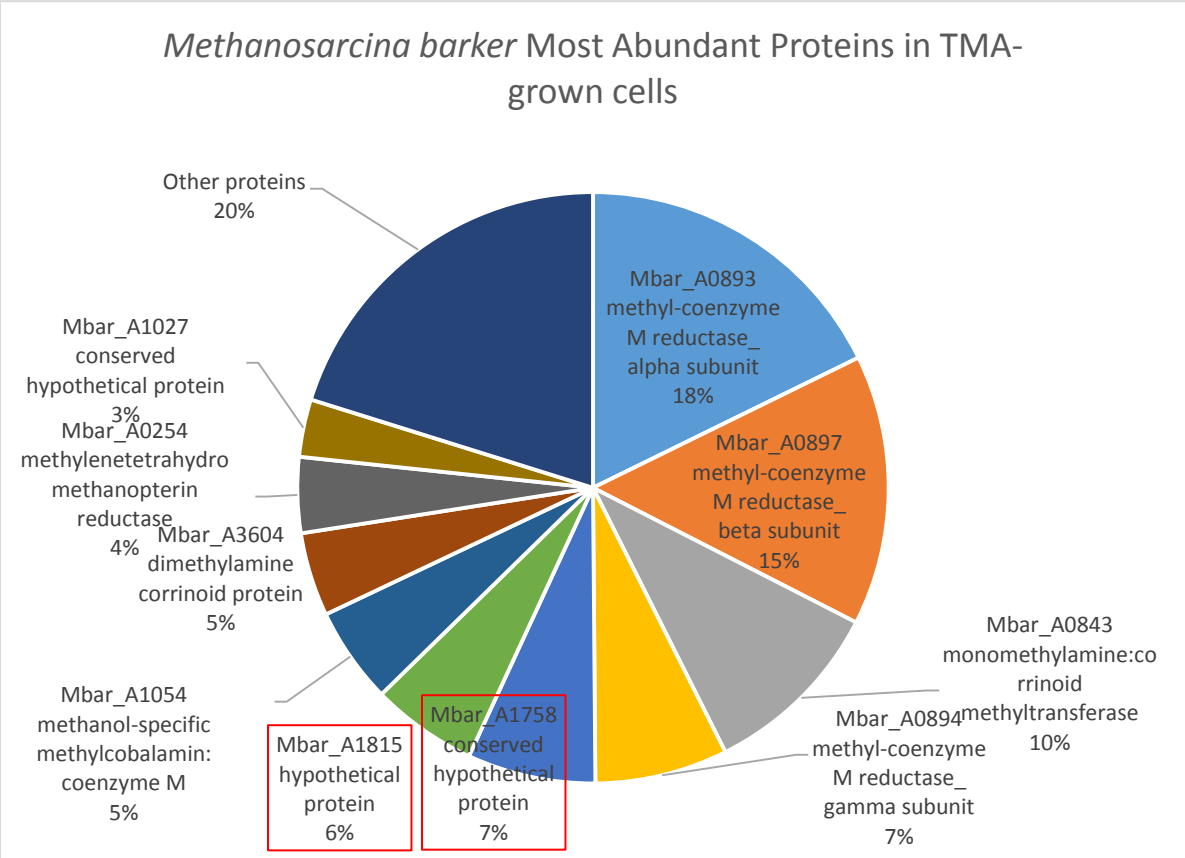

Figure A.4. *Methanosarcina barkeri* produces Mbar_A1815 and Mbar_A1758 surface-layer proteins when grown in TMA

Our initial analysis of *M. barkeri* cells showed that each methylotrophic-grown cell contained at least one surface-layer protein (Mbar_A1758 or Mbar_A1815) in the 10 most abundant proteins quantified **(Figures A.5-A.8)**. However, it is interesting to note that, in our second round of analyses, surface layer proteins Mbar_A1758 and Mbar_A1815 were among the 10 most abundant proteins from cells grown on methanol, monomethylamine, and trimethylamine. Noticeably, both S-layer proteins were abundant in the *M. barkeri* cells grown in trimethylamine

and monomethylamine, while no S-layer protein (SLP) was found in dimethylamine-grown cells, and only one SLP (Mbar_A1758) was found in methanol-grown cells. While additional biological replicates should be performed for the analysis of proteins in *M. barkeri* cells, preliminary data shows that 2 surface layer proteins (Mbar_A1758 and Mbar_A1815) each belonging to a different branch of the phylogenetic SLP tree in archaea **(Figure A.9)**, exists for *M. barkeri* cells grown in monomethylamine and trimethylamine **(Figures A.1-A.4)**.

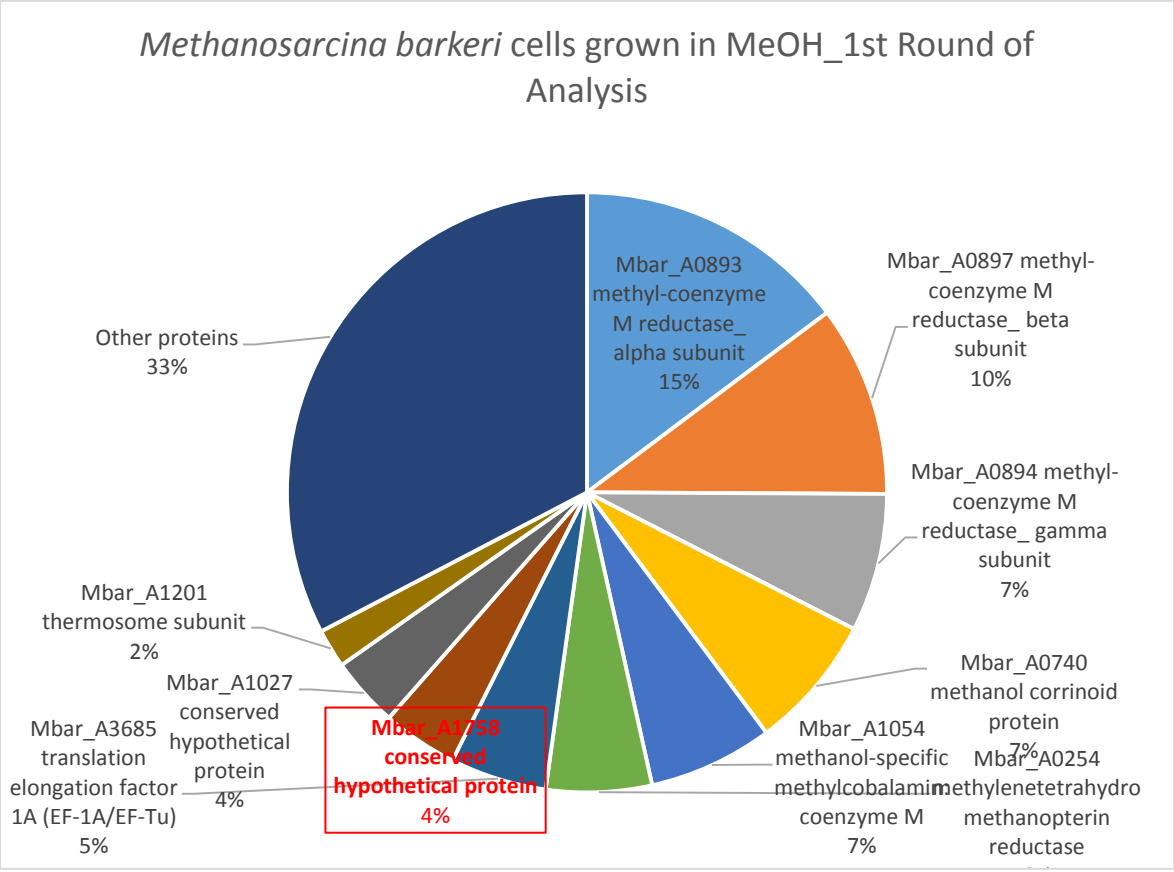

Figure A.5 *Methanosarcina barkeri* produces Mbar_A1758 surface-layer protein when grown in MeOH

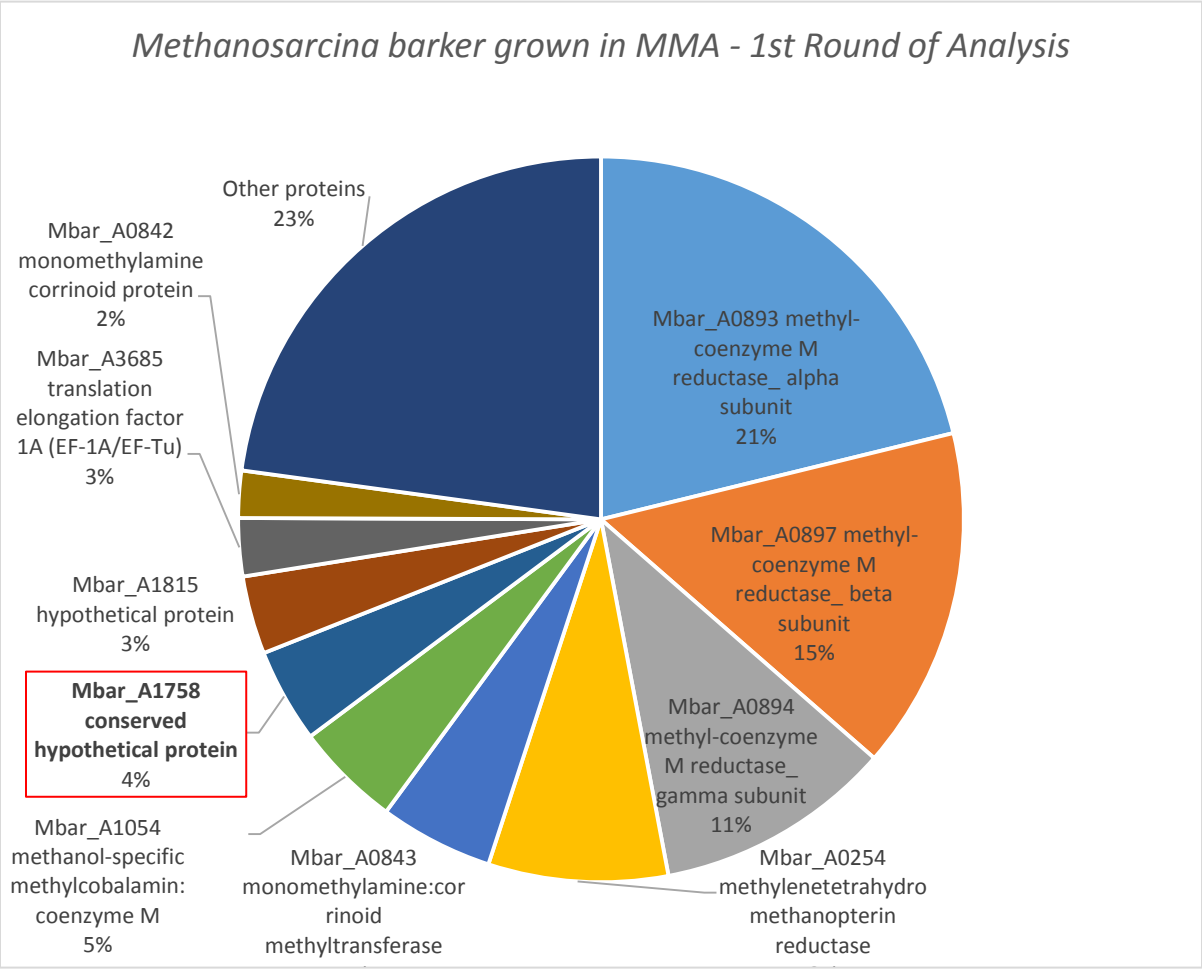

Figure A.6 *Methanosarcina barkeri* produces Mbar_A1758 surface-layer protein when grown in MMA

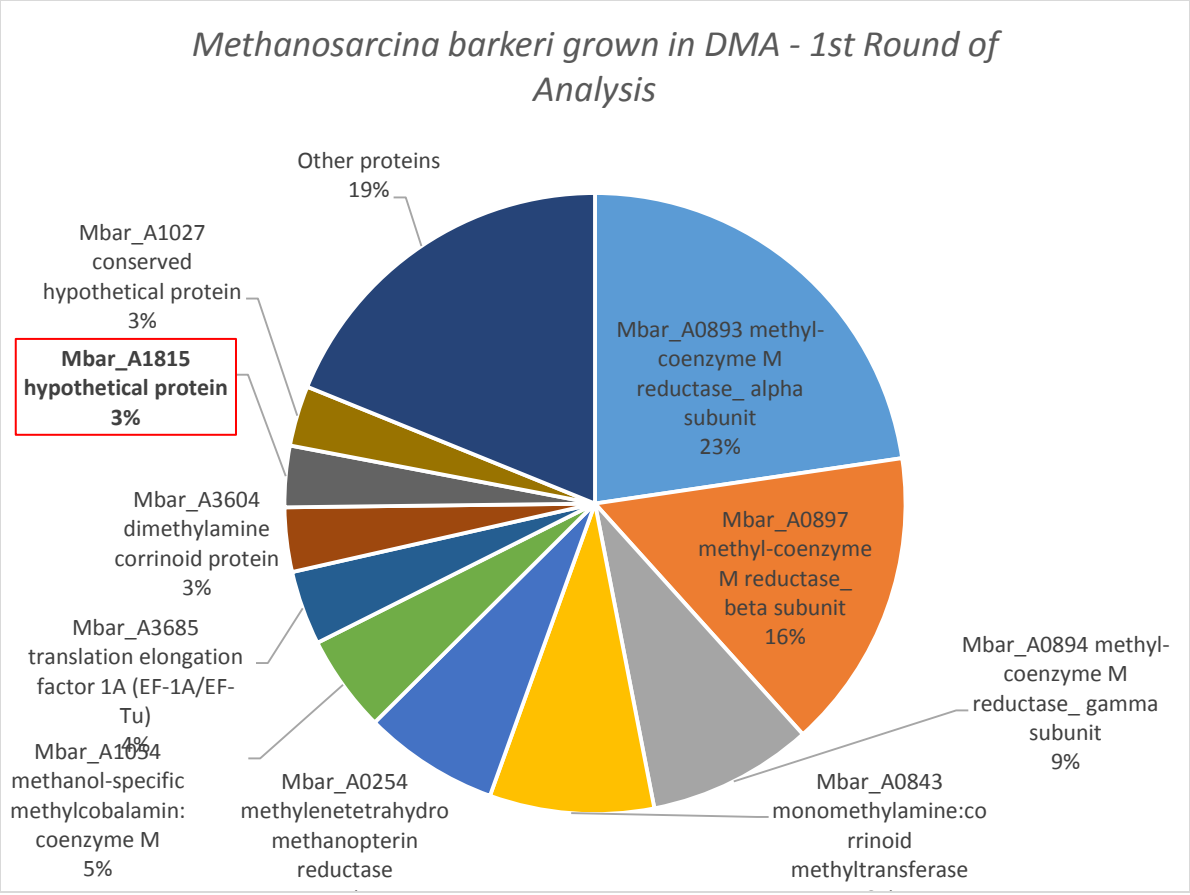

Figure A.7 *Methanosarcina barkeri* produces Mbar_A1815 surface-layer protein when grown in DMA

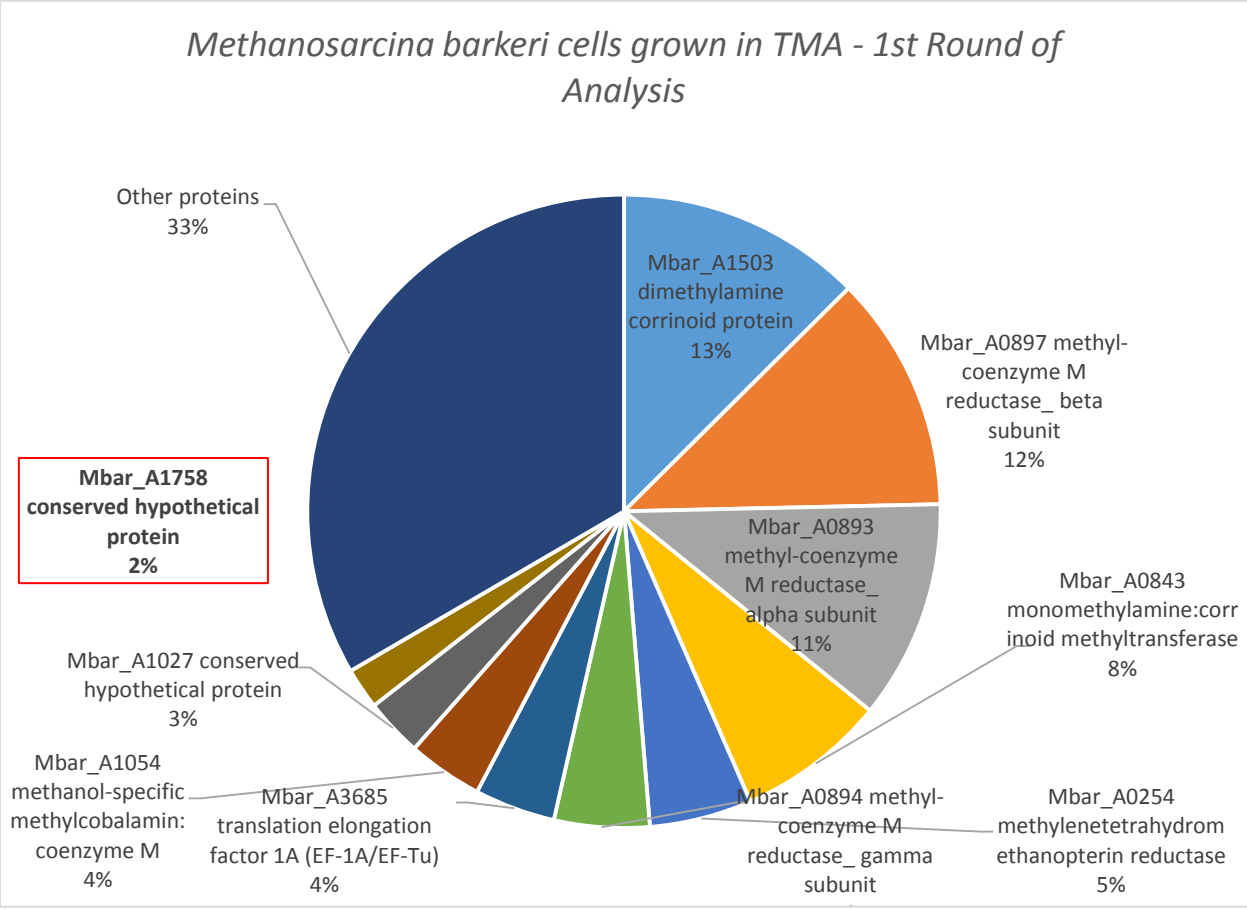

Figure A.8 *Methanosarcina barkeri* produces Mbar_A1758 surface-layer protein when grown in TMA

Figure A.9 Mbar_A1815 and Mbar_A1758 belong to different branches of the Archaea domain Surface Layer protein tree.

Discussion

Methanosarcina barkeri employs its corrinoid and methyltransferase enzymes in a substrate-dependent manner; however, the methylcoenzyme-M reductase enzymes it uses remain constant. Furthermore, *M. barkeri* cells, in a similar fashion to *M. mazei*, devote most of their energy (>40%) toward transferring the methyl group from the methylotrophic substrates to methyl-coenzyme M, a process performed by the triad of the methyltrasferase systems, and removing the methyl group from methyl-coenzyme M to form methane and the heterodisulfide coenzymeM-coenzymeB complex, a process performed by methyl-coenzyme M reductase. Both enzymes (methyltransferases with the corrinoid proteins and the methyl coenzyme M reductases) belong to the reductive steps of the methylotrophic pathway.

In an unexpected turn of events, *Methanosarcina barkeri* is able to synthesize 2 different surface layer proteins, each belonging to a different branch of the phylogenetic SLP tree in archaea, when cells are grown in monomethylamine and trimethylamine. The presence of both surface layer proteins in the list of the 10 most abundant proteins in *M. barkeri* indicates the cells are covered with a mosaic of surface layer proteins, each possibly serving different functions when the cells are exposed to various environments.

Conclusion

Methanosarcina barkeri is able to survive under hypo- and hyper-saline environments, and similar to *M. mazei*, as indicated in this study, can perform methanogenesis in a methylotrophic-substrate-dependent manner. Furthermore, the most abundant proteins were the methyltransferases with corrinoid proteins and methyl-coenzyme M reductases. However, in contrast to *M. mazei* cells, based upon our research, *M. barkeri* has the novel ability to produce 2 different surface layer proteins, each belonging to different branches of the phylogenetic SLP

tree, simultaneously when grown in monomethylamine as well as trimethylamine. This may be explained by the distorted genome distal to the origin of replication and the increase in transposases when compared to *M. mazei* and *M. acetivorans* cells (Maeder et al. 2006). While such a finding may have been unforeseen, it adds further insight into the structure of *M. barkeri* cells and their proteomic responses and adaptation to growth on different methylotrophic substrates.

In summary, *Methanosarcina barkeri* Fusaro exhibits many of the enzyme-switching properties as *Methanosarcina mazei* Gö1, and even has a surface-layer protein-switching mechanism that depends upon substrate availability.

References

1. Kandler, O.; Hippe, H. Lack of peptidoglycan in the cell walls of *Methanosarcina barkeri. Arch. Microbiol*. **1977**, *113*, 57-60.
2. Kreisl, P.; Kandler, O. Chemical structure of the cell wall polymer of *Methanosarcina*. *Sys. Appl. Microbiol.* **1986**, *7*, 293-299.
3. Maeder, D.L.; Anderson, I.; Brettin, T.S.; Bruce, D.C.; Gilna, P.; Han, C.S.; Lapidus, A.; Metcalf, W.W.; Saunders, E.; Tapia, R.; Sowers, K.R. The *Methanaosarcina barkeri* Genome: Comparative Analysis with *Methanosarcina acetivorans* and *Methanosarcina mazei* Reveals Extensive Rearrangement within Methanosarcinal Genomes. *Journal of Bacteriology.* **2006**, *185(22)*, 7922-7931.
4. Sowers, K.R. Growth of *Methanosarcina* spp. as single cells. **1998**, *In* F.T. Robb, K.R. Sowers, S. DasSharna, A.R. Place, H.J. Schrier, and E.M. Fleischmann (ed.), Archaea: a laboratory manual. Cold Spring Harbor Laboratory Press, Cold Spring Harbor, N.Y.